ENSEMBLES FOR THE PREDICTABILITY OF AVERAGE TEMPERATURES

by

Sarah Tarek Khankan

B.S., Mathematics, American University of Beirut, 2008

M.S., Computational Science, American University of Beirut, 2010

Submitted to the Graduate Faculty of

the Kenneth P. Dietrich School of Arts and Sciences in partial

fulfillment

of the requirements for the degree of

Doctor of Philosophy

University of Pittsburgh

2016

UNIVERSITY OF PITTSBURGH

DIETRICH SCHOOL OF ARTS AND SCIENCES

This dissertation was presented

by

Sarah Tarek Khankan

It was defended on

October 13th 2016

and approved by

William Layton, Professor

Michael Neilan, Professor

Catalin Trenchea, Professor

Noel Walkington, Professor

Dissertation Director: William Layton, Professor

ENSEMBLES FOR THE PREDICTABILITY OF AVERAGE TEMPERATURES

Sarah Tarek Khankan, PhD

University of Pittsburgh, 2016

The instability of the atmosphere places an upper bound on the predictability of instantaneous weather patterns. The lack of complete periodicity in the atmosphere's behavior is sufficient evidence for instability (Lorenz, 1963) [1], but it does not reveal the range at which the uncertainty in prediction must become large. Most estimates of this range have been based on numerical integrations of systems of equations of varying degrees of complexity, starting from two or more rather similar initial states. It has become common practice to measure the error which would be made by assuming one of these states to be correct, when in fact another is correct, by the root-mean-square difference between the two fields of wind, temperature, or some other element, and to express the rate of amplification of small errors in terms of a doubling time [1].

The purpose of this thesis is to build tools with rigorous support useful for studying predictability of average temperatures. We apply our tools to a simple Earth-like example and make use of the Bred Vector algorithm to generate initial perturbations. The numerical model used is that of the Natural Convection problem. The analysis is done in steps, first by analyzing the turbulent natural convection problem then by introducing a fast calculation of an ensemble of solutions of the Navier-Stokes equations coupled with the temperature equation. Complete stability and convergence analysis of the methods are presented. The turbulent Earth model and its stability conditions are introduced at the end of the thesis.

TABLE OF CONTENTS

LIST OF TABLES

LIST OF FIGURES

1.0 INTRODUCTION

Being able to predict the future state of a system, given its present state, stands at the foundations of scientific knowledge with important implications from a theoretical and applicative point of view [24]. The knowledge of the evolution law of the system may give the impression that this aim has been attained. This is the classical deterministic point of view as clearly stated by Laplace [26]: once the evolution laws of the system are known, the state at a certain time t_0 completely determines the subsequent states for every time $t > t_0$. However it is well established now that this cannot be accomplished in practice.

One limitation takes place in systems with many degrees of freedom, it is the impossibility to manage the huge amount of data required for a full description of a single state of a large scale body. Another source of difficulty, which arises even in low dimensional systems, is related to the unavoidable uncertainty in the initial condition. As clearly stated by Poincaré, this implies that one can make long-time predictions only if the evolution law does not amplify the initial uncertainty too rapidly. This aspect had a relevant role in the development of the theory of dynamical chaos.

Lorenz showed that the forecast skill of atmosphere models depends not only on the accuracy of the initial conditions and on the realism of the model (as it was generally believed at the time), but also on the instabilities of the flow itself [9]. He demonstrated that any nonlinear dynamical system with instabilities, like the atmosphere, has a finite limit of predictability. The growth of errors due to instabilities implies that the smallest imperfection in the forecast model or the tiniest error in the initial conditions, will inevitably lead to a total loss of skill in the eather forecasts after a finite forecast length. Lorenz estimated this limit of weather predictability as about two weeks. With his simple model he also pointed out that predictability is strongly dependent on the evolution of the atmosphere itself: some days the

forecasts can remain accurate for a week or longer, and on other days the forecast skill may break down after only 3 days [9].

Therefore, from the point of view of predictability, we need to know how an error in the initial state of the system grows in time. In deterministic chaotic systems, i.e., with sensitive dependence on initial condition, one has an exponential growth of errors and, consequently, a severe limitation on the ability to predict the future states. Another huge point of interest is predictability by scale; namely, the impact that the scale of the studied domain has on the ability to predict the state of the system in question.

In order to efficiently study the predictability of average temperatures, an ensemble algorithm for the Natural Convection problem has been developed. Ensemble predictions are commonly used in weather forecast worldwide, including National Centers for Environmental Prediction (US) and the European Centre for Medium-Range Weather Forecasts (ECMWF). Ensemble calculation is essential in uncertainty quantification, numerical weather prediction, sensitivity analysis, predicting probability distributions for quantities of interest and many other applications in Computational Fluid Dynamics (CFD), see for instance, [28], [29], [30], [31], [15], [33], [20], [61]. The algorithm results in J linear systems with the same coefficient matrix instead of J linear systems with J different coefficient matrices at each time step, which allows the use of block iterative methods, e.g., [34], [35], [36], [37], to reduce the computing time and required memory substantially. An ensemble system can be used to produce many forecasts. Instead of running a single forecast, the ensemble model will run a number of initial conditions that differ slightly from each other. The use of ensembles helps narrow the error and pick the most likely outcome. The initial differences between the ensemble members are small, which is consistent with uncertainties of the observations.

The final objective of this thesis is to study the predictability of average temperatures of the turbulent natural convection problems using ensembles. To reach this main goal, Chapter 2 presents some preliminary definitions, lemmas and notations. In Chapter 3, a complete analysis of a time stepping method for the turbulent coupled system of the Navier-Stokes equations and the temperature equation, with time and space dependent viscosity, is presented. Chapter 4 analyzes the ensemble system of the natural convection problem; some predictability results of the system are presented in Chapter 5. A section on Bred Vectors

is contained in Chapter 5, to generate the initial perturbations. Finally, the predictability of average temperatures using the ensemble algorithm for the turbulent natural convection problem is studied in Chapter 6. Chapter 7 contains some additional work on the Compression and reconstruction of turbulent flow data in which new averages are constructed using old ones.

2.0 NOTATION AND PRELIMINARIES

Let Ω, in $2d$ or $3d$, be a bounded, regular, open domain with Lipschitz boundary $\partial\Omega$. $\|\cdot\|$ and $(\cdot,\cdot)$ denote the L^2 norm and inner product, respectively, and $\|\cdot\|_\infty$ denotes the sup norm.

Consider the Sobolev spaces,

$$\begin{aligned} X := H_0^1(\Omega)^d &= \{v \in H^1(\Omega)^d : v = 0 \; on \; \partial\Omega\}, \\ Q := L_0^2 &= \{q \in L^2(\Omega) : \int_\Omega q dx = 0\}, \\ W &:= \{S \in H^1(\Omega) : S = 0 \; on \; \partial\Omega\}, \\ V &:= \{v \in X : (q, \nabla \cdot v) = 0 \; \forall q \in Q\}. \end{aligned}$$

V is called the space of divergence-free functions.

Furthermore, the Poincaré-Friedrichs (PF) inequality is satisfied:

$$\|\chi_{1,2}\| \leq C_{PF,1,2} \|\nabla \chi_{1,2}\| \quad \forall \chi_1 \in X, \; \forall \chi_2 \in W.$$

The following explicitly skew-symmetric trilinear forms are useful:

Definition 1.

$$\begin{aligned} b(u,v,w) &= \frac{1}{2}(u \cdot \nabla v, w) - \frac{1}{2}(u \cdot \nabla w, v) \quad \forall u, v, w \in X, \\ b^*(u,T,S) &= \frac{1}{2}(u \cdot \nabla T, S) - \frac{1}{2}(u \cdot \nabla S, T) \quad \forall u \in X, \; \forall T, S \in W. \end{aligned}$$

Furthermore, they satisfy the following continuity results.

Lemma 2.0.1. *For all u,v,w ∈ X and T,S ∈ W, b(u,v,w) and b*(u,T,S) satisfy*

$$\begin{aligned} b(u,v,w) &\le C'\|\nabla u\|\|\nabla v\|\|\nabla w\|, \\ b(u,v,w) &\le C_1\sqrt{\|u\|\|\nabla u\|}\|\nabla v\|\|\nabla w\|, \\ b^*(u,T,S) &\le \overline{C}\|\nabla u\|\|\nabla T\|\|\nabla S\|, \\ b^*(u,T,S) &\le C_2\sqrt{\|u\|\|\nabla u\|}\|\nabla T\|\|\nabla S\|, \end{aligned}$$

where all constants are dependent on Ω.

Proof. Follows from applications of Hölder and Sobolev embedding inequalities (see [10], Chapter 7). □

The following identities are useful.

Lemma 2.0.2. *Let u, v, and w ∈ X and T, S ∈ W, then the following identities hold*

$$\begin{aligned} b(u,v,w) &= \int_\Omega u\cdot\nabla v\cdot w dx + \frac{1}{2}\int_\Omega (\nabla\cdot u)v\cdot w dx, \\ b(u,T,S) &= \int_\Omega u\cdot\nabla T S dx + \frac{1}{2}\int_\Omega (\nabla\cdot u)TS dx. \end{aligned}$$

Proof. We have that

$$\begin{aligned} b(u,v,w) &= \frac{1}{2}(u\cdot\nabla v, w) - \frac{1}{2}(u\cdot\nabla w, v) \\ &= \frac{1}{2}(u\cdot\nabla v, w) + \frac{1}{2}(u\cdot\nabla v, w) + \frac{1}{2}\int_\Omega (\nabla\cdot u)v\cdot w dx \\ &= (u\cdot\nabla v, w) + \frac{1}{2}\int_\Omega (\nabla\cdot u)v\cdot w dx, \end{aligned}$$

where integration by parts was used on the second term in $b(u,v,w)$. Similarly,

$$\begin{aligned} b^*(u,T,S) &= \frac{1}{2}(u\cdot\nabla T, S) - \frac{1}{2}(u\cdot\nabla S, T) \\ &= \frac{1}{2}(u\cdot\nabla T, S) + \frac{1}{2}(u\cdot\nabla T, S) + \frac{1}{2}\int_\Omega (\nabla\cdot u)TS dx \\ &= (u\cdot\nabla T, S) + \frac{1}{2}\int_\Omega (\nabla\cdot u)TS dx. \end{aligned}$$

□

Using the above lemma, we have two vital continuity results for the skew-symmetric trilinear forms.

Lemma 2.0.3. *For all u,v,w ∈ X and T,S ∈ W, b(u,v,w) and b*(u,T,S) satisfy*

$$b(u,v,w) \leq C_3\|\nabla u\|\|\nabla v\|\sqrt{\|w\|\|\nabla w\|},$$
$$b^*(u,T,S) \leq C_4\|\nabla u\|\|\nabla T\|\sqrt{\|S\|\|\nabla S\|},$$

where all constants are dependent on Ω.

Proof. We have that for all u,v,w ∈ X,

$$|(u\cdot\nabla v,w)| \leq C\|u\|_{L^6}\|\nabla v\|\|w\|_{L^3} \leq C\|\nabla u\|\|\nabla v\|\sqrt{\|w\|\|\nabla w\|},$$

where Hölder, Ladyzhenskaya and Gagliardo−Nirenberg inequalities were used, respectively. Using the above result and inequalities,

$$\begin{aligned}
|b(u,v,w)| &= |(u\cdot\nabla v,w) + \frac{1}{2}\int_\Omega (\nabla\cdot u)v\cdot w dx| \\
&\leq |(u\cdot\nabla v,w)| + |\frac{1}{2}\int_\Omega (\nabla\cdot u)v\cdot w dx| \\
&\leq C\|\nabla u\|\|\nabla v\|\sqrt{\|w\|\|\nabla w\|} + C\|\nabla\cdot u\|\|v\|_{L^6}\|w\|_{L^3} \\
&\leq C\|\nabla u\|\|\nabla v\|\sqrt{\|w\|\|\nabla w\|} + C\|\nabla u\|\|\nabla v\|\sqrt{\|w\|\|\nabla w\|} \\
&\leq C\|\nabla u\|\|\nabla v\|\sqrt{\|w\|\|\nabla w\|}.
\end{aligned}$$

In similar fashion,

$$\begin{aligned}
|b^*(u,T,S)| &\leq |(u\cdot\nabla T,S)| + |\frac{1}{2}\int_\Omega (\nabla\cdot u)TS dx| \\
&\leq C\|\nabla u\|\|\nabla T\|\sqrt{\|S\|\|\nabla S\|} + C\|\nabla\cdot u\|\|T\|_{L^6}\|S\|_{L^3} \\
&\leq C\|\nabla u\|\|\nabla T\|\sqrt{\|S\|\|\nabla S\|} + C\|\nabla u\|\|\nabla T\|\sqrt{\|S\|\|\nabla S\|} \\
&\leq C\|\nabla u\|\|\nabla T\|\sqrt{\|S\|\|\nabla S\|},
\end{aligned}$$

where all constants depend on the size of the domain. □

The polarization identity and discrete Gronwall's inequality will be of great benefit in the stability and error analyses.

Lemma 2.0.4. *Polarization Identity:*

Let $u, v \in U$, where U is a an inner product vector space with inner product $(\cdot,\cdot)_U$ and norm $\|\cdot\|_U$. Then,

$$(u,v)_U = \frac{1}{2}\left(\|u\|_U^2 + \|v\|_U^2 - \|u-v\|_U^2\right).$$

Lemma 2.0.5. *Discrete Gronwall's Inequality:*

Let Δt, B, a_n, b_n, c_n, d_n for integers $n \geq 0$ be nonnegative numbers such that for $l \geq 1$, if

$$a_l + \Delta t \sum_{n=0}^{l} b_n \leq \Delta t \sum_{n=0}^{l-1} d_n a_n + \Delta t \sum_{n=0}^{l} c_n + B \text{ for } l \geq 0,$$

then for all $\Delta t \geq 0$,

$$a_l + \Delta t \sum_{n=0}^{l} b_n \leq \exp\left(\Delta t \sum_{n=0}^{l-1} d_n\right)\left(\Delta t \sum_{n=0}^{l} c_n + B\right) \text{ for } l \geq 0.$$

Proof. See [67], [68] pp 279-281. □

We define the following norms:

Definition 2. *Dual norm*

The norms on the dual spaces of bounded linear functions in X and V, respectively, by

$$\|f\|_{-1} := \sup_{0 \neq v \in X} \frac{(f,v)}{\|\nabla v\|} \text{ and } \|f\|_* := \sup_{0 \neq v \in V} \frac{(f,v)}{\|\nabla v\|}.$$

Definition 3. *Let $v : [0,T] \to X$. Define the discrete $(l^p(0,T), H^k(\Omega))$ norm on v by*

$$\|v\|_{l^p(H^k)} := \left(\Delta t \sum_{n=0}^{N} \|v^n\|_k^p\right)^{1/p}$$

2.1 SPACE DISCRETIZATION

We should now discuss those aspects relevant to finite element approximation. Consider a regular quasi-uniform mesh $\Omega_h = \{K\}$ of Ω with maximum triangle diameter length h. Consider a finite element discretization K of Ω, where h is the maximum element diameter in T_h. Let $X_h \subset X$, $Q_h \subset Q$ be the discrete velocity and pressure spaces, respectively, corresponding to K, assumed to satisfy the standard discrete inf-sup condition (see [10], Section 4.2), eg, [38, 39, 40] and given by:

$$X_h := \{v_h \in H_0^1(\Omega)^d : v_h|_K \in P_m(K)^d, \forall K \in \Omega^h\},$$
$$Q_h := \{q_h \in L_0^2(\Omega) \cap C^0(\Omega) : q_h|_K \in P_{m-1}(K), \forall K \in \Omega^h\},$$
$$W_h := \{S_h \in H^1(\Omega) : S_h|_K \in P_m(K), \forall K \in \Omega^h\},$$

with $1 < m$.

The discretely divergence-free subspace of X_h is

$$V_h := \{v_h \in X_h : (\nabla \cdot v_h, q_h) = 0 \text{ for all } q_h \in Q_h\}.$$

The following approximation properties will be useful for the error estimate.

Lemma 1. *([11], Chapter 4, Section 2, "Finite Element spaces for Model Problems") The aforementioned finite element spaces satisfy the following approximation properties for a given integer* $1 \leq k \leq m$,

$$\inf_{v_h \in X_h} \left\{ \|u - v_h\| + h\|\nabla(u - v_h)\| \right\} \leq Ch^{k+1}|u|_{k+1}, \tag{2.1}$$

$$\inf_{q_h \in Q_h} \|p - q_h\| \leq Ch^k|p|_k, \tag{2.2}$$

$$\inf_{S_h \in S_h} \left\{ \|T - S_h\| + h\|\nabla(T - S_h)\| \right\} \leq Ch^{k+1}|T|_{k+1}, \tag{2.3}$$

for all $u \in X \cap H^{k+1}(\Omega)$, $p \in Q \cap H^k(\Omega)$, *and* $T \in W \cap H^{k+1}(\Omega)$.

Furthermore, the discrete inf-sup condition is satisfied, ([10], Chapter 4, Section 4, pp 63-66)

$$\inf_{q_h \in Q_h} \sup_{v_h \in X_h} \frac{(q_h, \nabla \cdot v_h)}{\|q_h\| \|\nabla v_h\|} \geq \beta > 0, \tag{2.4}$$

where β is independent of h.

Let Δt be the time step and denote u^n, p^n, and T^n as the true solutions at time $t^n = n\Delta t$. Assume the solutions satisfy the following regularity assumptions:

$$\begin{aligned}
u &\in L^\infty(0, t^*; X \cap H^{k+1}(\Omega)), \\
T &\in L^\infty(0, t^*; W \cap H^{k+1}(\Omega)), \\
u_t, T_t &\in L^\infty(0, t^*; H^{k+1}(\Omega)), \\
u_{tt}, T_{tt} &\in L^\infty(0, t^*; L^2(\Omega)), \\
p &\in L^\infty(0, t^*; Q \cap H^k(\Omega)(\Omega)),
\end{aligned}$$

where the dimension has been suppressed. The error due to approximation is defined in the usual sense for each:

$$\begin{aligned}
e_u^n &= u^n - u_h^n, \\
e_T^n &= T^n - T_h^n, \\
e_p^n &= p^n - p_h^n.
\end{aligned}$$

3.0 TIME-STEPPING METHODS FOR THE EV-NSE

The following chapter is based on a joint work with Michael McLaughin and Victor Decaria [25].

Variable viscosity problems arise in many complex fluid flow processes of current interest, such as mantle convection ,e.g. Albers [41], Tackley [52], Moresi and Solomatov [58], models of viscoelastic flows, e.g. Renardy [47], Ervin and Miles [48], Ervin and Heuer [49], Ervin and Lee [50], eddy viscosity models of turbulence, e.g. Grinevich and Olshanskii [43], John, Kaiser and Novo [44], Furuichi, May and Tackley [46], materials with temperature-dependent properties, e.g. Cook, King, Herbs and Herschbach [53], Seddeek and Salama [54], Ellahi [55], Ratcliff, Tackleya, Schuberta and Zebib [56], Hooman and Gurgenci [57], Christensen and Harder [59], fluid mixing models, e.g. Geogievskii [45], fluids where viscosity depends on pressure, e.g. Bulicek, Malek and Rajagopal [62], Malek, Necas and Rajagopal [63], and other applications. The phenomena and numerical difficulties in complex flows have led to new problems for numerical methods, e.g. Yea, Mittala, Udaykumar and Shyy [64] and Mahesha, Constantinescu and Moin [65].

Critically for the present study, fluctuating viscosity problems arise when various eddy viscosity models are used for turbulent natural convection. Given the importance of these applications with highly fluctuating viscosity and the high impact it has on our main objective of studying the predictability of average temperature of turbulent Natural Convection models, we consider as a first step the Navier-Stokes equations with variable viscosity $\nu(x,t)$, which, step by step, will lead to the turbulent Natural Convection problem with variable Prandtl number and heat conductivity.. High fluctuations of $\nu(x,t)$ give difficulties for linear and nonlinear system solvers when using implicit time discretizations. In numerical studies of these flows, the focus has been primarily on using existing space-time discretization and

adapting the solvers used to variable $\nu = \nu(x, t, \cdots)$, e.g. John, Kaiser and Novo [44], Ervin and Heuer [49], Tromperta and Hansena [51]. In this chapter, we study a complementary approach in which the space-time discretization is itself adapted to variable $\nu(x, t)$ so that the linear systems that occur are the same as those in the common case of constant ν.

Herein we assume the viscosity $\nu(x, t)$ is known explicitly. This is not an algorithmic restriction since if $\nu(x, t)$ depends on unknowns calculated from other equations, or is extrapolated from previous time steps, it appears algorithmically in the NSE at t^{n+1} as a known but fluctuating $\nu(x, t)$. Thus, the case of known but fluctuating $\nu(x, t)$ is a simplification capturing one challenging computational aspect of a problem occurring in the applications above.

Given a function f representing external forces, we therefore consider the problem of finding $(u, p) \in (X, Q)$ such that

$$\begin{aligned} u_t + u \cdot \nabla u - \nu \Delta u - \nabla \cdot (\nu(x,t) \nabla u) + \nabla p = f, \text{ in } \Omega \times (0, T], \\ u(x, 0) = u_0(x), \text{ in } \Omega \text{ and } u = 0, \text{ on } \partial\Omega \\ \nabla \cdot u = 0, \text{ in } \Omega \times (0, T]. \end{aligned} \tag{3.1}$$

Let u_h be the discrete solution and, with time step Δt and $t^n = n\Delta t$, $u_h^n = u_h(t^n)$. We approach (3.1) by treating $\nu(x, t)$ as a constant at each time level and correct for it at the previous time level.

Remark 1. *The correct model in (3.1) is in terms of ∇^s instead of ∇. The mathematical results of (3.1) that follow extend to the model with ∇^s, due to Korn's inequality.*

Definition 4. *Let the maximal fixed value of $\nu(x, t)$ at the time level n be*

$$\nu_{max}^n = \sup_x \nu(x, t^n),$$

the fluctuation of the viscosity be

$$\nu'^n := \nu_{max}^n - \nu(x, t^n) \geq 0,$$

the linear extrapolation to t^{n+1} is denoted by

$$y^{*n+1} := 2y^n - y^{n-1},$$

and

$$\nu_+'^{*n+1}(x) := \max\{2\nu'^n(x) - \nu'^{n-1}(x), 0\}.$$

Suppressing the spatial discretization, we develop respectively the following first and nearly second-order methods for advancing in time.

Method 1:

$$
\begin{aligned}
&(\nabla \cdot u_h, q_h) = 0 \text{ and} \\
&\frac{u^{n+1}-u^n}{\Delta t} + u^n \cdot \nabla u^{n+1} - \nu \Delta u^{n+1} + \nabla p^{n+1} - \nabla \cdot (\nu^n_{max} \nabla u^{n+1}) \\
&\qquad = f^{n+1} - \nabla \cdot (\sqrt{\nu'^{n-1}} \sqrt{\nu'^n} \nabla u^n)
\end{aligned} \tag{3.2}
$$

Method 2 (second order except for treatment of ν'):

$$
\begin{aligned}
&(\nabla \cdot u_h, q_h) = 0 \text{ and} \\
&\frac{\frac{3}{2}u^{n+1} - 2u^n + \frac{1}{2}u^{n-1}}{\Delta t} + u^{*n+1} \cdot \nabla u^{n+1} - \nu \Delta u^{n+1} + \nabla p^{n+1} \\
&- \nabla \cdot \left(\nu^{*n+1} \nabla u^{n+1}\right) = f^{n+1} - \nabla \cdot \left(\sqrt{\nu'^{*n+1} \nu'^n} \nabla u^n\right).
\end{aligned} \tag{3.3}
$$

When $\nu'(x,t)$ arises from physical parametrizations of unresolved processes, it is expected to be small and tends to zero as Δx and Δt approach zero. Thus, Method 2 gives a second order treatment of large terms and, in this case, first order of small terms. In this sense, Method 2 is nearly second order. In Section 2, the unconditional stability of Methods 1 and 2, discretized in space by the finite element method, is proven. The error of Method 1 is analyzed in Section 3. (The error analysis of Method 2 is skipped since it is a combination of its stability proof in Section 3 and the error analysis of Method 1.) Finally, results from three numerical experiments are presented in Section 4 that support the theory.

Remark 2. *The existence of an unconditionally stable, fully second order method with the above properties is an open problem.*

The corresponding first and nearly second-order methods, respectively, are the following: for any $v_h \in X_h,\ q_h \in Q_h$, find $u_h \in X_h,\ p_h \in Q_h$ such that

Method 1:

$$
\begin{aligned}
&\left(\frac{u_h^{n+1}-u_h^n}{\Delta t}, v_h\right) + (u_h^n \cdot \nabla u_h^{n+1}, v_h) + (\nu \nabla u_h^{n+1}, \nabla v_h) + (\nabla p_h^{n+1}, v_h) \\
&\qquad + (\nu^n_{max} \nabla u_h^{n+1}, \nabla v_h) = (f^{n+1}, v_h) + \left(\sqrt{\nu'^{n-1}} \sqrt{\nu'^n} \nabla u_h^n, \nabla v_h\right),
\end{aligned} \tag{3.4}
$$

Method 2:

$$\left(\frac{\frac{3}{2}u_h^{n+1}-2u_h^n+\frac{1}{2}u_h^{n-1}}{\Delta t},v_h\right)+(\nu\nabla u_h^{n+1},\nabla v_h)+(u_h^{*n+1}\cdot\nabla u_h^{n+1},v_h) \tag{3.5}$$
$$+\int_\Omega \nu^{*n+1}\nabla u_h^{n+1}\cdot\nabla v_h\,dx-\int_\Omega\sqrt{\nu'^{*n+1}\nu'^n}\nabla u_h^n\cdot\nabla v_h\,dx=(f^{n+1},v_h).$$

3.1 STABILITY

In this section, we prove stability results for Methods 1 and 2.

3.1.1 Method 1

We now prove a discrete energy equality and, by corollary, unconditional stability for Method 1.

Proposition 1. *Discrete Energy Equality: Assuming that the velocity $u_h \in V_h$ at every time step, the numerical scheme in (3.4) is unconditionally stable and satisfies*

$$\begin{aligned}\frac{1}{2}\|u_h^{N+1}\|^2+\frac{1}{2}\sum_{n=1}^N\|u_h^{n+1}-u_h^n\|^2+\nu\Delta t\sum_{n=1}^N\|\nabla u_h^{n+1}\|^2\\ +\Delta t\sum_{n=1}^N\int_\Omega\nu(u_h^n)\left|\nabla u_h^{n+1}\right|^2dx+\Delta t\int_\Omega\nu'^N\left|\nabla u_h^{N+1}\right|^2dx\\ +\frac{\Delta t}{2}\sum_{n=1}^N\|\sqrt{\nu'^n}\nabla u_h^{n+1}-\sqrt{\nu'^{n-1}}\nabla u_h^n\|^2\\ =\frac{1}{2}\|u_h^1\|^2+\Delta t\int_\Omega\nu'^0|\nabla u_h^1|^2+\Delta t\sum_{n=1}^N\left(f^{n+1},u_h^{n+1}\right).\end{aligned}$$

Proof. The key step in this proof is the Polarization Identity applied to $(\sqrt{\nu'^{n-1}}\nabla u_h^n,\sqrt{\nu'^n}\nabla u_h^{n+1})$, leading to a telescoping series, where all terms, with the exception of the first and last, will cancel. We begin by taking the inner product of (3.4) with u_h^{n+1} and using the skew- symmmetrized form of the nonlinear term, yielding

$$\begin{aligned}\left(\frac{u_h^{n+1}-u_h^n}{\Delta t},u_h^{n+1}\right)+\nu\left(\nabla u_h^{n+1},\nabla u_h^{n+1}\right)+\left(\nu_{max}^n\nabla u_h^{n+1},\nabla u_h^{n+1}\right)\\ =\left(f^{n+1},u_h^{n+1}\right)+\left(\sqrt{\nu'^{n-1}}\sqrt{\nu'^n}\nabla u_h^n,\nabla u_h^{n+1}\right).\end{aligned}$$

By definition, $v_{max}^n = \nu'^n + \nu(x,t^n)$. Then, the equation above becomes

$$\left(\frac{u_h^{n+1}-u_h^n}{\Delta t}, u_h^{n+1}\right) + \nu\|\nabla u_h^{n+1}\|^2 + \left(\nu(x,t^n)\nabla u_h^{n+1}, \nabla u_h^{n+1}\right)$$
$$+ \left(\nu'^n \nabla u_h^{n+1}, \nabla u_h^{n+1}\right) - \left(\sqrt{\nu'^{n-1}}\nabla u_h^n, \sqrt{\nu'^n}\nabla u_h^{n+1}\right) = \left(f^{n+1}, u_h^{n+1}\right).$$

Using

$$(\sqrt{\nu'^{n-1}}\nabla u_h^n, \sqrt{\nu'^n}\nabla u_h^{n+1}) = \frac{1}{2}\int_\Omega \left(\nu'^n|\nabla u_h^{n+1}|^2 - \nu'^{n-1}|\nabla u_h^n|^2\right) dx$$
$$+ \frac{1}{2}\|\sqrt{\nu'^n}\nabla u_h^{n+1} - \sqrt{\nu'^{n-1}}\nabla u_h^n\|^2,$$

and the Polarization Identity on (u_h^n, u_h^{n+1}) yield

$$\frac{\|u_h^{n+1}\|^2}{\Delta t} - \frac{1}{\Delta t}\left(\frac{1}{2}\|u_h^n\|^2 + \frac{1}{2}\|u_h^{n+1}\|^2 - \frac{1}{2}\|u_h^{n+1}-u_h^n\|^2\right) + \nu\|\nabla u_h^{n+1}\|^2$$
$$+ \int_\Omega \nu(x,t^n)\left|\nabla u_h^{n+1}\right|^2 dx + \frac{1}{2}\int_\Omega \left(\nu'^n|\nabla u_h^{n+1}|^2 - \nu'^{n-1}|\nabla u_h^n|^2\right) dx$$
$$+ \frac{1}{2}\|\sqrt{\nu'^n}\nabla u_h^{n+1} - \sqrt{\nu'^{n-1}}\nabla u_h^n\|^2$$
$$= \frac{1}{2\Delta t}\|u_h^{n+1}\|^2 - \frac{1}{2\Delta t}\|u_h^n\|^2 + \frac{1}{2\Delta t}\|u_h^{n+1}-u_h^n\|^2 + \nu\|\nabla u_h^{n+1}\|^2$$
$$+ \int_\Omega \nu(x,t^n)\left|\nabla u_h^{n+1}\right|^2 dx + \frac{1}{2}\int_\Omega \left(\nu'^n|\nabla u_h^{n+1}|^2 - \nu'^{n-1}|\nabla u_h^n|^2\right) dx$$
$$+ \frac{1}{2}\|\sqrt{\nu'^n}\nabla u_h^{n+1} - \sqrt{\nu'^{n-1}}\nabla u_h^n\|^2 = \left(f^{n+1}, u_h^{n+1}\right).$$

Multiplying by Δt and summing from 1 to N prove unconditional stability. □

Next, we state a stability inequality relevant to Method 1, that puts all the unknowns on the left hand side.

Corollary 1. *Unconditional Stability: The following inequality holds:*

$$\frac{1}{2}\|u_h^{N+1}\|^2 + \frac{1}{2}\sum_{n=1}^N \|u_h^{n+1}-u_h^n\|^2 + \frac{\nu}{2}\Delta t\sum_{n=1}^N \|\nabla u_h^{n+1}\|^2$$
$$+ \Delta t\int_\Omega \sum_{n=1}^N \nu(u_h^n)\left|\nabla u_h^{n+1}\right|^2 dx + \Delta t\int_\Omega \nu'^N\left|\nabla u_h^{N+1}\right|^2 dx$$
$$+ \frac{\Delta t}{2}\sum_{n=1}^N \|\sqrt{\nu'^n}\nabla u_h^{n+1} - \sqrt{\nu'^{n-1}}\nabla u_h^n\|^2$$
$$\leq \frac{1}{2}\|u_h^1\|^2 + \Delta t\int_\Omega \nu'^0|\nabla u_h^1|^2 + \frac{\Delta t}{2\nu}\sum_{n=1}^N \|f^{n+1}\|_*^2.$$

Proof. The proof follows directly from the stability equality by applying the Cauchy-Schwarz-Young inequality to (f^{n+1}, u_h^{n+1}) with $\varepsilon = \nu$. □

3.1.2 Method 2

Method 2 is a variation of Method 1, and is second-order consistent in most terms, but is only first-order consistent in $\nabla \cdot (\nu(x,t)\nabla u)$. It consists of a combination of BDF2 and AB2, and the above treatment of $\nabla \cdot (\nu(x,t)\nabla u)$. In this subsection, we state and prove a stability result pertaining to the nearly second-order time-stepping method presented in (3.5).

Proposition 2. *Discrete Energy Inequality: Let* $w^n = \sqrt{\nu'^{*n}}\nabla u^n$. *Then, Method 2 is unconditionally stable, and*

$$\begin{aligned}
&\frac{1}{4}\left[||u^N||^2 + ||2u^N - u^{N-1}||^2 + 2\Delta t||w^N||^2\right] + \frac{1}{4}\sum_{n=1}^{N-1}||u^{n+1} - 2u^n + u^{n-1}|| \\
&\quad + \Delta t \sum_{n=1}^{N-1}\left(\frac{\nu}{2}||\nabla u^{n+1}||^2 + ||w^{n+1} - w^n||^2\right) \\
&\quad \leq \frac{1}{4}\left[||u^1||^2 + ||2u^1 - u^0||^2 + 2\Delta t||w^1||^2\right] + \Delta t \sum_{n=1}^{N-1}\frac{1}{2\nu}||f^{n+1}||_*^2.
\end{aligned}$$

Proof. We use the identity

$$\begin{aligned}
\frac{3}{2}||u^{n+1}||^2 - 2(u^n, u^{n+1}) + \frac{1}{2}(u^{n-1}, u^{n+1}) \qquad (3.6)\\
= \frac{1}{4}\left[||u^{n+1}||^2 + ||2u^{n+1} - u^n||^2\right] - \frac{1}{4}\left[||u^n||^2 + ||2u^n - u^{n-1}||^2\right] \\
+ \frac{1}{4}||u^{n+1} - 2u^n + u^{n-1}||^2
\end{aligned}$$

to simplify the left-hand side in (3.5), and use the Polarization Identity on the convenient change-of-variables w^n. Setting $v = u^{n+1}$, and multiplying by Δt gives

$$\begin{aligned}
\frac{3}{2}||u^{n+1}||^2 - 2(u^n, u^{n+1}) + \frac{1}{2}(u^{n-1}, u^{n+1}) \qquad (3.7)\\
+ \Delta t\nu||\nabla u^{n+1}||^2 \\
+ \Delta t\left(\int_\Omega |w^{n+1}|^2 dx - \int_\Omega \left(w^n \cdot w^{n+1}\right) dx\right) \\
= \Delta t(f^{n+1}, u^{n+1}).
\end{aligned}$$

For the first line of (3.7), we employ (3.6). The Polarization Identity applied to the term (w^n, w^{n+1}) yields

$$||w^{n+1}||^2 - (w^n, w^{n+1}) = \frac{1}{2}||w^{n+1}||^2 - \frac{1}{2}||w^n||^2 + \frac{1}{2}||w^{n+1} - w^n||^2.$$

We are left with

$$\begin{aligned}
&\frac{1}{4}||u^{n+1}||^2 + \frac{1}{4}||2u^{n+1} - u^n||^2 + \frac{1}{2}\Delta t||w^{n+1}||^2 \\
&\qquad - \frac{1}{4}\left[||u^n||^2 + ||2u^n - u^{n-1}||^2 + 2\Delta t||w^n||^2\right] \\
&\qquad + \frac{1}{4}||u^{n+1} - 2u^n + u^{n-1}||^2 + \left(\Delta t(\nu||\nabla u^{n+1}||^2 + \frac{1}{2}||w^{n+1} - w^n||^2\right) \\
&\qquad = \Delta t(f^{n+1}, u^{n+1}).
\end{aligned}$$

Summing over N yields

$$\begin{aligned}
&\frac{1}{4}\left[||u^N||^2 + ||2u^N - u^{N-1}||^2 + 2\Delta t||w^N||^2\right] + \frac{1}{4}\sum_{n=1}^{N-1}||u^{n+1} - 2u^n + u^{n-1}|| \\
&\quad + \Delta t\sum_{n=1}^{N-1}\left(\nu||\nabla u^{n+1}||^2 + ||w^{n+1} - w^n||^2\right) \\
&\quad = \frac{1}{4}\left[||u^1||^2 + ||2u^1 - u^0||^2 + 2\Delta t||w^1||^2\right] + \Delta t\sum_{n=1}^{N-1}(f^{n+1}, u^{n+1}) \\
&\quad \leq \frac{1}{4}\left[||u^1||^2 + ||2u^1 - u^0||^2 + 2\Delta t||w^1||^2\right] + \Delta t\sum_{n=1}^{N-1}||f^{n+1}||_*||\nabla u^{n+1}|| \\
&\quad \leq \frac{1}{4}\left[||u^1||^2 + ||2u^1 - u^0||^2 + 2\Delta t||w^1||^2\right] + \Delta t\sum_{n=1}^{N-1}\left(\frac{1}{2\nu}||f^{n+1}||_*^2 + \frac{\nu}{2}||\nabla u^{n+1}||^2\right),
\end{aligned}$$

from which the stability result follows. □

3.2 ERROR ANALYSIS

This section analyzes the error between the exact solution u of (3.1) and the solution of method (3.4)) u_h at every time step. The following few notations will be

Definition 5. *Let U^n to be the Stokes projection of u^n in V^h*

$$(\nabla(u^n - U^n), \nabla v_h) = 0 \text{ for all } v_h \in V^h.$$

Let

$$\eta^n = u^n - U^n, \ \phi^n = u_h^n - U^n$$

and define

$$e^n = \eta^n - \phi^n.$$

Let

$$\nu_{min}^n = \inf_x \nu(x, t^n).$$

Definition 6. *We define the residual $\tau(u^n; v_h)$ by*

$$\tau(u^n; v_h) := \left(\frac{u^{n+1} - u^n}{\Delta t} - u_t(t^{n+1}), v_h\right) + \left((u^n - u^{n+1}) \cdot \nabla u^{n+1}, v_h\right)$$
$$- \left(\nabla \cdot (\nu(x, t^{n+1})\nabla u^{n+1} - \nu_{max}^n \nabla u^n - \sqrt{\nu'^n \nu'^{n-1}}\nabla u^n), v_h\right).$$

In order to bound the error, we first show that it satisfies the following equality.

Proposition 3 (Error equation)**.** *Let e^n be as defined in Chapter 2. Then,*

$$\left(\frac{e^{n+1} - e^n}{\Delta t}, v_h\right) + \left(u^n \cdot \nabla u^{n+1} - u_h^n \cdot \nabla u_h^{n+1}, v_h\right) + \nu\left(\nabla e^{n+1}, \nabla v_h\right)$$
$$+ \left(\nu_{max}^n \nabla e^{n+1}, \nabla v_h\right) - (\sqrt{\nu'^n \nu'^{n-1}}\nabla e^n, \nabla v_h) = (p^{n+1} - p_h^{n+1}, \nabla \cdot v_h) + \tau(u^n; v_h),$$

Proof. This proof takes the inner product of each of (3.1) and (3.4) by $v_h \in X_h$, then makes (3.1) fit into (3.4). Then u^{n+1}, the true solution u at time t^{n+1}, satisfies

$$\begin{aligned}\left(\frac{u^{n+1}-u^n}{\Delta t}, v_h\right) + \left(u^n \cdot \nabla u^{n+1}, v_h\right) + \nu\left(\nabla u^{n+1}, \nabla v_h\right) - \left(p^{n+1}, \nabla \cdot v_h\right) \\ + \left(\nu^n_{max}\nabla u^{n+1}, \nabla v_h\right) - \left(\sqrt{\nu'^n \nu'^{n-1}}\nabla u^n), \nabla v_h\right) \\ = \left(f^{n+1}, v_h\right) + \tau(u^n; v_h).\end{aligned}$$

Subtracting the above form from the fully discrete finite element method in (3.4) and letting $e^n = u^n - u^n_h$ yields the desired error equation. □

The error analysis continues by bounding the error e^n by known terms. The error equation splits into terms involving ϕ^n on the left-hand side and terms involving η^n on the right-hand side. The inner product with ϕ^{n+1} is then taken and the Cauchy-Schwarz-Young inequality is applied successively to bound the right-hand side.

$$\begin{aligned}\left(u^n \cdot \nabla u^{n+1}, v_h\right) - \left(u^n_h \cdot \nabla u^{n+1}_h, v_h\right) &= \left(e^n \cdot \nabla u^{n+1}, v_h\right) + \left(u^n_h \cdot \nabla e^{n+1}, v_h\right) \\ &= b(e^n, u^{n+1}, v_h) + b(u^n_h, e^{n+1}, v_h).\end{aligned}$$

Let $q \in Q^h$ and set $v_h = \phi^{n+1}$. Plugging the above form into the error equation yields

$$\begin{aligned}&(\phi^{n+1} - \phi^n, \phi^{n+1}) + \Delta t(\nu + \nu^n_{max})\|\nabla\phi^{n+1}\|^2 = (\eta^{n+1} - \eta^n, \phi^{n+1}) \\ &+ \Delta t(\eta^n \cdot \nabla u^{n+1}, \phi^{n+1}) + \Delta t(u^n_h \cdot \nabla \eta^{n+1}, \phi^{n+1}) - \Delta t(\phi^n \cdot \nabla u^{n+1}, \phi^{n+1}) \\ &- \Delta t(p^{n+1} - q, \nabla \cdot \phi^{n+1}) + \Delta t(\sqrt{\nu'^n \nu'^{n-1}}\nabla\phi^n, \nabla\phi^{n+1}) - \Delta t\tau(u^n; \phi^{n+1}).\end{aligned}$$

Each of the terms in the right-hand side is bounded using the Cauchy-Schwartz-Young inequality, from which the term $\frac{\Delta t(\nu+\nu^n_{min})}{24}\|\nabla\phi^{n+1}\|^2$ appears.
$\Delta t(\sqrt{\nu'^n \nu'^{n-1}}\nabla\phi^n, \nabla\phi^{n+1})$ is written as follows:

$$\Delta t(\sqrt{\nu'^n\nu'^{n-1}}\nabla\phi^n,\nabla\phi^{n+1}) = \Delta t(\sqrt{\nu'^{n-1}}\nabla\phi^n,\sqrt{\nu'^n}\nabla\phi^{n+1})$$
$$= \frac{\Delta t}{2}\left((\nu'^n\nabla\phi^{n+1},\nabla\phi^{n+1}) + (\nu'^{n-1}\nabla\phi^n,\nabla\phi^n)\right)$$
$$- \frac{\Delta t}{2}\|\sqrt{\nu'^n}\nabla\phi^{n+1} - \sqrt{\nu'^{n-1}}\nabla\phi^n\|^2.$$

Note that ν^n_{max} is space-independent; and thus the above right-hand side can be moved to the left-hand side.

Next, we bound the consistency error.

Lemma 2. *The consistency error $\tau(u^n;\phi^{n+1})$ satisfies*

$$\Delta t\tau(u^n,\phi^{n+1}) \le \frac{\Delta t(\nu+\nu^n_{min})}{8}\|\nabla\phi^{n+1}\|^2 + \frac{C(\Delta t)^3}{8(\nu+\nu^n_{min})}\left(\|u_{tt}\|^2_* + \|u_t\|^2_\infty\right)$$
$$+ \frac{12(\Delta t)^3}{\nu+\nu^n_{min}}(\|u_t\|_\infty + \|\nu_t(x,t)\|_\infty)^2.$$

Proof. The main idea of the proof is to write all the terms at the time level t^{n+1} using the integral form of Taylor's Theorem, then apply the Cauchy-Schwartz-Young inequality to separate $\|\nabla\phi^{n+2}\|^2$ from the other terms. For $t\in(t^n,t^{n+1})$,

$$\Delta t\left(\frac{u^{n+1}-u^n}{\Delta t} - u_t(t^{n+1}),\phi^{n+1}\right) \le \Delta t\|\frac{u^{n+1}-u^n}{\Delta t} - u_t(t^{n+1})\|_*\|\nabla\phi^{n+1}\|$$
$$\le \frac{\Delta t(\nu+\nu^n_{min})}{24}\|\nabla\phi^{n+1}\|^2 + \frac{(6\Delta t)^3}{\nu+\nu^n_{min}}\|u_{tt}(t)\|^2_*.$$

Assuming $\|\nabla u(x,t)\|\le C<\infty$, and using, for $t\in(t^n,t^{n+1})$

$$\|u^n-u^{n+1}\|_\infty = \|\int_{t^{n+1}}^{t^n} u_t(t)dt\|_\infty \le \Delta t\|u_t(t)\|_\infty,$$

yields

$$\Delta t\left((u^n-u^{n+1})\cdot\nabla u^{n+1},\phi^{n+1}\right) \le \frac{\Delta t(\nu+\nu^n_{min})}{24}\|\nabla\phi^{n+1}\|^2 + \frac{6C^2(\Delta t)^3}{\nu+\nu^n_{min}}\|u_t(t)\|^2_\infty.$$

The integral form of Taylor's Theorem and the Cauchy-Schwartz-Young inequality yield

$$\Delta t\left(\nabla\cdot(\nu(x,t^{n+1})\nabla u^{n+1} - \nu^n_{max}\nabla u^n - \sqrt{\nu'^n\nu'^{n-1}}\nabla u^n),\phi^{n+1}\right)$$
$$\le \frac{\Delta t(\nu+\nu^n_{min})}{24}\|\nabla\phi^{n+1}\|^2 + \frac{12(\Delta t)^3}{\nu+\nu^n_{min}}\|\nabla u^{n+1}\|^2(\|\frac{\partial u}{\partial t}\|_\infty + \|\frac{\partial\nu}{\partial t}\|_\infty)^2.$$

Gathering the above bounds on $\Delta t\tau(u^n,\phi^{n+1})$ proves the result ∎

Using the Polarization Identity on $(\phi^{n+1}-\phi^n,\phi^{n+1})$ and combining all bounds yields

$$\begin{aligned}
&\frac{1}{2}(\|\phi^{n+1}\|^2-\|\phi^n\|^2)+\frac{1}{2}\|\phi^{n+1}-\phi^n\|^2+\Delta t\nu^n_{max}\|\nabla\phi^{n+1}\|^2-\frac{\Delta t}{2}\nu^{n-1}_{max}\|\nabla\phi^n\|^2\\
&+\frac{2\Delta t(\nu+\nu^n_{min})}{3}\|\nabla\phi^{n+1}\|^2+(\nu(x,t^n)\nabla\phi^{n+1},\nabla\phi^{n+1})\\
&+(\nu(x,t^{n-1})\nabla\phi^n,\nabla\phi^n)+\frac{\Delta t}{2}\|\sqrt{\nu'^n}\nabla\phi^{n+1}-\sqrt{\nu'^{n-1}}\nabla\phi^n\|^2\\
&\leq\frac{6}{\Delta t(\nu+\nu^n_{min})}(\|\eta^{n+1}\|_*+\|\eta^n\|_*)^2+\frac{C\Delta t}{\nu+\nu^n_{min}}\|\eta^n\|\|\nabla\eta^n\|\|\nabla u^{n+1}\|^2\\
&+\frac{C\Delta t}{\nu+\nu^n_{min}}(\|u^n_h\|\|\nabla u^n_h\|\|\nabla\eta^{n+1}\|^2+\|\phi^n\|\|\nabla\phi^n\|\|\nabla u^{n+1}\|^2+\|p^{n+1}-q\|^2)\\
&+\frac{C(\Delta t)^3}{8(\nu+\nu^n_{min})}\left(\|u_{tt}\|^2_*+\|u_t\|^2_\infty\right)+\frac{12(\Delta t)^3}{\nu+\nu^n_{min}}(\|u_t\|_\infty+\|\nu_t(x,t)\|_\infty)^2.
\end{aligned}$$

The term $\frac{\Delta t\nu^{n-1}_{max}}{2}\|\nabla\phi^n\|^2$ arising from the Cauchy-Schwartz-Young inequality applied to $\frac{C\Delta t}{\nu+\nu^n_{min}}\|\nabla u^{n+1}\|^2\|\nabla\phi^n\|\|\phi^n\|$ can be hidden on the left-hand side. Summing from $n=1$ to $n=N$ yields

$$\begin{aligned}
&\frac{1}{2}\|\phi^{N+1}\|^2+\Delta t\nu^N_{max}\|\nabla\phi^{N+1}\|^2+\sum_{n=1}^N\frac{1}{2}\|\phi^{n+1}-\phi^n\|^2\\
&+\sum_{n=1}^N\left[\frac{2\Delta t(\nu+\nu^n_{min})}{3}\|\nabla\phi^{n+1}\|^2+\|\sqrt{\nu(x,t^{n-1})}\nabla\phi^n\|^2\right]\\
&+\sum_{n=1}^N\left[(\nu(x,t^n)\nabla\phi^{n+1},\nabla\phi^{n+1})+\frac{\Delta t}{2}\|\sqrt{\nu'^n}\nabla\phi^{n+1}-\sqrt{\nu'^{n-1}}\nabla\phi^n\|^2\right]\\
&\leq\frac{1}{2}\|\phi^1\|^2+\nu^0\|\nabla\phi^1\|^2+\sum_{n=1}^N\frac{6}{\Delta t(\nu+\nu^n_{min})}(\|\eta^{n+1}\|_*+\|\eta^n\|_*)^2\\
&+\sum_{n=1}^N\frac{C\Delta t}{\nu+\nu^n_{min}}\|p^{n+1}-q\|^2+\sum_{n=1}^N\frac{C\Delta t}{\nu+\nu^n_{min}}\|u^n_h\|\|\nabla u^n_h\|\|\nabla\eta^{n+1}\|^2\\
&+\sum_{n=1}^N\frac{C\Delta t}{\nu+\nu^n_{min}}\|\eta^n\|\|\nabla\eta^n\|\|\nabla u^{n+1}\|^2+\sum_{n=1}^N\frac{\Delta tC^2}{2\nu^{n-1}_{max}(\nu+\nu^n_{min})^2}\|\nabla u^{n+1}\|^4\|\phi^n\|^2\\
&+\sum_{n=1}^N\frac{C(\Delta t)^3}{8(\nu+\nu^n_{min})}\left(\|u_{tt}\|^2_*+\|u_t\|^2_\infty\right)+\sum_{n=1}^N\frac{12(\Delta t)^3}{\nu+\nu^n_{min}}(\|u_t\|_\infty+\|\nu_t(x,t)\|_\infty)^2,
\end{aligned}$$

giving the desired result.

The error analysis continues by estimating the terms on the right-hand side of the result above. Using the Approximation Assumptions,

$$\begin{aligned}\sum_{n=1}^{N}\frac{6}{\Delta t(\nu+\nu_{min}^{n})}(\|\eta^{n+1}\|_{*}+\|\eta^{n}\|_{*})^{2} &\leq \frac{C}{\Delta t}\sum_{n=1}^{N}\frac{1}{\nu+\nu_{min}^{n}}h^{2k+2}|u^{n+1}|_{k+1}^{2}\\ &\leq \frac{C}{\Delta t}h^{2k+2}\|u\|_{l^{2}(H^{k+1})}^{2}\sum_{n=1}^{N}\frac{1}{\nu+\nu_{min}^{n}}.\end{aligned}$$

Using the Approximation Assumptions and the fact that $\nu_{min}^{n}\geq 0$,

$$\begin{aligned}\sum_{n=1}^{N}\frac{C\Delta t}{\nu+\nu_{min}^{n}}\|\eta^{n}\|\|\nabla\eta^{n}\|\|\nabla u^{n+1}\|^{2} &\leq \sum_{n=1}^{N}\frac{C\Delta t}{\nu+\nu_{min}^{n}}h^{k+1}|u^{n}|_{k+1}h^{k}|u^{n}|_{k+1}\|\nabla u^{n+1}\|^{2}\\ &\leq C\Delta t h^{2k+1}\sum_{n=1}^{N}\frac{1}{\nu+\nu_{min}^{n}}|u^{n}|_{k+1}^{2}\|\nabla u^{n+1}\|^{2}\\ &\leq \frac{C\Delta t}{\nu}h^{2k+1}\left(\sum_{n=1}^{N}|u^{n}|_{k+1}^{4}+\sum_{n=1}^{N}\|\nabla u^{n+1}\|^{4}\right)\\ &\leq \frac{C\Delta t}{\nu}h^{2k+1}\left(\|u\|_{l^{4}(H^{k+1})}^{4}+\|\nabla u\|_{l^{4}(H^{0})}^{4}\right).\end{aligned}$$

Using the *a priori* estimate for $\|u_{h}^{n}\|$ in the stability analysis and the fact that $\nu_{min}^{n}\geq 0$ for any n,

$$\begin{aligned}\sum_{n=1}^{N}\frac{C\Delta t}{\nu+\nu_{min}^{n}}\|u_{h}^{n}\|\|\nabla u_{h}^{n}\|\|\nabla\eta^{n+1}\|^{2} &\leq \frac{C\Delta t}{\nu}\sum_{n=1}^{N}\|\nabla u_{h}^{n}\|\|\nabla\eta^{n+1}\|^{2}\\ &\leq \frac{C\Delta t}{\nu}\sum_{n=1}^{N}\|\nabla u_{h}^{n}\||u^{n+1}|_{k+1}^{2}h^{2k}\\ &\leq \frac{C\Delta t}{\nu}h^{2k}\left(\sum_{n=1}^{N}\|\nabla u_{h}^{n}\|^{2}+\sum_{n=1}^{N}|u^{n+1}|_{k+1}^{4}\right)\\ &\leq \frac{C\Delta t}{\nu}h^{2k}\left(\nu^{-1}\|u^{h}\|^{2}+\nu^{-1}\||f|\|_{2,*}^{2}+\|u\|_{l^{4}(H^{k+1})}^{4}\right).\end{aligned}$$

Adding and subtracting terms, using Taylor series expansion and the Approximation Assumptions, the pressure term on the right-hand side is bounded by

$$
\begin{aligned}
6\Delta t\sum_{n=1}^{N}\frac{1}{\nu+\nu_{min}^{n}}\|p^{n+1}-q\|^2 &\leq \frac{C\Delta t}{\nu}\sum_{n=1}^{N}\left(\|p(t^{n+1})-q\|^2+\|p^{n+1}-p(t^{n+1})\|^2\right)\\
&\leq \frac{C}{\nu}\left(h^{2s+2}\Delta t\sum_{n=1}^{N}\|p(t^{n+1})\|_{s+1}^2+\Delta t\sum_{n=1}^{N}C(\Delta t)^3\int_{t^{n-1}}^{t^{n+1}}\|p_{tt}\|^2dt\right)\\
&\leq \frac{C}{\nu}\left(\Delta t h^{2s+2}\|p\|_{2,s+1}^2+(\Delta t)^4\|p_{tt}\|_{2,0}^2\right).
\end{aligned}
$$

Gathering all bounds,

$$
\begin{aligned}
&\frac{1}{2}\|\phi^{N+1}\|^2+\Delta t\nu_{max}^{n}\|\nabla\phi^{N+1}\|^2+\sum_{n=1}^{N}\frac{1}{2}\|\phi^{n+1}-\phi^{n}\|^2\\
&+\sum_{n=1}^{N}\frac{2\Delta t(\nu+\nu_{min}^{n})}{3}\|\nabla\phi^{n+1}\|^2+\sum_{n=1}^{N}\frac{\Delta t}{2}\|\sqrt{\nu'^{n}}\nabla\phi^{n+1}-\sqrt{\nu'^{n-1}}\nabla\phi^{n}\|^2\\
&+\sum_{n=1}^{N}\left[(\nu(x,t^{n})\nabla\phi^{n+1},\nabla\phi^{n+1})+(\nu(x,t^{n-1})\nabla\phi^{n},\nabla\phi^{n})\right]\\
&\leq\frac{1}{2}\|\phi^{1}\|^2+\nu^{0}\|\nabla\phi^{1}\|^2+\frac{C}{\Delta t}h^{2k+2}\|u\|_{l^2(H^{k+1})}^2\sum_{n=1}^{N}\frac{1}{\nu+\nu_{min}^{n}}\\
&+\frac{C}{\nu}\left(\Delta t h^{2s+2}\|p\|_{2,s+1}^2+(\Delta t)^4\|p_{tt}\|_{2,0}^2\right)\\
&+\frac{C\Delta t}{\nu}h^{2k+1}\left(\|u\|_{l^4(H^{k+1})}^4+\|\nabla u\|_{l^4(H^{0})}^4\right)+\sum_{n=1}^{N}\frac{\Delta t C^2}{2\nu_{max}^{n-1}(\nu+\tilde{\nu}^{n})^2}\|\nabla u^{n+1}\|^4\|\phi^{n}\|^2\\
&+\frac{C\Delta t}{\nu}h^{2k}\left(\nu^{-1}\|u^{h}\|^2+\nu^{-1}\|f\|_{l^2(H^{*})}^2+\|u\|_{l^4(H^{k+1})}^4\right)\\
&+\sum_{n=1}^{N}\frac{C(\Delta t)^3}{8(\nu+\nu_{min}^{n})}\left(\|u_{tt}\|_{*}^2+\|u_t\|_{\infty}^2\right)+\sum_{n=1}^{N}\frac{12(\Delta t)^3}{\nu+\nu_{min}^{n}}(\|u_t\|_{\infty}+\|\nu_t(x,t)\|_{\infty})^2.
\end{aligned}
$$

At this point, (2.0.5) is applied and the error estimate follows by using the Triangle Inequality.

3.3 NUMERICAL RESULTS

In this section, we test the stability and accuracy of Methods 1 and 2, using Taylor-Hood elements to approximate the velocity (piecewise continuous quadratic elements) and pressure (piecewise continuous linear elements). The software used for all tests is FreeFem++ [93]. In these tests, $e = u - u_h$ and all errors are relative.

3.3.1 Numerical Test 1

An exact solution, used to test accuracy, to (3.1) is given in [44]. Let

$$\phi(x,t) = 1000x^2(1-x)^4y^3(1-y)^2(1+\cos^2 t).$$

The velocity u and variable viscosity $\nu(x,t)$ are given by

$$u(x,t) = (\partial_y\phi, -\partial_x\phi) \text{ and}$$
$$\nu(x,t) = xy(1+\cos^2 t).$$

We set $\mathrm{Re} = 1000$, $\nu = \frac{1}{\mathrm{Re}}$, and $\Omega = (0,1)^2$. A Delaunay triangulation of Ω generated by 120 points on $\partial\Omega$ is used. The maximum edge length is $h_{\max} = .055131 \approx \frac{1}{30}$. The projected rate of convergence is 3, we choose $\Delta t = O(h_{\max}^3)$.

To isolate the effect of the treatment of $\nu(x,t)$ in Methods 1 and 2 on the total error, we also compute the error using the standard implicit method

Method 3:

$$\begin{aligned}\left(\frac{u^{n+1}-u^n}{\Delta t}, v_h\right) + (u^n\cdot\nabla u^{n+1}, v_h) + \nu(\nabla u^{n+1}, \nabla v_h) + (\nu(x,t^n)\nabla u^{n+1}, \nabla v_h)\\ +(\nabla p^{n+1}, v_h) = (f^{n+1}, v_h)\\ (\nabla\cdot u^{n+1}, q_h) = 0.\end{aligned} \tag{3.8}$$

For this numerical test, Methods 3 and 1 are implemented. Table 1 presents relative errors and rates of convergence for Methods 3 and 1, which are visualized in Figures 1 and 2. For both methods, a convergence rate of 3 is expected, which Methods 3 and 1 satisfy. In addition, both methods reliably give 3 significant digits of error in u and 2 significant digits

in ∇u on the given mesh and time step. We see that the treatment of $\nu(x,t)$ in Method 1 does not contribute appreciably to the velocity error.

	Method 3	Method 1
$\|\|e\|\|_{\infty,0}$	.00022	.00059
$\|\|e\|\|_{2,0}$	.00021	.00033
$\|\|\nabla e\|\|_{\infty,0}$	.0048	.0048
$\|\|\nabla e\|\|_{2,0}$	.0048	.0048
Initial rate	2.98	2.98
Final rate	2.90	2.57
Average rate	2.92	2.79

Table 1: Time stepping methods: Test 1

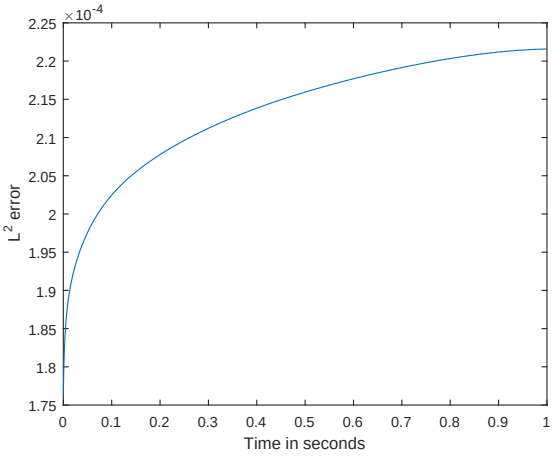

(a) Relative L^2 errors

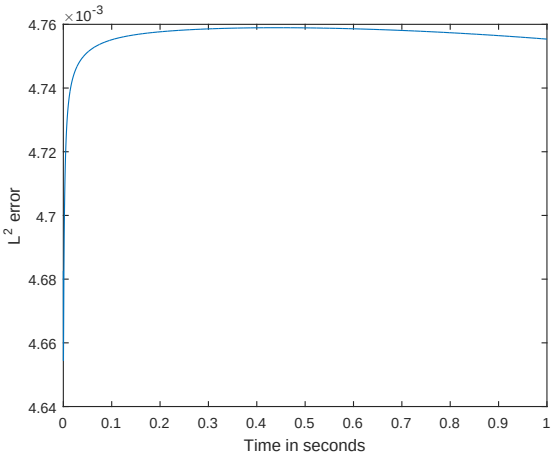

(b) Relative L^2 grad errors

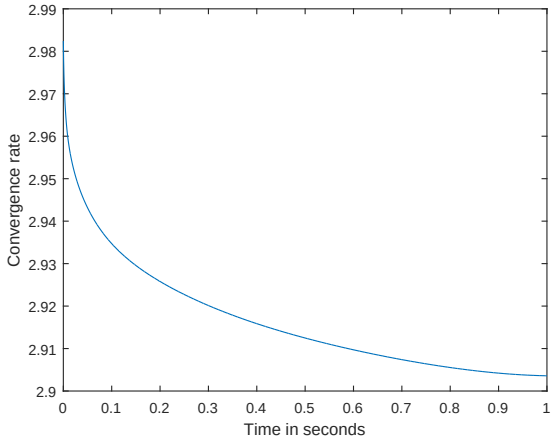

(c) Convergence rates

Figure 1: Test 1: Errors and rates for Method 3.

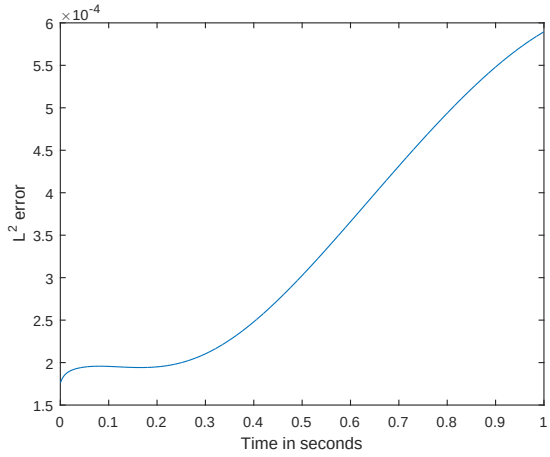

(a) Relative L^2 errors

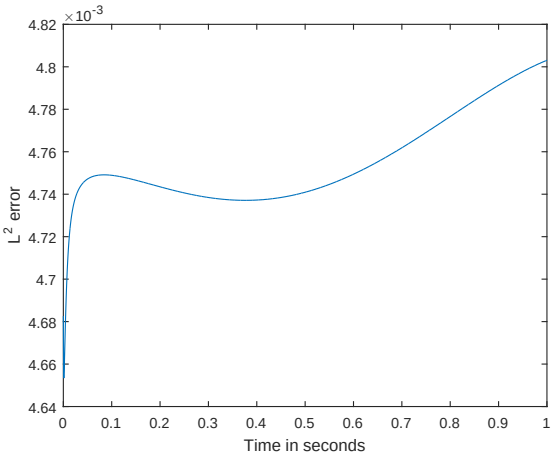

(b) Relative L^2 grad errors

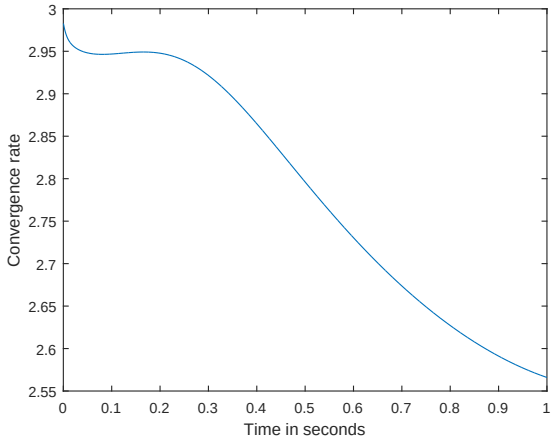

(c) Convergence rates

Figure 2: Test 1: Errors and rates for Method 1

3.3.2 Numerical Test 2: Perturbation of a Power Law for Fluids

For these tests, an exact solution to (3.1) is given by

$$u(x,t) = (1+\cos^2 t)(-4y(1-x^2-y^2),\ 4x(1-x^2-y^2)),$$

for all $x \in \Omega := B(0,1) \subset \mathbb{R}^2$ and $t \in [0,1]$. For the variable viscosity, we use a perturbation of the power law for fluids. Indeed, let $\frac{1}{2}(\nabla u + \nabla u^T)$ be the deformation tensor, $||\cdot||_F$ the Frobenius norm, and

$$s = \left|\left|\frac{1}{2}\left(\nabla u + \nabla u^T\right)\right|\right|_F.$$

We say that a fluid obeys the power law if, given $\alpha \in \mathbb{R}$ and $\frac{1}{r} + \frac{1}{r'} = 1$, then

$$\nu(x,t) = \alpha s^{r-2}.$$

For this test, we let $r = 1$ and $\alpha = 1$. However, the chosen velocity flow u yields a singularity for $\nu(x,t)$ at the origin, so the denominator is regularized to eliminate the singularity, yielding

$$\nu(x,t) = \frac{1}{\frac{1}{2} + s}.$$

As with Test 1, we triangulate Ω via the Delaunay algorithm generated by 40 points around $\partial\Omega$. The maximum edge length is $h := h_{\max} = .24109$. We expect Method 1 to have a convergence rate of 3, so we choose $\Delta t = O(h^3)$ ($\Delta t = \frac{1}{125}$). Table 2 presents relative errors and rates of convergence for Methods 3 and 1, which are visualized in Figures 3 and 4. For both methods, a convergence rate of 3 is expected, which Methods 3 and 1 satisfy. In addition, Method 3 reliably gives 2 significant digits of error in u and 1 significant digit in ∇u on the given mesh and time step, whereas Method 1 gives 1 significant digit in u and ∇u. We see that the treatment of $\nu(x,t)$ in Method 1 does not contribute appreciably to the velocity error. In Figure 5, plots of the approximate solution at $t = 1$, as well as plots of the vorticity are given.

	Method 3	Method 1
$\|\|e\|\|_{\infty,0}$	.0069	.0308
$\|\|e\|\|_{2,0}$	.0077	.0148
$\|\|\nabla e\|\|_{\infty,0}$	.0254	.0541
$\|\|\nabla e\|\|_{2,0}$	.0310	.0365
Initial rate	3.91	3.91
Final rate	3.43	2.40
Average rate	3.43	3.11

Table 2: Perturbation of the power law: errors and rates

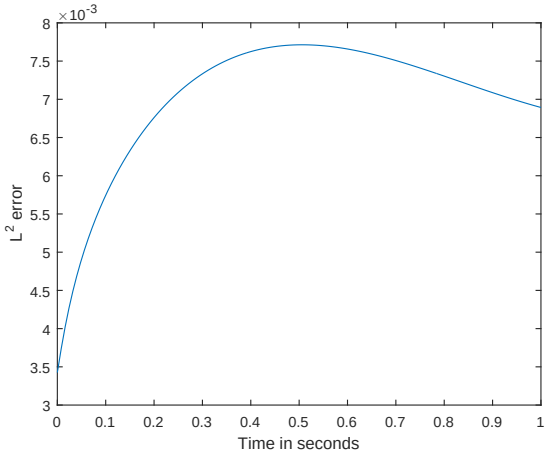

(a) Relative L^2 errors

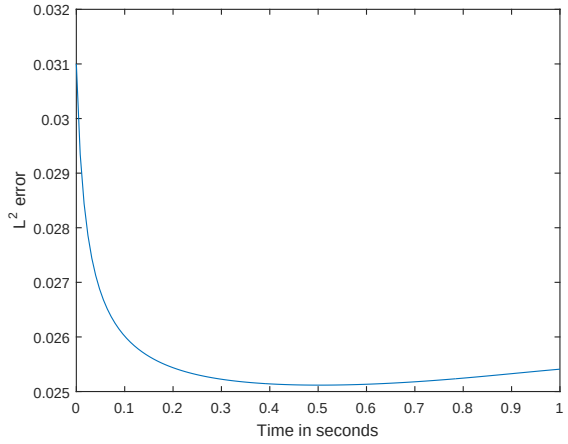

(b) Relative L^2 grad errors

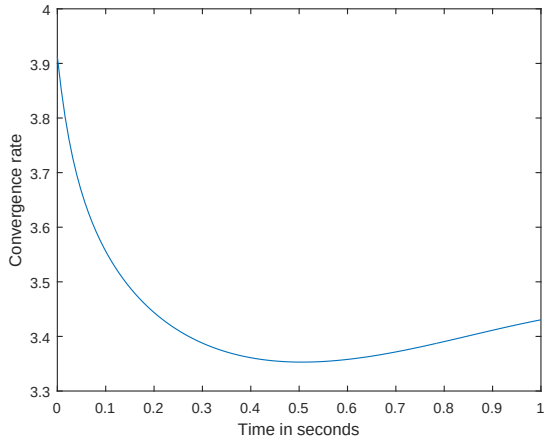

(c) Convergence rates

Figure 3: Test 2: Errors and rates for Method 3.

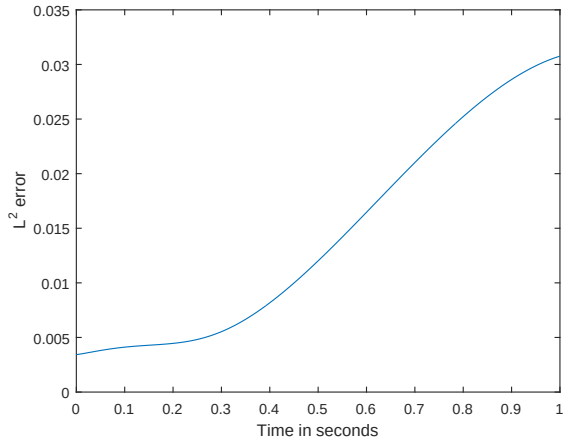

(a) Relative L^2 errors

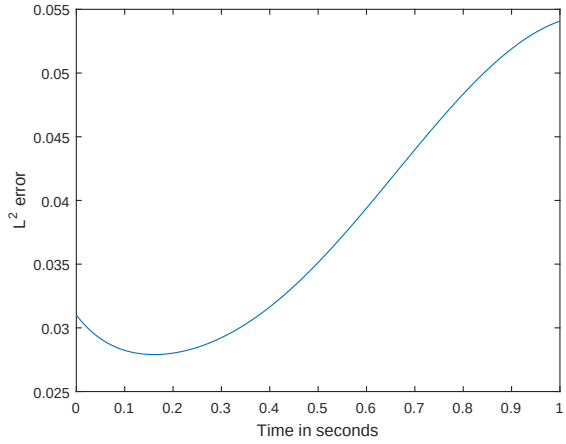

(b) Relative L^2 grad errors

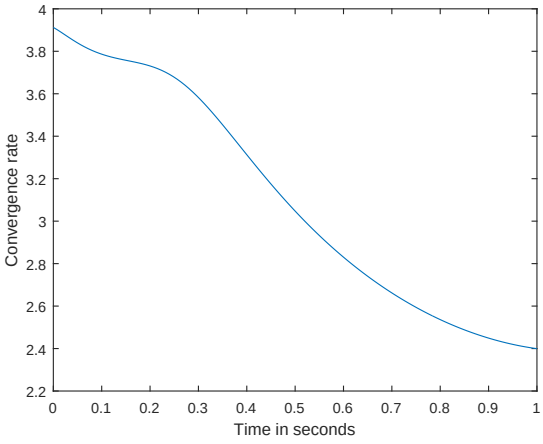

(c) Convergence rates

Figure 4: Test 2: Errors and rates for Method 1.

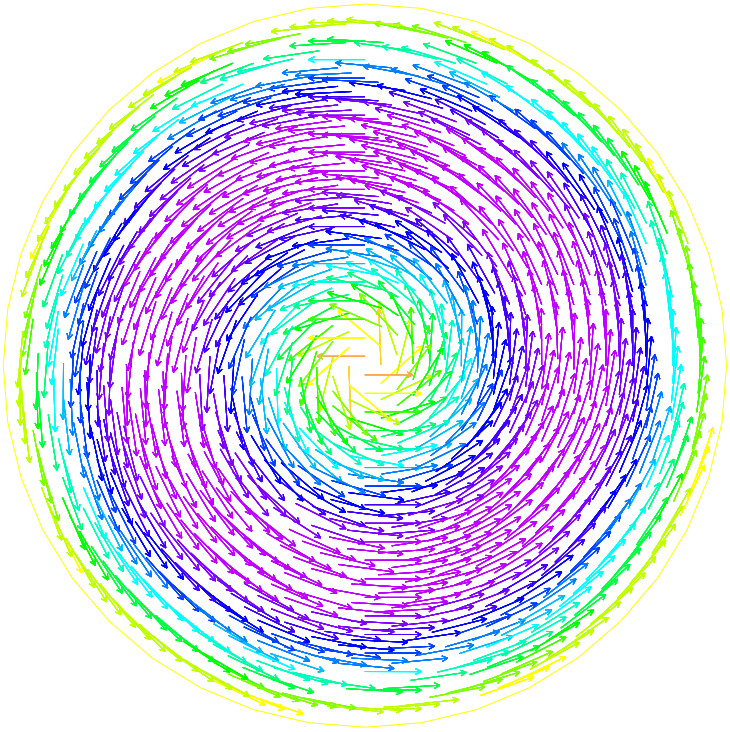

(a) Velocity Flow

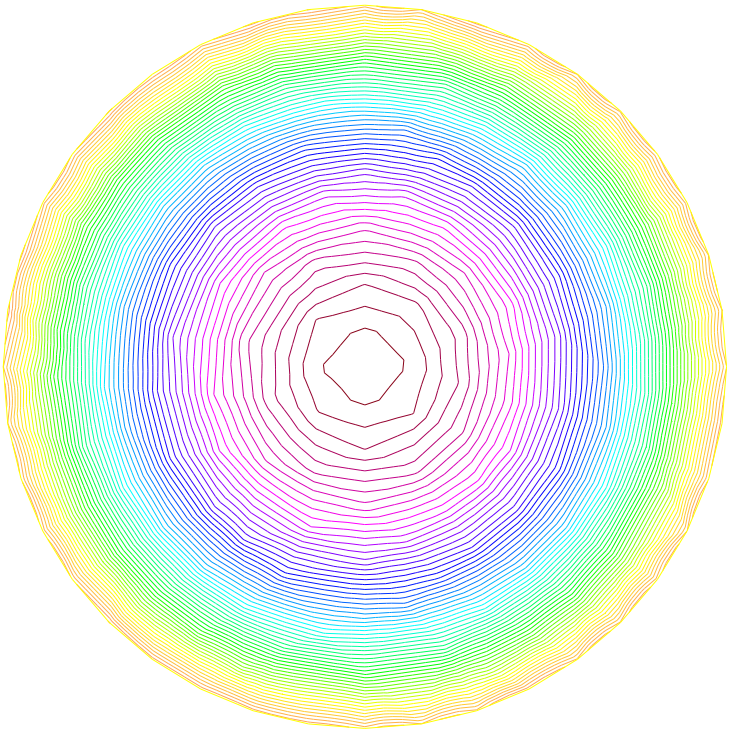

(b) Vorticity

Figure 5: Test 2: Method 1 at $t = 1$.

In Figure 6, we show plots of u and its vorticity on Ω, but with an obstruction located to the right of the origin.

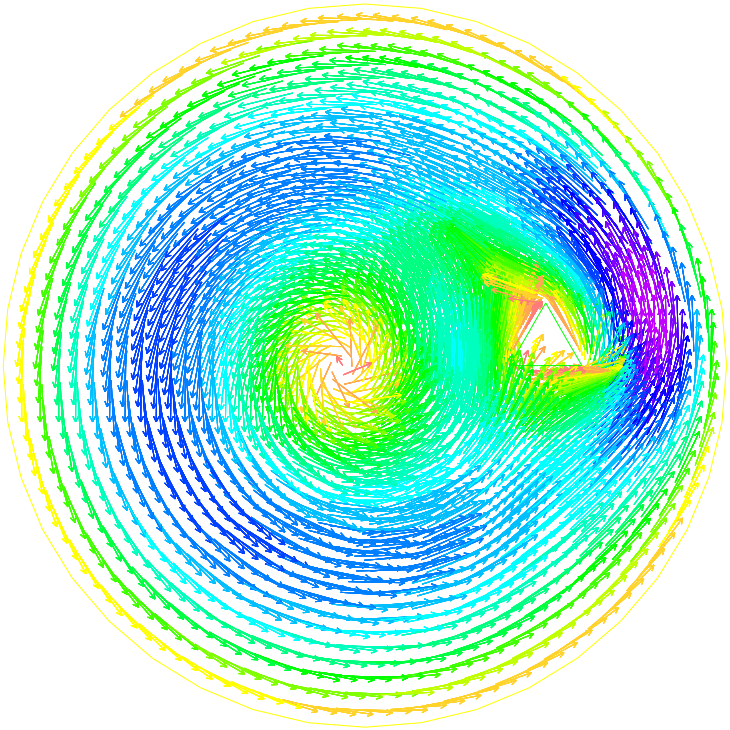

(a) Velocity Flow

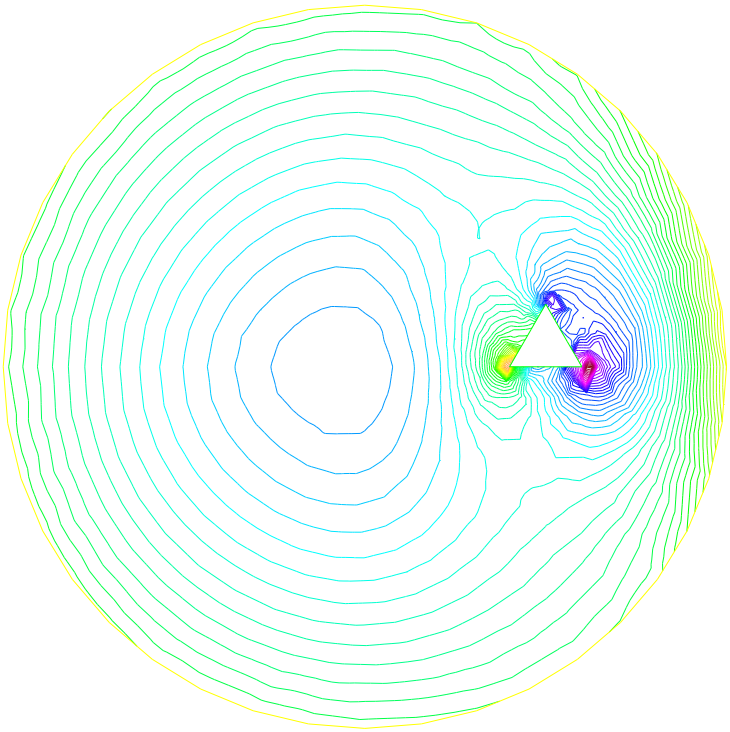

(b) Vorticity

Figure 6: Test 2: Method 1 with an obstruction at $t = 1$.

3.3.3 Numerical Test 3: Method 2

For this test, we approximate (3.1) using Method 2. For consistency, we repeat the experiment used in Test 2. Again, $\Omega = B(0,1) \subset \mathbb{R}^2$, and we triangulate Ω using 40 points on $\partial\Omega$. Again, $h := h_{\max} = .24109$, and we choose $\Delta t = O(h^3)$, specifically $\Delta t = \frac{1}{125}$. Table 3 presents relative errors and rates of convergence for Method 2, which are visualized in Figure 7. For both methods, a convergence rate of 3 is expected, which Method 2 satisfies. In addition, Method 2 reliably gives 1 significant digits of error in both u and ∇u on the given mesh and time step.

	Method 2
$\|\|e\|\|_{\infty,0}$	.0257
$\|\|e\|\|_{2,0}$	.0127
$\|\|\nabla e\|\|_{\infty,0}$	.0525
$\|\|\nabla e\|\|_{2,0}$	.0399
Initial rate	3.91
Final rate	2.52
Average rate	3.16

Table 3: Errors and rates for Method 2.

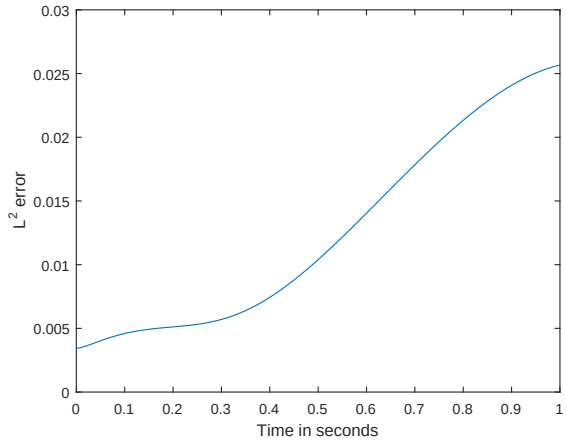

(a) Relative L^2 errors

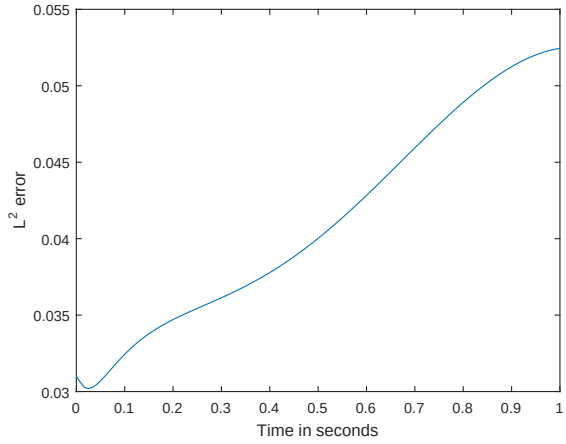

(b) Relative L^2 grad errors

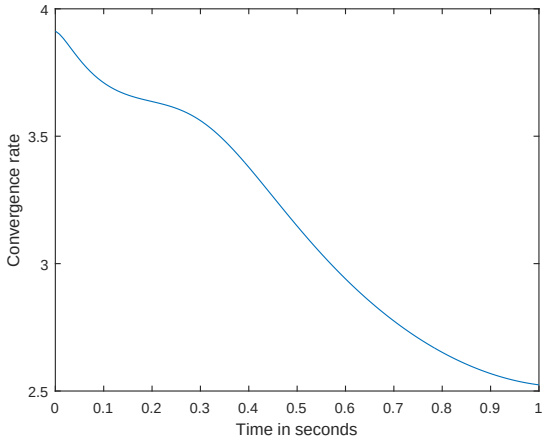

(c) Convergence rates

Figure 7: Test 3: Errors and rates for Method 2.

In Figure 8, plots of the approximate solution at $t = 1$, as well as plots of the vorticity are given.

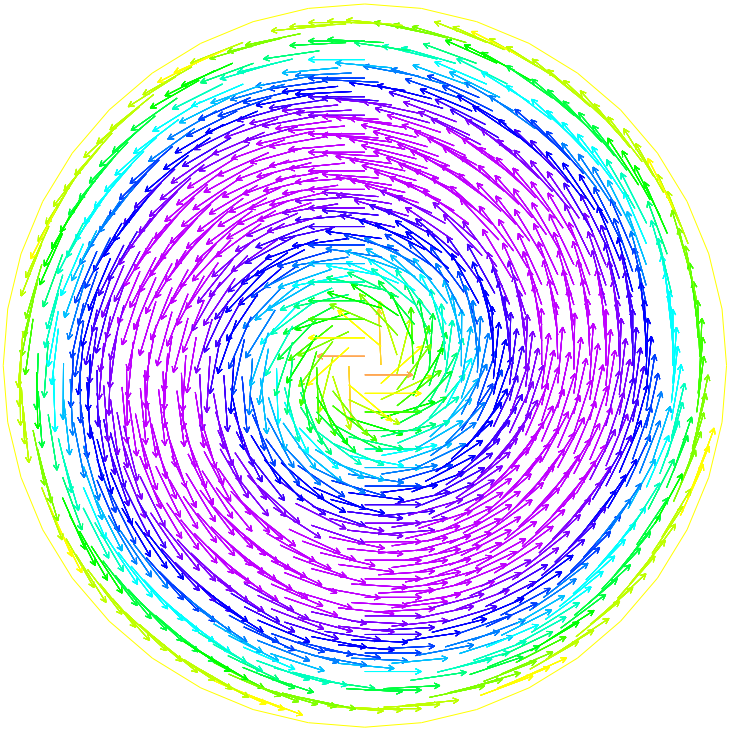

(a) Velocity Flow

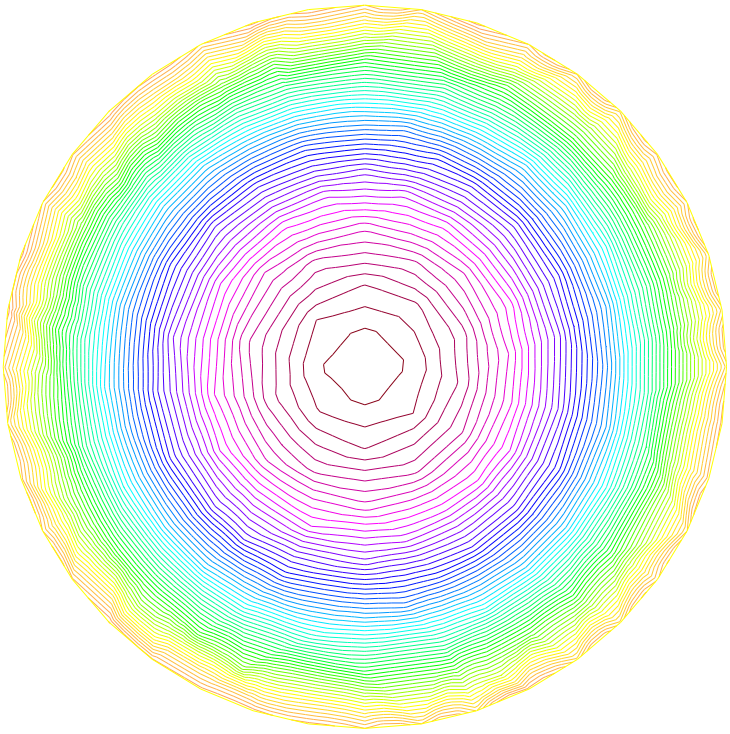

(b) Vorticity

Figure 8: Test 3: Method 2 at $t = 1$

In Figure 9, we show the plots for the velocity flow and vorticity at three different times, using Method 2 on Ω, but with an obstruction to the right of the origin.

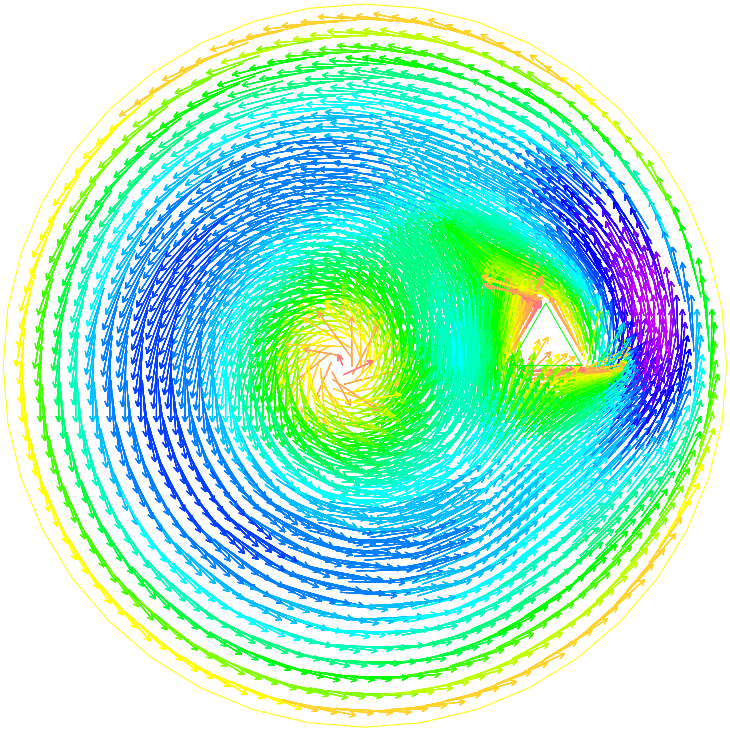

(a) Velocity Flow

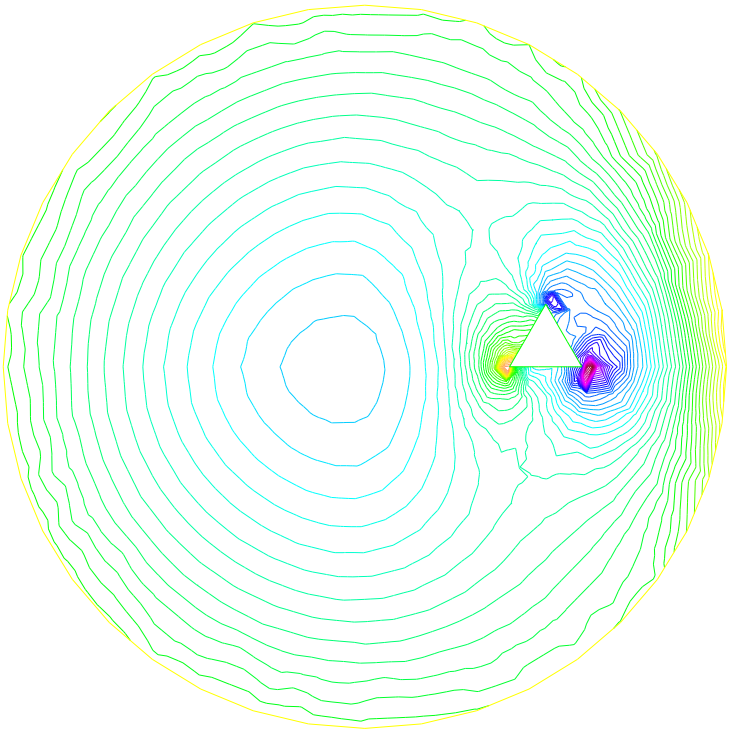

(b) Vorticity

Figure 9: Test 3: Method 2 with an obstruction at $t = 1$.

First and (nearly) second-order time-stepping methods for the Navier-Stokes equations with variable viscosity were developed in this chapter. These methods are unique in that they are adapted specifically to handle the Navier-Stokes equations with variable viscosity. Stability was shown in Section 1 for each of the two methods, and error bounds were derived for the first-order method. We showed in Section 2 that the error depends on the maximum and minimum values attained by the fluctuating viscosity and its derivatives, emphasizing the important influence of the variations of the viscosity on the model. Numerical experiments in Section 3 confirmed the theory. This was the first step in dealing with systems with variable viscosity and will be used in the analysis of the turbulent Natural convection problem.

4.0 ENSEMBLES FOR THE NATURAL CONVECTION PROBLEM

The following chapter is based on a joint work with Joseph Fiordilino and Professor William Layton [32].

Ensemble calculations are useful in the study of chaotic systems, e.g. weather forecasting [9], ocean modeling [13], turbulence [7], etc. Ensemble methods involve, for example, the solution of a system of J equations with J slightly different initial conditions. Flow statistics such as the mean yield superior long-term behavior compared to single realization solves, extending the horizon of predictability and the potential to measure it [9]. Furthermore, the deviation of realizations from one another or from the mean (variance) allows for the quantification of the uncertainty in a prediction, e.g., a high degree of spread indicates that the flow is not easily predicted and, consequently, the accuracy of the ensemble average may be severely compromised.

The benefits of computing ensembles are many, however, the number of realizations computed is in direct competition with the resolution in the simulations. This competition is the motivation for the methods presented herein; that is, our algorithms reduce the storage requirement to compute multiple realizations. In contrast with solving J different matrix equations, our methods reduce the storage necessary by reducing the problem to the solution of a single matrix equation, at each time step, with multiple right hands, which can be solved using block conjugate gradient methods, QMR, etc.

In subsequent sections, we will present two generic natural convection problems that will be the setting for this study. First, we collect and present necessary mathematical tools needed for the study of these problems in the context of finite element method. Then, we present algorithms for calculating an ensemble of solutions to natural convection problems are presented. In particular, we extend the methods of [6] to natural convection problems.

4.1 SCENARIO 1: THICK WALLED CAVITY

Consider the natural convection problem enclosed in a medium with non-zero wall thickness. Let $\Omega_f \subset \Omega$ be polyhedral domains in $\mathbb{R}^d (d = 2, 3)$ with boundaries $\partial\Omega_f$ and $\partial\Omega$, respectively, such that dist($\partial\Omega_f$,$\partial\Omega$) > 0. The boundary $\partial\Omega$ is partitioned such that $\partial\Omega = \Gamma_1 \cup \Gamma_2$ with $\Gamma_1 \cap \Gamma_2 = \emptyset$ and $|\Gamma_2| > 0$. Let $u(x,t) : \Omega \times (0,t^*] \to \mathbb{R}^d$, $p(x,t) : \Omega \times (0,t^*] \to \mathbb{R}$, and $T(x,t) : \Omega \times (0,t^*] \to \mathbb{R}$ satisfy

$$u_t + u \cdot \nabla u - Pr\Delta u + \nabla p = PrRa\gamma T + f \ \ in\ \Omega_f, \tag{4.1}$$

$$\nabla \cdot u = 0 \ \ in\ \Omega_f, \tag{4.2}$$

$$T_t + u \cdot \nabla T - \nabla \cdot (\kappa \nabla T) = g \ \ in\ \Omega, \tag{4.3}$$

$$u(x,0) = u^0(x)\ and\ T(x,0) = T^0(x) \ \ in\ \Omega, \tag{4.4}$$

$$u = 0 \ \ on\ \partial\Omega_f, \ \ u = 0 \ \ in\ \Omega - \Omega_f, \ \ T = 0 \ \ on\ \Gamma_2 \ \ and \ \ n \cdot \nabla T = 0 \ \ on\ \Gamma_1, \tag{4.5}$$

where n denotes the usual outward normal to the pertinent boundary, $\gamma = g/|g|$ denotes the unit vector in the direction of gravity, Pr is the Prandtl number, Ra is the Rayleigh number, and $\kappa = \kappa_f$ in Ω_f is the thermal conductivity of the fluid; all of which are positive constants. Further, f and g are forcing terms dependent on space and time.

Let $J \in \mathbb{N}$ and $j = 1, ..., J$. We now consider J systems of the above equations with J slightly perturbed initial conditions

$$u^0(x,t;\omega_j) \text{ and } T^0(x,t;\omega_j)$$

and body forces

$$f(x,t;\omega_j) \text{ and } g(x,t;\omega_j).$$

Let $u(x,t;\omega_j) : \Omega \times (0,t^*] \to \mathbb{R}^d$, $p_j(x,t;\omega_j) : \Omega \times (0,t^*] \to \mathbb{R}$, and $T_j(x,t;\omega_j) : \Omega \times (0,t^*] \to \mathbb{R}$ satisfy the system (4.1) - (4.1). To make the essential features clearer, we shall suppress the spacial discretization until Section 3.

Definition 7. *We define the average velocity* $< u >^n$ *at each time step* n *by*

$$< u >^n := \frac{1}{J} \sum_{j=1}^{J} u^n \tag{4.6}$$

Applying an implicit-explicit time-discretization, while keeping the coefficient matrix independent of the ensemble members, leads to the following method:

$$\frac{u^{n+1}-u^n}{\Delta t} - Pr\triangle u^{n+1} + < u >^n \cdot\nabla u^{n+1} + (u^n - < u >^n)\cdot\nabla u^n + \nabla p^{n+1} = PrRa\gamma T^{n+1} + f^{n+1}, \quad (4.7)$$

$$\nabla \cdot u^{n+1} = 0, \quad (4.8)$$

$$\frac{T^{n+1}-T^n}{\Delta t} - \kappa\nabla T^{n+1} + < u >^n \cdot\nabla T^{n+1} + (u^n - < u >^n)\cdot\nabla T^n = g^{n+1}, \quad (4.9)$$

Remark 3. *The block linear system for the ensemble problem above can be briefly schematized as follows [61]:*

$$A\left[\begin{array}{c|c|c} u_1 & \cdots & u_J \\ p_1 & \cdots & p_J \\ T_1 & \cdots & T_J \end{array}\right] = \left[RHS_1 \,|\cdots|\, RHS_J\right]. \quad (4.10)$$

where A is a common block matrix for all the J different initial conditions. In (4.7), the block matrix A looks like

$$A = \left[\begin{array}{c|c|c} \frac{1}{\Delta t} - Pr\triangle + < u >^n \cdot\nabla & \nabla & -PrRa\gamma \\ \nabla\cdot & 0 & 0 \\ 0 & 0 & \frac{1}{\Delta t} - \kappa\nabla + < u >^n \cdot\nabla \end{array}\right] \quad (4.11)$$

Note that all the entries in A are independent of the unknowns u_j^{n+1}, p_j^{n+1}, and T_j^{n+1}; and thus A is a constant matrix for all $j = 1\cdots J$.

4.2 SCENARIO 2: THIN WALLED CAVITY

Consider the natural convection problem enclosed in a square cavity with zero wall thickness. Let Ω be a polyhedral domain in $\mathbb{R}^d$ $(d = 2, 3)$, with outward unit normal n, and boundary $\partial\Omega$ such that $\partial\Omega = \Gamma_1 \cup \Gamma_2$. Let $u(x,t) : \Omega \times [0,t^*] \to \mathbb{R}^d$, $p(x,t) : \Omega \times [0,t^*] \to \mathbb{R}$, and $T(x,t) : \Omega \times [0,t^*] \to \mathbb{R}$ satisfy

$$u_t + u \cdot \nabla u - Pr\Delta u + \nabla p = PrRa\gamma T + f \;\; in\ \Omega, \tag{4.12}$$

$$\nabla \cdot u = 0 \;\; in\ \Omega, \tag{4.13}$$

$$T_t + u \cdot \nabla T - \nabla \cdot (\kappa \nabla T) = u_1 + g \;\; in\ \Omega, \tag{4.14}$$

$$u(x,0) = u^0(x)\ and\ T(x,0) = T^0(x) \;\; in\ \Omega, \tag{4.15}$$

$$u = 0 \;\; on\ \partial\Omega, \quad T = 0 \;\; on\ \Gamma_1, \quad n \cdot \nabla T = 0 \;\; on\ \Gamma_2, \tag{4.16}$$

Remark 4. *Check Appendix A for the derivation of u_1 in the temperature equation.*

As in the above section, consider J systems of the above equations with J slightly perturbed initial conditions $u^0(x,t;\omega_j)$ and $T^0(x,t;\omega_j)$ and body forces $f(x,t;\omega_j)$ and $g(x,t;\omega_j)$. Let $u(x,t;\omega_j) : \Omega \times (0,t^*] \to \mathbb{R}^d$, $p_j(x,t;\omega_j) : \Omega \times (0,t^*] \to \mathbb{R}$, and $T_j(x,t;\omega_j) : \Omega \times (0,t^*] \to \mathbb{R}$ satisfy the system (4.12) - (4.16). In similar fashion, we discretize in time arriving at the ensemble method given by:

$$\frac{u^{n+1} - u^n}{\Delta t} - Pr\triangle u^{n+1} + < u >^n \cdot \nabla u^{n+1} + (u^n - < u >^n) \cdot \nabla u^n + \nabla p^{n+1} = PrRa\gamma T^n + f^{n+1}, \tag{4.17}$$

$$\nabla \cdot u^{n+1} = 0, \tag{4.18}$$

$$\frac{T^{n+1} - T^n}{\Delta t} - \kappa \nabla T^{n+1} + < u >^n \cdot \nabla T^{n+1} + (u^n - < u >^n) \cdot \nabla T^n = u_1^n + g^{n+1}, \tag{4.19}$$

Remark: Note that the buoyancy and velocity terms on the right-hand sides have been lagged.

The weak formulation of system (4.1) - (4.5) is:

Find $u : [0,t^*] \to X$, $p : [0,t^*] \to Q$, $T : [0,t^*] \to W$ for a.e. $t \in (0,t^*]$ satisfying for $j = 1, ..., J$:

$$(u_t, v) + b(u,u,v) + Pr(\nabla u, \nabla v) - (p, \nabla \cdot v) = PrRa(\gamma T, v) + (f, v) \ \ \forall v \in X, \tag{4.20}$$

$$(q, \nabla \cdot u) = 0 \ \ \forall q \in Q, \tag{4.21}$$

$$(T_t, S) + \kappa(\nabla T, \nabla S) + b^*(u, T, S) = (g, S) \ \ \forall S \in W. \tag{4.22}$$

Similarly, the weak formulation of system (4.12) - (4.16) is:

Find $u : [0,t^*] \to X$, $p : [0,t^*] \to Q$, $T : [0,t^*] \to W$ for a.e. $t \in (0,t^*]$ satisfying for $j = 1, ..., J$:

$$(u_t, v) + b(u,u,v) + Pr(\nabla u, \nabla v) - (p, \nabla \cdot v) = PrRa(\gamma T, v) + (f, v) \ \ \forall v \in X, \tag{4.23}$$

$$(q, \nabla \cdot u) = 0 \ \ \forall q \in Q, \tag{4.24}$$

$$(T_t, S) + \kappa(\nabla T, \nabla S) + b^*(u, T, S) = (u_1, S) + (g, S) \ \ \forall S \in W. \tag{4.25}$$

For the system (4.1) - (4.5), suppose that $\partial\Omega_f$ and $\partial\Omega - \partial\Omega_f$ lie along the meshlines of the triangulation of Ω. The inf-sup condition implies that we may approximate functions in V well by functions in V_h; that is,

Lemma 4.2.1. *Suppose the discrete inf-sup condition (2.4) holds, then for any $v \in V$*

$$\inf_{v_h \in V_h} \|\nabla(v - v_h)\| \leq \big(1 + \frac{\sqrt{d}}{\beta}\big) \inf_{v_h \in X_h} \|\nabla(v - v_h)\| \tag{4.26}$$

Proof. See [66], Chapter 2, Section 1, p60. □

We will also assume that the mesh and finite element spaces satisfy the following inverse inequality:

$$\|\nabla \chi_{1,2}\| \leq C_{inv,1,2} h^{-1} \|\chi_{1,2}\| \quad \forall \chi_1 \in X_h, \ \forall \chi_2 \in W_h.$$

The discrete time analysis will utilize the following norms $\forall\ 1 \leq k \leq \infty$:

$$|||v|||_{\infty,k} := \max_{0 \leq n \leq N} \|v^n\|_k,$$

$$|||v|||_{p,k} := \big(\Delta t \sum_{n=0}^{N} \|v^n\|_k^p\big)^{1/p}.$$

4.3 NUMERICAL SCHEME

In subsequent discussion, we continue to suppress the dependence of the solution variables on the realization number j and the following notational simplicity is enforced:

$$u'^{n}_{h} = u^{n}_{h} - < u_h >^{n} . \tag{4.27}$$

Denote the fully discrete solutions u^n_h, p^n_h, and T^n_h at time levels $t^n = n\Delta t$, $n = 0, 1, ..., N$, such that $t^* = N\Delta t$. Introducing the finite element approximation in space and applying a backward Euler discretization in time, the fully discrete approximation of (4.1) - (4.5) is: Given $(u^n_h, p^n_h, T^n_h) \in (X_h, Q_h, W_h)$, find $(u^{n+1}_h, p^{n+1}_h, T^{n+1}_h) \in (X_h, Q_h, W_h)$ satisfying, for every $n = 0, 1, ..., N$,

$$\begin{aligned}(\frac{u^{n+1}_h - u^n_h}{\Delta t}, v_h) + b(< u_h >^n, u^{n+1}_h, v_h) + b(u'^{n}_{h}, u^n_h, v_h) \\ + Pr(\nabla u^{n+1}_h, \nabla v_h) - (p^{n+1}_h, \nabla \cdot v_h) = PrRa(\gamma T^{n+1}_h, v_h) + (f^{n+1}, v_h) \ \ \forall v_h \in X_h, \end{aligned} \tag{4.28}$$

$$(q_h, \nabla \cdot u^{n+1}_h) = 0 \ \ \forall q_h \in Q_h,$$

$$\begin{aligned}(\frac{T^{n+1}_h - T^n_h}{\Delta t}, S_h) + b^*(< u_h >^n, T^{n+1}_h, S_h) + b^*(u'^{n}_{h}, T^n_h, S_h) \\ + \kappa(\nabla T^{n+1}_h, \nabla S_h) = (g^{n+1}, S_h) \ \ \forall S_h \in W_h. \end{aligned} \tag{4.29}$$

Similarly, the fully discrete approximation of (4.12) - (4.16) is:
Given $(u^n_h, p^n_h, T^n_h) \in (X_h, Q_h, W_h)$, find $(u^{n+1}_h, p^{n+1}_h, T^{n+1}_h) \in (X_h, Q_h, W_h)$ satisfying, for every $n = 0, 1, ..., N$,

$$\begin{aligned}(\frac{u^{n+1}_h - u^n_h}{\Delta t}, v_h) + b(< u_h >^n, u^{n+1}_h, v_h) + b(u'^{n}_{h}, u^n_h, v_h) \\ + Pr(\nabla u^{n+1}_h, \nabla v_h) - (p^{n+1}_h, \nabla \cdot v_h) = PrRa(\gamma T^{n}_h, v_h) + (f^{n+1}, v_h) \ \ \forall v_h \in X_h, \end{aligned} \tag{4.30}$$

$$(q_h, \nabla \cdot u^{n+1}_h) = 0 \ \ \forall q_h \in Q_h,$$

$$\begin{aligned}(\frac{T^{n+1}_h - T^n_h}{\Delta t}, S_h) + b^*(< u_h >^n, T^{n+1}_h, S_h) + b^*(u'^{n}_{h}, T^n_h, S_h) \\ + \kappa(\nabla T^{n+1}_h, \nabla S_h) = (u^n_1, S_h) + (g^{n+1}, S_h) \ \ \forall S_h \in W_h. \end{aligned} \tag{4.31}$$

4.4 NUMERICAL ANALYSIS

In this section, we present the major stability and error results for the ensemble method. The method is shown to be conditionally stable.

4.4.1 Stability Analysis

After presenting the numerical schemes for the two problems mentioned above, we prove a conditional stability result for the the thick walled cavity problem.

Theorem 4.4.1. *The scheme (4.28) -(4.29) is conditionally stable with respect to the timestep Δt in the following sense: Suppose $f \in L^\infty(0,t^*;H^{-1}(\Omega)^d)$, $g \in L^\infty(0,t^*;H^{-1}(\Omega))$ and for all $N \geq 1$ and $j = 1,...,J$ if*

$$\frac{C\Delta t}{h}\|\nabla u'^n_h\|^2 \leq 1,$$

then for all $0 < t \leq t^*$,

$$\begin{aligned}
&\frac{1}{2}\big(\|T_h^N\|^2 + \|u_h^N\|^2\big) + \frac{1}{4}\sum_{n=0}^{N-1}\big(\|T_h^{n+1}-T_h^n\|^2 + \|u_h^{n+1}-u_h^n\|^2\big) \\
&\qquad + \frac{\kappa\Delta t}{2}\|\nabla T_h^N\|^2 + \frac{Pr\Delta t}{2}\|\nabla u_h^N\|^2 \\
&\qquad \leq \sum_{n=0}^{N-1}\big(\frac{\Delta t}{2\kappa}\sum_{n=0}^{N-1}\|g^{n+1}\|_*^2 + \frac{1}{2}\|T_h^0\|^2 + \frac{\kappa\Delta t}{2}\|\nabla T_h^0\|^2\big) \\
&\qquad + \frac{\Delta t}{Pr}\sum_{n=0}^{N-1}\|f^{n+1}\|_*^2 + \frac{1}{2}\|u_h^0\|^2 + \frac{Pr\Delta t}{2}\|\nabla u_h^0\|^2,
\end{aligned}$$

where $C \equiv C(|\Omega|,\alpha_{min},\kappa,Pr)$. Further,

$$\begin{aligned}
\beta\Delta t\sum_{n=0}^{N-1}\|p_h^{n+1}\| \leq 2\Delta t\sum_{n=0}^{N-1}\big(&C'\|\nabla < u_h >^n\|\|\nabla u_h^{n+1}\| + C'\|\nabla u_h^n\|\|\nabla u'^n_h\| \\
&+ Pr\|\nabla u_h^{n+1}\| + PrRaC_{PF,1}\|T_h^{n+1}\| + \Delta t\|f^{n+1}\|_*\big).
\end{aligned}$$

Proof. Let $S_h = T_h^{n+1}$ in equation (4.29) and use the polarization identity. Then,

$$\begin{aligned}
\frac{1}{2\Delta t}\Big\{\|T_h^{n+1}\|^2 - \|T_h^n\|^2 + \|T_h^{n+1}-T_h^n\|^2\Big\} + \kappa\|\nabla T_h^{n+1}\|^2 \\
+ b^*(u'^n_h, T_h^n, T_h^{n+1}) = (g^{n+1}, T_h^{n+1}),
\end{aligned} \tag{4.32}$$

Multiply by Δt on both sides, use Cauchy-Schwarz-Young on the right hand side term,

$$\frac{1}{2}\Big\{\|T_h^{n+1}\|^2 - \|T_h^n\|^2 + \|T_h^{n+1} - T_h^n\|^2\Big\} + \kappa\Delta t\|\nabla T_h^{n+1}\|^2 \tag{4.33}$$
$$+ \Delta t b^*(u'^n_h, T_h^n, T_h^{n+1}) \leq \frac{\Delta t}{2\epsilon}\|g^{n+1}\|_*^2 + \frac{\Delta t\epsilon}{2}\|\nabla T_h^{n+1}\|^2.$$

We need to estimate $\Delta t b^*(u'^n_h, T_h^n, T_h^{n+1})$. Use Lemma 2.0.3 and the inverse estimate, this gives

$$\begin{aligned} |-\Delta t b^*(u'^n_h, T_h^n, T_h^{n+1})| &= |-\Delta t b^*(u'^n_h, T_h^n, T_h^{n+1} - T_h^n)| \\ &\leq \Delta t C_4\|\nabla u'^n_h\|\|\nabla T_h^n\|\sqrt{\|T_h^{n+1} - T_h^n\|\|\nabla(T_h^{n+1} - T_h^n)\|} \\ &\leq \frac{\Delta t C_2 C_{inv,2}^{1/2}}{h^{1/2}}\|\nabla u'^n_h\|\|\nabla T_h^n\|\|T_h^{n+1} - T_h^n\|. \end{aligned} \tag{4.34}$$

Lastly, apply Cauchy-Shwartz-Young to the right hand side,

$$|-\Delta t b^*(u'^n_h, T_h^n, T_h^{n+1})| \leq \frac{\overline{C}^*\Delta t^2}{h}\|\nabla u'^n_h\|^2\|\nabla T_h^n\|^2 + \frac{1}{4}\|T_h^{n+1} - T_h^n\|^2, \tag{4.35}$$

where $\overline{C}^* \equiv \overline{C}^*(|\Omega|, \alpha_{min})$. Now, use this estimate,

$$\frac{1}{2}\Big\{\|T_h^{n+1}\|^2 - \|T_h^n\|^2 + \|T_h^{n+1} - T_h^n\|^2\Big\} + \kappa\Delta t\|\nabla T_h^{n+1}\|^2 \leq \frac{\Delta t}{2\epsilon}\|g^{n+1}\|_*^2 \tag{4.36}$$
$$+ \frac{\Delta t\epsilon}{2}\|\nabla T_h^{n+1}\|^2 + \frac{\overline{C}^*\Delta t^2}{h}\|\nabla u'^n_h\|^2\|\nabla T_h^n\|^2 + \frac{1}{4}\|T_h^{n+1} - T_h^n\|^2.$$

Let $\epsilon = \kappa$, add/subtract $\frac{\kappa\Delta t}{2}\|\nabla T_h^n\|^2$ to the left-hand side, and regrouping terms leads to,

$$\frac{1}{2}\Big\{\|T_h^{n+1}\|^2 - \|T_h^n\|^2\Big\} + \frac{1}{4}\|T_h^{n+1} - T_h^n\|^2 + \frac{\kappa\Delta t}{2}\Big\{\|\nabla T_h^{n+1}\|^2 - \|\nabla T_h^n\|^2\Big\} \tag{4.37}$$
$$+ \frac{\kappa\Delta t}{2}\|\nabla T_h^n\|^2\Big[1 - \frac{2\overline{C}^*\Delta t}{\kappa h}\|\nabla u'^n_h\|^2\Big] \leq \frac{\Delta t}{2\kappa}\|g^{n+1}\|_*^2.$$

By hypothesis, $\frac{2\overline{C}^*\Delta t}{\kappa h}\|\nabla u'^n_h\|^2 \leq 1$ for $j = 1, \cdots, J$, which leaves us with:

$$\frac{1}{2}\Big\{\|T_h^{n+1}\|^2 - \|T_h^n\|^2\Big\} + \frac{1}{4}\|T_h^{n+1} - T_h^n\|^2 + \frac{\kappa\Delta t}{2}\Big\{\|\nabla T_h^{n+1}\|^2 - \|\nabla T_h^n\|^2\Big\} \leq \frac{\Delta t}{2\kappa}\|g^{n+1}\|_*^2. \tag{4.38}$$

Sum over n from $n = 0$ to $n = N - 1$,

$$\frac{1}{2}\Big\{\|T_h^N\|^2 - \|T_h^0\|^2\Big\} + \frac{1}{4}\sum_{n=0}^{N-1}\|T_h^{n+1} - T_h^n\|^2 \tag{4.39}$$
$$+ \frac{\kappa\Delta t}{2}\Big\{\|\nabla T_h^N\|^2 - \|\nabla T_h^0\|^2\Big\} \leq \frac{\Delta t}{2\kappa}\sum_{n=0}^{N-1}\|g^{n+1}\|_*^2.$$

Putting all data on the right hand side,

$$\frac{1}{2}\|T_h^N\|^2 + \frac{1}{4}\sum_{n=0}^{N-1}\|T_h^{n+1} - T_h^n\|^2 + \frac{\kappa\Delta t}{2}\|\nabla T_h^N\|^2 \tag{4.40}$$
$$\leq \frac{\Delta t}{2\kappa}\sum_{n=0}^{N-1}\|g^{n+1}\|_*^2 + \frac{1}{2}\|T_h^0\|^2 + \frac{\kappa\Delta t}{2}\|\nabla T_h^0\|^2.$$

Therefore, the left hand side is bounded by data on the right hand side. The temperature approximation is stable.

We follow an almost identical form of attack for the velocity as we did for the temperature. Let $v_h = u_h^{n+1} \in V_h$ in (4.28) and use the polarization identity. Then,

$$\frac{1}{2\Delta t}\Big\{\|u_h^{n+1}\|^2 - \|u_h^n\|^2 + \|u_h^{n+1} - u_h^n\|^2\Big\} + Pr\|\nabla u_h^{n+1}\|^2 \tag{4.41}$$
$$+ b(u'^n_h, u_h^n, u_h^{n+1}) = PrRa(\gamma T_h^{n+1}, u_h^{n+1}) + (f^{n+1}, u_h^{n+1})$$

Multiply by Δt on both sides, use Cauchy-Shwartz-Young on the right hand side terms and note that $\|\gamma\| = 1$,

$$\frac{1}{2}\Big\{\|u_h^{n+1}\|^2 - \|u_h^n\|^2 + \|u_h^{n+1} - u_h^n\|^2\Big\} + Pr\Delta t\|\nabla u_h^{n+1}\|^2 + \Delta t b(u'^n_h, u_h^n, u_h^{n+1}) \tag{4.42}$$
$$\leq \frac{\Delta t Pr^2 Ra^2}{2\epsilon}\|T_h^{n+1}\|^2 + \frac{\Delta t}{2\epsilon}\|f^{n+1}\|_*^2 + \Delta t\epsilon\|\nabla u_h^{n+1}\|^2$$

An estimation of $\Delta t b(u'^n_h, u_h^n, u_h^{n+1})$ is needed. We estimate this term in similar fashion as we did for the skew-symmetric trilinear term in the temperature stability analysis,

$$|-\Delta t b(u'^n_h, u_h^n, u_h^{n+1})| \leq \frac{C^*\Delta t^2}{h}\|\nabla u'^n_h\|^2\|\nabla u_h^n\|^2 + \frac{1}{4}\|u_h^{n+1} - u_h^n\|^2, \tag{4.43}$$

where $C^* \equiv C^*(|\Omega|, \alpha_{min})$. Continuing,

$$\frac{1}{2}\Big\{\|u_h^{n+1}\|^2 - \|u_h^n\|^2 + \|u_h^{n+1} - u_h^n\|^2\Big\} + Pr\Delta t\|\nabla u_h^{n+1}\|^2 \tag{4.44}$$
$$\leq \frac{\Delta t Pr^2 Ra^2}{2\epsilon}\|T_h^{n+1}\|^2 + \frac{\Delta t}{2\epsilon}\|f^{n+1}\|_*^2 + \Delta t\epsilon\|\nabla u_h^{n+1}\|^2$$
$$+ \frac{C^*\Delta t^2}{h}\|\nabla u'^n_h\|^2\|\nabla u_h^n\|^2 + \frac{1}{4}\|u_h^{n+1} - u_h^n\|^2.$$

where we have applied the above estimate. Let $\epsilon = Pr/2$, add/subtract $\frac{Pr\Delta t}{2}\|\nabla u_h^n\|^2$ to the left hand side, and regrouping terms leads to,

$$\frac{1}{2}\Big\{\|u_h^{n+1}\|^2 - \|u_h^n\|^2\Big\} + \frac{1}{4}\|u_h^{n+1} - u_h^n\|^2 + \frac{Pr\Delta t}{2}\Big\{\|\nabla u_h^{n+1}\|^2 - \|\nabla u_h^n\|^2\Big\}$$
$$+ \frac{\mathrm{Pr}\,\Delta t}{2}\|\nabla u_h^n\|^2\Big[1 - \frac{2C^*\Delta t}{Prh}\|\nabla u'^n_h\|^2\Big] \leq \Delta t Pr Ra^2\|T_h^{n+1}\|^2 + \frac{\Delta t}{Pr}\|f^{n+1}\|_*^2. \tag{4.45}$$

By hypothesis, $\frac{2C^*\Delta t}{Prh}\|\nabla u'^n_h\|^2 \leq 1$ for $j = 1, \cdots, J$, which leaves us with:

$$\frac{1}{2}\Big\{\|u_h^{n+1}\|^2 - \|u_h^n\|^2\Big\} + \frac{1}{4}\|u_h^{n+1} - u_h^n\|^2 + \frac{Pr\Delta t}{2}\Big\{\|\nabla u_h^{n+1}\|^2 - \|\nabla u_h^n\|^2\Big\}$$
$$\leq \Delta t Pr Ra^2\|T_h^{n+1}\|^2 + \frac{\Delta t}{Pr}\|f^{n+1}\|_*^2. \tag{4.46}$$

Sum over n from $n = 0$ to $n = N - 1$, putting all data on right hand side,

$$\frac{1}{2}\|u_h^n\|^2 + \frac{1}{4}\sum_{n=0}^{N-1}\|u_h^{n+1} - u_h^n\|^2 + \frac{Pr\Delta t}{2}\|\nabla u_h^n\|^2 \tag{4.47}$$
$$\leq \Delta t Pr Ra^2\sum_{n=0}^{N-1}\|T_h^{n+1}\|^2 + \frac{\Delta t}{Pr}\sum_{n=0}^{N-1}\|f^{n+1}\|_*^2$$
$$+ \frac{1}{2}\|u_h^0\|^2 + \frac{Pr\Delta t}{2}\|\nabla u_h^0\|^2.$$

Together with the stability of the temperature approximation, the left hand side is bounded above by data; that is, the velocity approximation is stable. Adding the resulting inequality relations together and taking $\max(2C^*/Pr, 2\overline{C^*}/\kappa)$ leaves us with the result.

We now prove stability of the pressure approximation.

Consider (4.28) and pick $0 \neq v_h \in V_h$. Then,

$$(\frac{u_h^{n+1} - u_h^n}{\Delta t}, v_h) + b(< u_h >^n, u_h^{n+1}, v_h) + b(u'^n_h, u_h^n, v_h)$$
$$+ Pr(\nabla u_h^{n+1}, \nabla v_h) = PrRa(\gamma T_h^{n+1}, v_h) + (f^{n+1}, v_h). \tag{4.48}$$

We will isolate the first velocity term to form an estimate we will need in finalizing the analysis. We will need estimates of all other terms before doing so. Applying Lemma 2.0.1 to the skew-symmetric trilinear terms, Cauchy-Schwarz, and Poincaré-Friedrichs,

$$|-b(<u_h>^n, u_h^{n+1}, v_h)| \leq C'\Delta t\|\nabla <u_h>^n\|\|\nabla u_h^{n+1}\|\|\nabla v_h\|, \tag{4.49}$$

$$|-b(u'^n_h, u_h^n, v_h)| \leq C'\Delta t\|\nabla u_h^n\|\|\nabla u_h^n\|\|\nabla v_h\|, \tag{4.50}$$

$$|-Pr(\nabla u_h^{n+1}, \nabla v_h)| \leq Pr\Delta t\|\nabla u_h^{n+1}\|\|\nabla v_h\|, \tag{4.51}$$

$$|PrRa(\gamma T_h^{n+1}, v_h)| \leq PrRa\Delta t\|T_h^{n+1}\|\|v_h\| \leq PrRaC_{PF,1}\Delta t\|T_h^{n+1}\|\|\nabla v_h\|, \tag{4.52}$$

$$|(f^{n+1}, v_h)| \leq \Delta t\|f^{n+1}\|_*\|\nabla v_h\|. \tag{4.53}$$

Isolate the first velocity term on the left hand side, multiply by Δt, apply the above estimates and then divide by the common factor $\|\nabla v_h\|$ on both sides,

$$\begin{aligned}\frac{(u_h^{n+1}-u_h^n, v_h)}{\|\nabla v_h\|} \leq\ & C'\Delta t\|\nabla <u_h>^n\|\|\nabla u_h^{n+1}\| + C'\Delta t\|\nabla u'^n_h\|\|\nabla u_h^n\| \\ & + Pr\Delta t\|\nabla u_h^{n+1}\| + PrRaC_{PF,1}\Delta t\|T_h^{n+1}\| + \Delta t\|f^{n+1}\|_*. \end{aligned}\tag{4.54}$$

Take the supremum over all $0 \neq v_h \in V_h$,

$$\begin{aligned}\|u_h^{n+1}-u_h^n\|_* \leq\ & C'\Delta t\|\nabla <u_h>^n\|\|\nabla u_h^{n+1}\| + C'\Delta t\|\nabla u'^n_h\|\|\nabla u_h^n\| \\ & + Pr\Delta t\|\nabla u_h^{n+1}\| + PrRaC_{PF,1}\Delta t\|T_h^{n+1}\| + \Delta t\|f^{n+1}\|_*. \end{aligned}\tag{4.55}$$

Now consider equation (4.28). Multiply by Δt and isolate the pressure term,

$$\begin{aligned}\Delta t(p_h^{n+1}, \nabla\cdot v_h) =\ & (u_h^{n+1}-u_h^n, v_h) \\ & + \Delta t b(<u_h>^n, u_h^{n+1}, v_h) + \Delta t b(u'^n_h, u_h^n, v_h) \\ & + Pr\Delta t(\nabla u_h^{n+1}, \nabla v_h) - PrRa\Delta t(\gamma T_h^{n+1}, v_h) - \Delta t(f^{n+1}, v_h) \quad \forall v_h \in X_h \end{aligned}\tag{4.56}$$

Use all of the above estimates on the right hand side terms,

$$\begin{aligned}\Delta t(p_h^{n+1}, \nabla\cdot v_h) \leq\ & (u_h^{n+1}-u_h^n, v_h) \\ & + \big(C'\Delta t\|\nabla <u_h>^n\|\|\nabla u_h^{n+1}\| + C'\Delta t\|\nabla u'^n_h\|\|\nabla u_h^n\| \\ & + Pr\Delta t\|\nabla u_h^{n+1}\| + PrRaC_{PF,1}\Delta t\|T_h^{n+1}\| + \Delta t\|f^{n+1}\|_*\big)\|\nabla v_h\| \end{aligned}\tag{4.57}$$

Divide by $\|\nabla v_h\|$, and note that $\frac{(u_h^{n+1}-u_h^n, v_h)}{\|\nabla v_h\|} \leq \|u_h^{n+1} - u_h^n\|_*$. Take the supremum over all $0 \neq v_h \in X_h$,

$$\sup_{0\neq v_h \in X_h} \Delta t \frac{(p_h^{n+1}, \nabla \cdot v_h)}{\|\nabla v_h\|} \leq 2\big(C'\Delta t \|\nabla < u_h >^n \| \|\nabla u_h^{n+1}\| + C'\Delta t \|\nabla u'^n_h\| \|\nabla u_h^n\| + Pr\Delta t \|\nabla u_h^{n+1}\| + PrRaC_{PF,1}\Delta t \|T_h^{n+1}\| + \Delta t \|f^{n+1}\|_*\big) \quad (4.58)$$

Use the inf-sup condition,

$$\beta \Delta t \|p_h^{n+1}\| \leq 2\big(C'\Delta t \|\nabla < u_h >^n \| \|\nabla u_h^{n+1}\| + C'\Delta t \|\nabla u'^n_h\| \|\nabla u_h^n\| + Pr\Delta t \|\nabla u_h^{n+1}\| + PrRaC_{PF,1}\Delta t \|T_h^{n+1}\| + \Delta t \|f^{n+1}\|_*\big). \quad (4.59)$$

Summing over n from $n = 0$ to $n = N - 1$ gives us stability of the pressure approximation, built on the stability of the temperature and velocity. □

Next we prove a conditional stability result for the thin walled cavity numerical scheme.

Theorem 4.4.2. *The scheme (4.30) -(4.31) is conditionally stable with respect to the timestep Δt in the following sense: Suppose $f \in L^\infty(0, t^*; H^{-1}(\Omega)^d)$, $g \in L^\infty(0, t^*; H^{-1}(\Omega))$ and for all $N \geq 1$ and $j = 1, ..., J$ if*

$$\frac{C\Delta t}{h} \|\nabla u'^n_h\|^2 \leq 1,$$

then

$$\begin{aligned} &\|u_h^N\|^2 + \|T_h^N\|^2 + \frac{1}{2}\sum_{n=0}^{N-1} \|u_h^{n+1} - u_h^n\|^2 + \frac{1}{2}\sum_{n=0}^{N-1} \|T_h^{n+1} - T_h^n\|^2 \\ &\quad + Pr\Delta t \|\nabla u_h^N\|^2 + \kappa \Delta t \|\nabla T_h^N\|^2 \\ &\quad \leq \exp(2Ct^*)\big\{\Delta t \sum_{n=0}^{N-1} (\frac{1}{Pr}\|f^{n+1}\|^2 + \frac{1}{\kappa}\|g^{n+1}\|^2) + \|u_h^0\|^2 + \|T_h^0\|^2 \\ &\quad + Pr\Delta t \|\nabla u_h^0\|^2 + \kappa \Delta t \|\nabla T_h^0\|^2\big\}, \end{aligned}$$

where $C \equiv C(|\Omega|, \alpha_{min}, \kappa, Pr)$. Further,

$$\beta \Delta t \sum_{n=0}^{N-1} \|p_h^{n+1}\| \leq 2 \sum_{n=0}^{N-1} \big(C'\Delta t \|\nabla < u_h >^n \| \|\nabla u_h^{n+1}\| + C'\Delta t \|\nabla u'^n_h\| \|\nabla u_h^n\| + Pr\Delta t \|\nabla u_h^{n+1}\| + PrRaC_{PF,1}\Delta t \|T_h^n\| + \Delta t \|f^{n+1}\|_*\big).$$

Proof. Add equations (4.30) and (4.31), let $S_h = T_h^{n+1}$ and $v_h = u_h^{n+1}$ and use the polarization identity. Then,

$$\frac{1}{2\Delta t}\Big\{\|u_h^{n+1}\|^2 - \|u_h^n\|^2 + \|u_h^{n+1} - u_h^n\|^2\Big\} \tag{4.60}$$

$$+ \frac{1}{2\Delta t}\Big\{\|T_h^{n+1}\|^2 - \|T_h^n\|^2 + \|T_h^{n+1} - T_h^n\|^2\Big\} \tag{4.61}$$

$$+ Pr\|\nabla u_h^{n+1}\|^2 + \kappa\|\nabla T_h^{n+1}\|^2 + b(u'^n_h, u_h^n, u_h^{n+1}) + b^*(u'^n_h, T_h^n, T_h^{n+1})$$

$$= PrRa(\gamma T_h^{n+1}, u_h^{n+1}) + (u_{1h}^n, T_h^{n+1}) + (f^{n+1}, u_h^{n+1}) + (g^{n+1}, T_h^{n+1}),$$

Apply similar techniques and estimates as in the previous analysis,

$$\frac{1}{2}\Big\{\|u_h^{n+1}\|^2 - \|u_h^n\|^2 + \|u_h^{n+1} - u_h^n\|^2\Big\} + \frac{1}{2}\Big\{\|T_h^{n+1}\|^2 - \|T_h^n\|^2 + \|T_h^{n+1} - T_h^n\|^2\Big\} \tag{4.62}$$

$$+ \frac{Pr\Delta t}{2}\big\{\|\nabla u_h^{n+1}\|^2 - \|\nabla u_h^n\|^2\big\} + \frac{\kappa\Delta t}{2}\big\{\|\nabla T_h^{n+1}\|^2 - \|\nabla T_h^n\|^2\big\}$$

$$+ \frac{Pr\Delta t}{2}\|\nabla u_h^n\|^2\Big\{1 - \frac{2\Delta t C^*}{Prh}\|\nabla u'^n_h\|^2\Big\} + \frac{\kappa\Delta t}{2}\|\nabla T_h^n\|^2\Big\{1 - \frac{2\Delta t\overline{C}^*}{\kappa h}\|\nabla u'^n_h\|^2\Big\}$$

$$\leq \frac{\Delta t PrRa^2 C_{PF,1}^2}{2}\|T_h^n\|^2 + \frac{\Delta t C_{PF,2}^2}{2\kappa}\|u_h^n\|^2 + \frac{\Delta t}{2Pr}\|f^{n+1}\|^2 + \frac{\Delta t}{2\kappa}\|g^{n+1}\|^2.$$

Using the timestep condition and taking a maximum over constants in the first two terms leaves us with,

$$\frac{1}{2}\Big\{\|u_h^{n+1}\|^2 - \|u_h^n\|^2 + \|u_h^{n+1} - u_h^n\|^2\Big\} + \frac{1}{2}\Big\{\|T_h^{n+1}\|^2 - \|T_h^n\|^2 + \|T_h^{n+1} - T_h^n\|^2\Big\} \tag{4.63}$$

$$+ \frac{Pr\Delta t}{2}\big\{\|\nabla u_h^{n+1}\|^2 - \|\nabla u_h^n\|^2\big\} + \frac{\kappa\Delta t}{2}\big\{\|\nabla T_h^{n+1}\|^2 - \|\nabla T_h^n\|^2\big\}$$

$$\leq \Delta t C\big\{\|T_h^n\|^2 + \|u_h^n\|^2\big\} + \frac{\Delta t}{2Pr}\|f^{n+1}\|^2 + \frac{\Delta t}{2\kappa}\|g^{n+1}\|^2.$$

Multiplying by 2 and summing over n from $n = 0$ to $n = N - 1$ leads to,

$$\|u_h^N\|^2 + \|T_h^N\|^2 + \frac{1}{2}\sum_{n=0}^{N-1}\|u_h^{n+1} - u_h^n\|^2 + \frac{1}{2}\sum_{n=0}^{N-1}\|T_h^{n+1} - T_h^n\|^2 \tag{4.64}$$

$$+ Pr\Delta t\|\nabla u_h^N\|^2 + \kappa\Delta t\|\nabla T_h^N\|^2$$

$$\leq 2C\Delta t\sum_{n=0}^{N-1}\big\{\|T_h^n\|^2 + \|u_h^n\|^2\big\} + 2\Delta t\sum_{n=0}^{N-1}\big\{\frac{1}{2Pr}\|f^{n+1}\|^2 + \frac{1}{2\kappa}\|g^{n+1}\|^2\big\}$$

$$+ \|u_h^0\|^2 + \|T_h^0\|^2 + Pr\Delta t\|\nabla u_h^0\|^2 + \kappa\Delta t\|\nabla T_h^0\|^2.$$

Apply Lemma 2.0.4,

$$\|u_h^N\|^2 + \|T_h^N\|^2 + \frac{1}{2}\sum_{n=0}^{N-1}\|u_h^{n+1} - u_h^n\|^2 + \frac{1}{2}\sum_{n=0}^{N-1}\|T_h^{n+1} - T_h^n\|^2 \tag{4.65}$$
$$+ Pr\Delta t\|\nabla u_h^N\|^2 + \kappa\Delta t\|\nabla T_h^N\|^2$$
$$\leq \exp(2Ct^*)\big\{\Delta t\sum_{n=0}^{N-1}(\frac{1}{Pr}\|f^{n+1}\|^2 + \frac{1}{\kappa}\|g^{n+1}\|^2) + \|u_h^0\|^2 + \|T_h^0\|^2$$
$$+ Pr\Delta t\|\nabla u_h^0\|^2 + \kappa\Delta t\|\nabla T_h^0\|^2\big\}.$$

Thus, velocity and temperature are stable. Pressure follows by similar arguments as in Theorem 4.4.1. □

Remark: For ocean and atmosphere dynamics, the Gronwall constant will typically behave like $e^{Ra^2 t^*}$.

4.5 ERROR ANALYSIS

In this section, an error estimate is presented for the ensemble method (4.28)-(4.29).

Theorem 4.5.1. *For (u,p,T) satisfying (4.1) - (4.5), suppose the approximation assumptions hold and that* $(u_h^0, p_h^0, T_h^0) \in (X_h, Q_h, W_h)$ *are approximations of* (u^0, p^0, T^0) *to within the accuracy of the interpolant. Further, suppose that* $\frac{C\Delta t}{h}\|\nabla u_h'^n\|^2 \leq 1$, *holds for all* $j = 1, ..., J$. *Then there exists a constant C such that*

$$
\begin{aligned}
&\|e_T^N\|^2 + \|e_u^N\|^2 + \frac{1}{2}\sum_{n=0}^{N-1}\big(\|e_T^{n+1} - e_T^n\|^2 + \|e_u^{n+1} - e_u^n\|^2\big) \qquad (4.66)\\
&+ \frac{\kappa\Delta t}{2}\|\nabla e_T^N\|^2 + \frac{Pr\Delta t}{2}\|\nabla e_u^N\|^2\\
&\le C\Big\{\Delta t h^{2k}|||T|||^2_{\infty,k+1} + \Delta t h^{2k}|||u|||^2_{\infty,k+1} + \Delta t h^{2k+2}|||T_t|||^2_{\infty,k+1} + \Delta t^3|||\nabla u_t|||^2_{\infty,k+1}\\
&+ \Delta t^3|||\nabla T_t|||^2_{\infty,0} + \Delta t^3|||T_{tt}|||^2_{\infty,0} + \Delta t h^{2k}|||p|||^2_{\infty,k} + \Delta t h^{2k+2}|||u_t|||^2_{\infty,k+1} + \Delta t^3|||u_{tt}|||^2_{\infty,0}\Big\}\\
&+ C\big(\|\zeta_h^0\|^2 + \frac{\kappa\Delta t}{2}\|\nabla\zeta_h^0\|^2 + \|\eta_h^0\|^2 + \frac{Pr\Delta t}{2}\|\nabla\eta_h^0\|^2\big) + \|e_T^0\|^2 + \|e_u^0\|^2\\
&+ \frac{\kappa\Delta t}{2}\|\nabla e_T^0\|^2 + \frac{Pr\Delta t}{2}\|\nabla e_u^0\|^2\\
&\le C(\Delta t h^{2k} + \Delta t h^{2k+2} + \Delta t^3 + \Delta t\|\nabla\eta_h^0\|^2 + \Delta t\|\nabla\zeta_h^0\|^2 + \|\eta_h^0\|^2\\
&+ \|\zeta_h^0\|^2 + \|e_T^0\|^2 + \|e_u^0\|^2 + \Delta t\|\nabla e_T^0\|^2 + \Delta t\|\nabla e_u^0\|^2).
\end{aligned}
$$

Proof. We have that the true solutions satisfy:

$$
\begin{aligned}
(\frac{u^{n+1}-u^n}{\Delta t}, v_h) + b(u^{n+1}, u^{n+1}, v_h) + Pr(\nabla u^{n+1}, \nabla v_h) - (p^{n+1}, \nabla\cdot v_h) \qquad (4.67)\\
= PrRa(\gamma T^{n+1}, v_h) + (f^{n+1}, v_h) + \tau(u^{n+1}; v_h)\ \ \forall v_h \in X_h,
\end{aligned}
$$

$$
(q_h, \nabla\cdot u^{n+1}) = 0\ \ \forall q_h \in Q_h, \qquad (4.68)
$$

$$
\begin{aligned}
(\frac{T^{n+1}-T^n}{\Delta t}, S_h) + b^*(u^{n+1}, T^{n+1}, S_h) + \kappa(\nabla T^{n+1}, \nabla S_h) \qquad (4.69)\\
= (g^{n+1}, S_h) + \tau(T^{n+1}; S_h)\ \ \forall S_h \in W_h,
\end{aligned}
$$

where the consistency errors are given by,

$$
\begin{aligned}
\tau(u^n; v_h) &= \big(\frac{u^n - u^{n-1}}{\Delta t} - u_t^n, v_h\big),\\
\tau(T^n; S_h) &= \big(\frac{T^n - T^{n-1}}{\Delta t} - T_t^n, S_h\big).
\end{aligned}
$$

The error equation for temperature is

$$
\begin{aligned}
(\frac{e_T^{n+1}-e_T^n}{\Delta t}, S_h) + b^*(u^{n+1}, T^{n+1}, S_h) - b^*(u_h^{n+1} - u'^{n+1}_h, T_h^{n+1}, S_h) \qquad (4.70)\\
- b^*(u'^n_h, T_h^n, S_h) + \kappa(\nabla e_T^{n+1}, \nabla S_h) = \tau(T^{n+1}, S_h)\ \ \forall S_h \in W_h.
\end{aligned}
$$

Letting $e_T^n = (T^n - \tilde{T}^n) - (T_h^n - \tilde{T}^n) = \zeta^n - \psi_h^n$ and rearranging,

$$(\frac{\psi_h^{n+1} - \psi_h^n}{\Delta t}, S_h) - b^*(u^{n+1}, T^{n+1}, S_h) + b^*(u_h^{n+1} - u'^{n+1}_h, T_h^{n+1}, S_h) + b^*(u'^n_h, T_h^n, S_h)$$
$$+ \kappa(\nabla\psi_h^{n+1}, \nabla S_h) = (\frac{\zeta^{n+1} - \zeta^n}{\Delta t}, S_h) + \kappa(\nabla\zeta^{n+1}, \nabla S_h) - \tau(T^{n+1}, S_h) \ \ \forall S_h \in W_h. \quad (4.71)$$

Set $S_h = \psi_h^{n+1} \in W_h$,

$$\frac{1}{2\Delta t}\Big\{\|\psi_h^{n+1}\|^2 - \|\psi_h^n\|^2 + \|\psi_h^{n+1} - \psi_h^n\|^2\Big\} + \kappa\|\nabla\psi_h^{n+1}\|^2 \quad (4.72)$$
$$= \frac{1}{\Delta t}(\zeta^{n+1} - \zeta^n, \psi_h^{n+1}) + \kappa(\nabla\zeta^{n+1}, \nabla\psi_h^{n+1}) - \tau(T^{n+1}, \psi_h^{n+1})$$
$$+ b^*(u^{n+1}, T^{n+1}, \psi_h^{n+1}) - b^*(u_h^{n+1} - u'^{n+1}_h, T_h^{n+1}, \psi_h^{n+1}) - b^*(u'^n_h, T_h^n, \psi_h^{n+1})$$

Add/subtract $b^*(u^{n+1}, T_h^{n+1}, \psi_h^{n+1})$ and $b^*(u^n, T_h^{n+1}, \psi_h^{n+1})$.
Denote $LHS = \frac{1}{2\Delta t}\Big\{\|\psi_h^{n+1}\|^2 - \|\psi_h^n\|^2 + \|\psi_h^{n+1} - \psi_h^n\|^2\Big\} + \kappa\|\nabla\psi_h^{n+1}\|^2$, then

$$LHS = \frac{1}{\Delta t}(\zeta^{n+1} - \zeta^n, \psi_h^{n+1}) + \kappa(\nabla\zeta^{n+1}, \nabla\psi_h^{n+1}) - \tau(T^{n+1}, \psi_h^{n+1}) \quad (4.73)$$
$$+ b^*(u^{n+1}, e_T^{n+1}, \psi_h^{n+1}) + b^*(u^{n+1} - u^n, T_h^{n+1}, \psi_h^{n+1}) + b^*(u^{n+1}, T_h^{n+1}, \psi_h^{n+1})$$

Add/subtract $b^*(u'^n_h, T^{n+1} - T^n, \psi_h^{n+1})$ and expanding out terms,

$$LHS = \frac{1}{\Delta t}(\zeta^{n+1} - \zeta^n, \psi_h^{n+1}) + \kappa(\nabla\zeta^{n+1}, \nabla\psi_h^{n+1}) - \tau(T^{n+1}, \psi_h^{n+1}) \quad (4.74)$$
$$+ b^*(u^{n+1}, \zeta^{n+1}, \psi_h^{n+1}) + b^*(u^{n+1} - u^n, T_h^{n+1}, \psi_h^{n+1})$$
$$+ b^*(e_u^n, T_h^{n+1}, \psi_h^{n+1}) + b^*(u'^n_h, T_h^{n+1}, \psi_h^{n+1}) - b^*(u'^n_h, T_h^n, \psi_h^{n+1})$$
$$+ b^*(u'^n_h, T^{n+1}, \psi_h^{n+1}) - b^*(u'^n_h, T^{n+1}, \psi_h^{n+1}) + b^*(u'^n_h, T^n, \psi_h^{n+1})$$
$$- b^*(u'^n_h, T^n, \psi_h^{n+1}) \quad (4.75)$$

leads to,

$$\frac{1}{2\Delta t}\Big\{\|\psi_h^{n+1}\|^2 - \|\psi_h^n\|^2 + \|\psi_h^{n+1} - \psi_h^n\|^2\Big\} + \kappa\|\nabla\psi_h^{n+1}\|^2 \quad (4.76)$$
$$= \frac{1}{\Delta t}(\zeta^{n+1} - \zeta^n, \psi_h^{n+1}) + \kappa(\nabla\zeta^{n+1}, \nabla\psi_h^{n+1}) + b^*(u^{n+1}, \zeta^{n+1}, \psi_h^{n+1})$$
$$+ b^*(u^{n+1} - u^n, T_h^{n+1}, \psi_h^{n+1}) + b^*(\eta^n, T_h^{n+1}, \psi_h^{n+1}) - b^*(\phi_h^n, T_h^{n+1}, \psi_h^{n+1})$$
$$+ b^*(u'^n_h, \zeta^{n+1}, \psi_h^{n+1}) - b^*(u'^n_h, \zeta^n, \psi_h^{n+1}) + b^*(u'^n_h, \psi^n, \psi_h^{n+1})$$
$$+ b^*(u'^n_h, T^{n+1} - T^n, \psi_h^{n+1}) - \tau(T^{n+1}, \psi_h^{n+1}).$$

Following analogously for the velocity error equation and letting $v_h = \phi_h^{n+1} \in V_h$, we have

$$\begin{aligned}
&\frac{1}{2\Delta t}\Big\{\|\phi_h^{n+1}\|^2 - \|\phi_h^n\|^2 + \|\phi_h^{n+1} - \phi_h^n\|^2\Big\} + Pr\|\nabla\phi_h^{n+1}\|^2 \qquad (4.77)\\
&\quad = \frac{1}{\Delta t}(\eta^{n+1} - \eta^n, \phi_h^{n+1}) + Pr(\nabla\eta^{n+1}, \nabla\phi_h^{n+1}) - (p^{n+1} - q_h^{n+1}, \nabla\cdot\phi_h^{n+1})\\
&\quad + PrRa(\gamma\zeta^{n+1}, \phi_h^{n+1+}) - PrRa(\gamma\psi_h^{n+1}, \phi_h^{n+1+}) + b(u^{n+1}, \eta^{n+1}, \phi_h^{n+1})\\
&\quad + b(u^{n+1} - u^n, u_h^{n+1}, \phi_h^{n+1}) + b(\eta^n, u_h^{n+1}, \phi_h^{n+1}) - b(\phi_h^n, u_h^{n+1}, \phi_h^{n+1})\\
&\quad + b(u'^n_h, \eta^{n+1}, \phi_h^{n+1}) - b(u'^n_h, \eta^n, \phi_h^{n+1}) + b(u'^n_h, \phi^n, \phi_h^{n+1})\\
&\quad + b(u'^n_h, u^{n+1} - u^n, \phi_h^{n+1}) - \tau(u^{n+1}, \phi_h^{n+1}),
\end{aligned}$$

where $e_u^n = (u^n - \tilde{u}^n) - (u_h^n - \tilde{u}^n) = \eta^n - \phi_h^n$. Our goal now is to estimate all terms on the right hand side in such a way that we may hide the unknown pieces ψ into the left hand side. The following estimates are formed using Lemma 2.0.1 in conjunction with Cauchy-Schwartz-Young,

$$\begin{aligned}
|b^*(u^{n+1}, \zeta^{n+1}, \psi_h^{n+1})| &\le \overline{C}\|\nabla u^{n+1}\|\|\nabla\zeta^{n+1}\|\|\nabla\psi_h^{n+1}\| \qquad (4.78)\\
&\le \frac{C_r\overline{C}^2}{\epsilon_3}\|\nabla u^{n+1}\|^2\|\nabla\zeta^{n+1}\|^2 + \frac{\epsilon_3}{r}\|\nabla\psi_h^{n+1}\|^2,
\end{aligned}$$

$$\begin{aligned}
|b^*(\eta^n, T_h^{n+1}, \psi_h^{n+1})| &\le \overline{C}\|\nabla\eta^n\|\|\nabla T_h^{n+1}\|\|\nabla\psi_h^{n+1}\| \qquad (4.79)\\
&\le \frac{C_r\overline{C}^2}{\epsilon_5}\|\nabla\eta^n\|^2\|\nabla T_h^{n+1}\|^2 + \frac{\epsilon_5}{r}\|\nabla\psi_h^{n+1}\|^2,
\end{aligned}$$

$$\begin{aligned}
|b^*(u'^n_h, \zeta^{n+1}, \psi_h^{n+1})| &\le \overline{C}\|u'^n_h\|\|\zeta^{n+1}\|\|\psi_h^{n+1}\| \qquad (4.80)\\
&\le \frac{C_r\overline{C}^2}{\epsilon_7}\|\nabla u'^n_h\|^2\|\nabla\zeta^{n+1}\|^2 + \frac{\epsilon_7}{r}\|\nabla\psi_h^{n+1}\|^2,
\end{aligned}$$

$$\begin{aligned}
|-b^*(u'^n_h, \zeta^n, \psi_h^{n+1})| &\le \overline{C}\|\nabla u'^n_h\|\|\nabla\zeta^n\|\|\nabla\psi_h^{n+1}\| \qquad (4.81)\\
&\le \frac{C_r\overline{C}^2}{\epsilon_8}\|\nabla u'^n_h\|^2\|\nabla\zeta^n\|^2 + \frac{\epsilon_8}{r}\|\nabla\psi_h^{n+1}\|^2.
\end{aligned}$$

Now, we apply Lemma 2.0.1, Cauchy-Schwartz-Young, and use Taylor's theorem for the following estimates,

$$|b^*(u^{n+1}-u^n, T_h^{n+1}, \psi_h^{n+1})| \leq \overline{C}\|\nabla(u^{n+1}-u^n)\|\|\nabla T_h^{n+1}\|\|\nabla\psi_h^{n+1}\| \tag{4.82}$$

$$\leq \frac{C_r\overline{C}^2}{\epsilon}\|\nabla(u^{n+1}-u^n)\|^2\|\nabla T_h^{n+1}\|^2 + \frac{\epsilon}{r}\|\nabla\psi_h^{n+1}\|^2$$

$$\leq \frac{C_r\overline{C}^2\Delta t^2}{\epsilon_4}\|\nabla T_h^{n+1}\|^2\|\nabla u_t\|^2_{L^\infty(t^n,t^{n+1};L^2(\Omega))}$$

$$+ \frac{\epsilon_4}{r}\|\nabla\psi_h^{n+1}\|^2, \tag{4.83}$$

$$|b^*(u_h^n, T^{n+1}-T^n, \psi_h^{n+1})| \leq \overline{C}\|\nabla u_h^n\|\|\nabla(T^{n+1}-T^n)\|\|\nabla\psi_h^{n+1}\| \tag{4.84}$$

$$\leq \frac{C_r\overline{C}^2\Delta t^2}{\epsilon_{10}}\|\nabla u_h^n\|^2\|\nabla T_t\|^2_{L^\infty(t^n,t^{n+1};L^2(\Omega))}$$

$$+ \frac{\epsilon_{10}}{r}\|\nabla\psi_h^{n+1}\|^2. \tag{4.85}$$

Apply Lemma 2.0.1 and Cauchy-Schwartz-Young twice,

$$|-b^*(\phi_h^n, T_h^{n+1}, \psi_h^{n+1})| \leq C_2\sqrt{\|\phi_h^n\|\|\nabla\phi_h^n\|}\|\nabla T_h^{n+1}\|\|\nabla\psi_h^{n+1}\| \tag{4.86}$$

$$\leq C_2C_T(j)\sqrt{\|\phi_h^n\|\|\nabla\phi_h^n\|}\|\psi_h^{n+1}\|$$

$$\leq \frac{C_2C_T\epsilon_6}{2}\|\nabla\psi_h^{n+1}\|^2 + \frac{C_2C_T\delta_6}{4\epsilon_6}\|\nabla\phi_h^n\|^2 + \frac{C_2C_T}{4\epsilon_6\delta_6}\|\phi_h^n\|^2.$$

Use Lemma 2.0.3, the inverse estimate, and Cauchy-Schwartz-Young,

$$|\Delta t b^*(u'^n_h, \psi_h^n, \psi_h^{n+1})| = |\Delta t b^*(u'^n_h, \psi_h^n, \psi_h^{n+1}-\psi_h^n)| \tag{4.87}$$

$$\leq |\Delta t C_4\|\nabla u'^n_h\|\|\nabla\psi^n\|\sqrt{\|\psi_h^{n+1}-\psi_h^n\|\|\nabla(\psi_h^{n+1}-\psi_h^n)\|}$$

$$\leq \frac{\Delta t C_2 C_{inv,2}^{1/2}}{h^{1/2}}\|\nabla u'^n_h\|\|\nabla\psi^n\|\|\psi_h^{n+1}-\psi_h^n\|$$

$$\leq \frac{\overline{C^*}\Delta t}{2h\epsilon_9}\|\nabla u'^n_h\|^2\|\nabla\psi_h^n\|^2 + \frac{\epsilon_9}{2}\|\psi_h^{n+1}-\psi_h^n\|^2.$$

Use Cauchy-Schwartz-Young, Poincaré−Friedrichs and Taylor's theorem

$$|\frac{1}{\Delta t}(\zeta^{n+1}-\zeta^n, \psi_h^{n+1})| \leq \frac{C_{PF,2}^2C_r}{\epsilon_1}\|\zeta_t\|^2_{L^\infty(t^n,t^{n+1};L^2(\Omega))} + \frac{\epsilon_1}{r}\|\nabla\psi_h^{n+1}\|^2,$$

$$|-\tau(T^{n+1};\psi_h^{n+1})| \leq \frac{C_{PF,2}^2C_r\Delta t^2}{\epsilon_1 1}\|T_{tt}\|^2_{L^\infty(t^n,t^{n+1};L^2(\Omega))} + \frac{\epsilon_1 1}{r}\|\nabla\psi_h^{n+1}\|^2.$$

Lastly, use Cauchy-Schwartz-Young,

$$|\kappa(\nabla\zeta^{n+1},\nabla\psi_h^{n+1})| \leq \frac{C_r\kappa}{\epsilon_2}\|\nabla\zeta^{n+1}\|^2 + \frac{\epsilon_2}{r}\|\nabla\psi^{n+1}\|^2.$$

Similar estimates follow for equation 4.77, however, we must treat an additional pressure term and error term,

$$\begin{aligned}|-(p^{n+1}-q_h^{n+1},\nabla\cdot\phi_h^{n+1})| &\leq \sqrt{d}\|p^{n+1}-q_h^{n+1}\|\|\nabla\phi_h^{n+1}\| \\ &\leq \frac{dC_r}{\epsilon_{14}}\|p^{n+1}-q_h^{n+1}\|^2 + \frac{\epsilon_{14}}{r}\|\nabla\phi_h^{n+1}\|^2,\end{aligned}$$

$$|PrRa(\gamma\zeta^{n+1},\phi_h^{n+1+})| \leq \frac{Pr^2Ra^2C_{PF,1}^2C_{PF,2}^2C_r}{\epsilon_{15}}\|\nabla\zeta^{n+1}\|^2 + \frac{\epsilon_{15}}{r}\|\nabla\phi_h^{n+1}\|^2,$$

$$|-PrRa(\gamma\psi^{n+1},\phi_h^{n+1+})| \leq \frac{Pr^2Ra^2C_{PF,1}^2C_{PF,2}^2C_r}{\epsilon_{16}}\|\nabla\psi^{n+1}\|^2 + \frac{\epsilon_{16}}{r}\|\nabla\phi_h^{n+1}\|^2,$$

Introducing the inequalities into the temperature and velocity equations and multiplying by Δt:

$$\begin{aligned}&\frac{1}{2}\Big\{\|\psi_h^{n+1}\|^2 - \|\psi_h^n\|^2 + \|\psi_h^{n+1}-\psi_h^n\|^2\Big\} + \kappa\Delta t\|\nabla\psi_h^{n+1}\|^2 \\ &\quad\leq \frac{\Delta tC_rC_{PF,2}^2}{\epsilon_1}\|\zeta_t\|^2_{L^\infty(t^n,t^{n+1};L^2(\Omega))} + \frac{\Delta t\epsilon_1}{r}\|\nabla\psi_h^{n+1}\|^2 + \frac{C_r\kappa\Delta t}{\epsilon_2}\|\nabla\zeta^{n+1}\|^2 \\ &\quad+ \frac{\Delta t\epsilon_2}{r}\|\nabla\psi_h^{n+1}\|^2 + \frac{\overline{C}^2C_r\Delta t}{\epsilon_3}\|\nabla u^{n+1}\|^2\|\nabla\zeta^{n+1}\|^2 + \frac{\Delta t\epsilon_3}{r}\|\nabla\psi_h^{n+1}\|^2 \\ &\quad+ \frac{C_r\overline{C}^2\Delta t^3}{\epsilon_4}\|\nabla T_h^{n+1}\|^2\|\nabla u_t\|^2_{L^\infty(t^n,t^{n+1};L^2(\Omega))} + \frac{\Delta t\epsilon_4}{r}\|\nabla\psi_h^{n+1}\|^2 + \frac{\overline{C}_rC^2\Delta t}{\epsilon_5}\|\nabla\eta^n\|^2\|\nabla T_h^{n+1}\|^2 \\ &\quad+ \frac{\Delta t\epsilon_5}{r}\|\nabla\psi_h^{n+1}\|^2 + \frac{C_2C_T\Delta t\epsilon_6}{2}\|\nabla\psi_h^{n+1}\|^2 + \frac{C_2C_T\Delta t\delta_6}{4\epsilon_6}\|\nabla\phi_h^n\|^2 \\ &\quad+ \frac{C_2C_T\Delta t}{4\epsilon_6\delta_6}\|\phi^n\|^2 + \frac{C_r\overline{C}^2\Delta t}{\epsilon_7}\|\nabla u_h'^n\|^2\|\nabla\zeta^{n+1}\|^2 + \frac{\Delta t\epsilon_7}{r}\|\nabla\psi_h^{n+1}\|^2 \\ &\quad+ \frac{C_r\overline{C}^2\Delta t}{\epsilon_8}\|\nabla u_h'^n\|^2\|\nabla\zeta^n\|^2 + \frac{\Delta t\epsilon_8}{r}\|\nabla\psi_h^{n+1}\|^2 + \frac{\overline{C}^*\Delta t^2}{h\epsilon_9}\|\nabla u_h'^n\|^2\|\nabla\psi_h^{n+1}\|^2 \\ &\quad+ \frac{\epsilon_9}{2}\|\psi_h^{n+1}-\psi_h^n\|^2 + \frac{C_r\overline{C}^2\Delta t^3}{\epsilon_{10}}\|\nabla u_h'^n\|^2\|\nabla T_t\|^2_{L^\infty(t^n,t^{n+1};L^2(\Omega))} + \frac{\Delta t\epsilon_{10}}{r}\|\nabla\psi_h^{n+1}\|^2 \\ &\quad+ \frac{C_{PF,2}^2C_r\Delta t^3}{\epsilon_{11}}\|T_{tt}\|^2_{L^\infty(t^n,t^{n+1};L^2(\Omega))} + \frac{\epsilon_{11}}{r}\|\nabla\psi_h^{n+1}\|^2.\end{aligned}$$

and

$$
\begin{aligned}
&\frac{1}{2}\Big\{\|\phi_h^{n+1}\|^2-\|\phi_h^n\|^2+\|\phi_h^{n+1}-\phi_h^n\|^2\Big\}+Pr\Delta t\|\nabla\phi_h^{n+1}\|^2\\
&\quad\le\frac{\Delta tC_rC_{PF,1}^2}{\epsilon_{12}}\|\eta_t\|^2_{L^\infty(t^n,t^{n+1};L^2(\Omega))}+\frac{\Delta t\epsilon_{12}}{r}\|\nabla\phi_h^{n+1}\|^2+\frac{C_rPr\Delta t}{\epsilon_{13}}\|\nabla\eta^{n+1}\|^2\\
&\quad+\frac{\Delta t\epsilon_{13}}{r}\|\nabla\phi_h^{n+1}\|^2+\frac{dC_r\Delta t}{\epsilon_{14}}\|p^{n+1}-q_h^{n+1}\|^2+\frac{\Delta\epsilon_{14}}{r}\|\nabla\phi_h^{n+1}\|^2\\
&\quad+\Delta tPr^2Ra^2C_{PF,1}^2C_{PF,2}^2C_r\big(\frac{1}{\epsilon_{15}}\|\nabla\zeta^{n+1}\|^2+\frac{1}{\epsilon_{16}}\|\nabla\psi_h^{n+1}\|^2\big)\\
&\quad+\frac{\Delta t}{r}\big(\frac{1}{\epsilon_{15}}\|\nabla\phi_h^{n+1}\|^2+\frac{1}{\epsilon_{16}}\|\nabla\phi_h^{n+1}\|^2\big)+\frac{C'C_r\Delta t}{\epsilon_{17}}\|\nabla u^{n+1}\|^2\|\nabla\eta^{n+1}\|^2\\
&\quad+\frac{\Delta t\epsilon_{17}}{r}\|\nabla\phi_h^{n+1}\|^2+\frac{C_rC'^2\Delta t^3}{\epsilon_{18}}\|\nabla u_h^{n+1}\|^2\|\nabla u_t\|^2_{L^\infty(t^n,t^{n+1};L^2(\Omega))}+\frac{\Delta t\epsilon_{18}}{r}\|\nabla\phi_h^{n+1}\|^2\\
&\quad+\frac{C_rC'\Delta t}{\epsilon_{19}}\|\nabla\eta^n\|^2\|\nabla u_h^{n+1}\|^2+\frac{\Delta t\epsilon_{19}}{r}\|\nabla\phi_h^{n+1}\|^2+\frac{C_1C_u\Delta t\epsilon_{20}}{2}\|\nabla\phi_h^{n+1}\|^2\\
&\quad+\frac{C_1C_u\Delta t\delta_{20}}{4\epsilon_{20}}\|\nabla\phi_h^n\|^2+\frac{C_1C_u\Delta t}{4\epsilon_{20}\delta_{20}}\|\phi^n\|^2+\frac{C_rC'^2\Delta t}{\epsilon_{21}}\|\nabla u_h'^n\|^2\|\nabla\eta^{n+1}\|^2\\
&\quad+\frac{\Delta t\epsilon_{21}}{r}\|\nabla\phi_h^{n+1}\|^2+\frac{C_rC'\Delta t}{\epsilon_{22}}\|\nabla u_h'^n\|^2\|\nabla\eta^n\|^2+\frac{\Delta t\epsilon_{22}}{r}\|\nabla\phi_h^{n+1}\|^2\\
&\quad+\frac{C^*\Delta t^2}{h\epsilon_{23}}\|\nabla u_h'^n\|^2\|\nabla\phi_h^{n+1}\|^2+\frac{\epsilon_{23}}{2}\|\phi_h^{n+1}-\phi_h^n\|^2+\frac{C_rC'\Delta t^3}{\epsilon_{24}}\|\nabla u_h'^n\|^2\|\nabla u_t\|^2_{L^\infty(t^n,t^{n+1};L^2(\Omega))}\\
&\quad+\frac{\Delta t\epsilon_{24}}{r}\|\nabla\phi_h^{n+1}\|^2+\frac{C_{PF,1}^2C_r\Delta t^3}{\epsilon_{26}}\|u_{tt}\|^2_{L^\infty(t^n,t^{n+1};L^2(\Omega))}+\frac{\Delta\epsilon_{26}}{r}\|\nabla\phi_h^{n+1}\|^2.
\end{aligned}
$$

Combining, choosing free parameters appropriately, using the time-step condition in stability, and taking maximum over constants (leaving Δt) yields

$$
\begin{aligned}
&\frac{1}{2}\big(\|\psi_h^{n+1}\|^2-\|\psi_h^n\|^2\big)+\frac{1}{4}\|\psi_h^{n+1}-\psi_h^n\|^2+\frac{\kappa\Delta t}{4}\big(\|\nabla\psi_h^{n+1}\|^2-\|\nabla\psi_h^n\|^2\big)\\
&\quad+\frac{1}{2}\big(\|\phi_h^{n+1}\|^2-\|\phi_h^n\|^2\big)+\frac{1}{4}\|\phi_h^{n+1}-\phi_h^n\|^2+\frac{Pr\Delta t}{4}\big(\|\nabla\phi_h^{n+1}\|^2-\|\nabla\phi_h^n\|^2\big)\\
&\quad\le C\Big\{\Delta t\|\zeta_t\|^2_{L^\infty(t^n,t^{n+1};L^2(\Omega))}+\Delta t\|\nabla\zeta^{n+1}\|^2+\Delta t\|\nabla u^{n+1}\|^2\|\nabla\zeta^{n+1}\|^2\\
&\quad+\Delta t^3\|\nabla T_h^{n+1}\|^2\|\nabla u_t\|^2_{L^\infty(t^n,t^{n+1};L^2(\Omega))}+\Delta t\|\nabla\eta^n\|^2\|\nabla T_h^{n+1}\|^2+\Delta t\|\phi^n\|^2\\
&\quad+\Delta t\|\nabla u_h'^n\|^2\|\nabla\zeta^{n+1}\|^2+\Delta t\|\nabla u_h'^n\|^2\|\nabla\zeta^n\|^2+\Delta t^3\|\nabla u_h'^n\|^2\|\nabla T_t\|^2_{L^\infty(t^n,t^{n+1};L^2(\Omega))}\\
&\quad+\Delta t^3\|T_{tt}\|^2_{L^\infty(t^n,t^{n+1};L^2(\Omega))}+\Delta t\|p^{n+1}-q_h^{n+1}\|^2+\Delta t\|\eta_t\|^2_{L^\infty(t^n,t^{n+1};L^2(\Omega))}+\Delta t\|\nabla\eta^{n+1}\|^2\\
&\quad+\Delta t\|\nabla\zeta^{n+1}\|^2+\Delta t\|\nabla u^{n+1}\|^2\|\nabla\eta^{n+1}\|^2+\Delta t^3\|\nabla u_h^{n+1}\|^2\|\nabla u_t\|^2_{L^\infty(t^n,t^{n+1};L^2(\Omega))}\\
&\quad+\Delta t\|\nabla\eta^n\|^2\|\nabla u_h^{n+1}\|^2+\Delta t\|\nabla u_h'^n\|^2\|\nabla\eta^{n+1}\|^2+\Delta t\|\nabla u_h'^n\|^2\|\nabla\eta^n\|^2\\
&\quad+\Delta t^3\|\nabla u_h'^n\|^2\|\nabla u_t\|^2\|\nabla u_h^{n+1}\|^2+\Delta t^3\|u_{tt}\|^2\|\nabla u_h^{n+1}\|^2\Big\}.
\end{aligned}
$$

Multiplying by two, summing over n from $n = 0$ to $n = N-1$, applying the discrete Gronwall Lemma, and renorming yields

$$\begin{aligned}
&\|\psi_h^N\|^2 + \|\phi_h^N\|^2 + \frac{1}{2}\sum_{n=0}^{N-1}\left(\|\psi_h^{n+1} - \psi_h^n\|^2 + \|\phi_h^{n+1} - \phi_h^n\|^2\right) + \frac{\kappa\Delta t}{2}\|\nabla\psi_h^N\|^2 + \frac{Pr\Delta t}{2}\|\nabla\phi_h^N\|^2 \\
&\quad \le C\Big\{(2 + \|\nabla u^{n+1}\|^2 + \|\nabla u_h'^n\|^2)\Delta t|||\nabla\zeta|||_{\infty,0}^2 \\
&\quad + (1 + \|\nabla T_h^{n+1}\|^2 + \|\nabla u^{n+1}\|^2 + \|\nabla u_h^{n+1}\|^2 + 2\|\nabla u_h'^n\|^2)\Delta t|||\nabla\eta|||_{\infty,0}^2 \\
&\quad + \Delta t|||\zeta_t|||_{\infty,0}^2 + \left(\|\nabla T_h^{n+1}\|^2 + \|\nabla u_h^{n+1}\|^2 + \|u_h'^n\|^2\right)\Delta t^3|||\nabla u_t|||_{\infty,0}^2 \\
&\quad + \Delta t^3\|u_h'^n\|^2|||\nabla T_t|||_{\infty,0}^2 + \Delta t^3|||T_{tt}|||_{2,0}^2 + \Delta t|||p - q_h|||_{\infty,0}^2 + \Delta t|||\eta_t|||_{\infty,0}^2 + \Delta t^3|||u_{tt}|||_{\infty,0}^2\Big\} \\
&\quad + \|\psi_h^0\|^2 + \frac{\kappa\Delta t}{2}\|\nabla\psi_h^0\|^2 + \|\phi_h^0\|^2 + \frac{Pr\Delta t}{2}\|\nabla\phi_h^0\|^2 \\
&\quad \le C\Big\{\Delta t|||\nabla\zeta|||_{\infty,0}^2 + \Delta t|||\nabla\eta|||_{\infty,0}^2 + \Delta t|||\zeta_t|||_{\infty,0}^2 + \Delta t^3|||\nabla u_t|||_{\infty,0}^2 \\
&\quad + \Delta t^3|||\nabla T_t|||_{\infty,0}^2 + \Delta t|||p - q_h|||_{\infty,0}^2 + \Delta t|||\eta_t|||_{\infty,0}^2 + \Delta t^3|||u_{tt}|||_{\infty,0}^2\Big\} \\
&\quad + \|\psi_h^0\|^2 + \frac{\kappa\Delta t}{2}\|\nabla\psi_h^0\|^2 + \|\phi_h^0\|^2 + \frac{Pr\Delta t}{2}\|\nabla\phi_h^0\|^2.
\end{aligned}$$

Applying Lemma 4.2.1, the approximation assumptions 2.1, and triangle inequality gives

$$\begin{aligned}
&\|e_T^N\|^2 + \|e_u^N\|^2 + \frac{1}{2}\sum_{n=0}^{N-1}\left(\|e_T^{n+1} - e_T^n\|^2 + \|e_u^{n+1} - e_u^n\|^2\right) + \frac{\kappa\Delta t}{2}\|\nabla e_T^N\|^2 + \frac{Pr\Delta t}{2}\|\nabla e_u^N\|^2 \\
&\quad \le C\Big\{\Delta t h^{2k}|||T|||_{\infty,k+1}^2 + \Delta t h^{2k}|||u|||_{\infty,k+1}^2 + \Delta t h^{2k+2}|||T_t|||_{\infty,k+1}^2 + \Delta t^3|||\nabla u_t|||_{\infty,k+1}^2 \\
&\quad + \Delta t^3|||\nabla T_t|||_{\infty,0}^2 + \Delta t^3|||T_{tt}|||_{\infty,0}^2 + \Delta t h^{2k}|||p|||_{\infty,k}^2 + \Delta t h^{2k+2}|||u_t|||_{\infty,k+1}^2 + \Delta t^3|||u_{tt}|||_{\infty,0}^2\Big\} \\
&\quad + C\left(\|\zeta_h^0\|^2 + \frac{\kappa\Delta t}{2}\|\nabla\zeta_h^0\|^2 + \|\eta_h^0\|^2 + \frac{Pr\Delta t}{2}\|\nabla\eta_h^0\|^2\right) + \|e_T^0\|^2 + \|e_u^0\|^2 \\
&\quad + \frac{\kappa\Delta t}{2}\|\nabla e_T^0\|^2 + \frac{Pr\Delta t}{2}\|\nabla e_u^0\|^2 \\
&\quad \le C(\Delta t h^{2k} + \Delta t h^{2k+2} + \Delta t^3 + \Delta t\|\nabla\eta_h^0\|^2 + \Delta t\|\nabla\zeta_h^0\|^2 + \|\eta_h^0\|^2 \\
&\quad + \|\zeta_h^0\|^2 + \|e_T^0\|^2 + \|e_u^0\|^2 + \Delta t\|\nabla e_T^0\|^2 + \Delta t\|\nabla e_u^0\|^2).
\end{aligned}$$

□

After bounding the error in the velocity, we show a bound for the error in the pressure of the system (4.28)-(4.29).

Theorem 4.5.2. *Suppose the assumptions of Theorem 4.4.1 hold. Then the error in the pressure satisfies*

$$\Delta t \sum_{n=0}^{N-1} \|e_p^{n+1}\| \leq C\Delta t \sum_{n=0}^{N-1} \Big\{ \|\nabla e_u^{n+1}\| + \|\nabla e_u^n\| + \Delta t \|\nabla u_t\|_{L^\infty(t^n,t^{n+1};L^2(\Omega))} + \|p^{n+1} - q_h^{n+1}\| + \|e_T^{n+1}\| + \Delta t \|u_{tt}\|_{L^\infty(t^n,t^{n+1};L^2(\Omega))} \Big\}.$$

Proof. Begin with the error equation for the velocity,

$$\begin{aligned}(\frac{e_u^{n+1} - e_u^n}{\Delta t}, v_h) + b(u^{n+1}, u^{n+1}, v_h) - b(u_h^n - {u'}_h^n, u_h^{n+1}, v_h) \\ - b({u'}_h^n, u_h^n, v_h) + Pr(\nabla e_u^{n+1}, \nabla v_h) - (e_p^{n+1}, \nabla \cdot v_h) \\ = PrRa(\gamma e_T^{n+1}, v_h) + \tau(u^{n+1}; v_h).\end{aligned}$$

As in the proof of Theorem 4.4.1, add/subtract $b(u^{n+1} - u^n, u_h^{n+1}, v_h)$ and $b({u'}_h^n, u^{n+1} - u^n, v_h)$ which leads to

$$\begin{aligned}(\frac{e_u^{n+1} - e_u^n}{\Delta t}, v_h) + b(u^{n+1}, e_u^{n+1}, v_h) + b(e^n, u_h^{n+1}, v_h) + b(u^{n+1} - u^n, u_h^{n+1}, v_h) \\ + b({u'}_h^n, e_u^n, v_h) - b({u'}_h^n, e_u^{n+1}, v_h) + b({u'}_h^n, u^{n+1} - u^n, v_h) + Pr(\nabla e_u^{n+1}, \nabla v_h) \\ - (e_p^{n+1}, \nabla \cdot v_h) = PrRa(\gamma e_T^{n+1}, v_h) + \tau(u^{n+1}; v_h).\end{aligned}$$

We now isolate $(\frac{e_u^{n+1} - e_u^n}{\Delta t}, v_h)$ and estimate the explicitly skew-symmetric trilinear terms. Apply Lemma 2.0.1 on each to obtain

$$|-b(u^{n+1}, e_u^{n+1}, v_h)| \leq C\|\nabla u^{n+1}\|\|\nabla e_u^{n+1}\|\|\nabla v_h\|,$$

$$|-b(e_u^n, u_h^{n+1}, v_h)| \leq C\|\nabla e_u^n\|\|\nabla u_h^{n+1}\|\|\nabla v_h\|,$$

$$|-b(u^{n+1} - u^n, u_h^{n+1}, v_h)| \leq C\|\nabla u^{n+1} - u^n\|\|\nabla u_h^{n+1}\|\|\nabla v_h\|,$$

$$|-b({u'}_h^n, e_u^n, v_h)| \leq C\|\nabla {u'}_h^n\|\|\nabla e_u^n\|\|\nabla v_h\|,$$

$$|b({u'}_h^n, e_u^{n+1}, v_h)| \leq C\|\nabla {u'}_h^n\|\|\nabla e_u^{n+1}\|\|\nabla v_h\|,$$

$$|b({u'}_h^n, u^{n+1} - u^n, v_h)| \leq C\|\nabla {u'}_h^n\|\|\nabla (u^{n+1} - u^n)\|\|\nabla v_h\|.$$

If we let $v_h \in V_h$, we have that $(e_p^{n+1}, \nabla \cdot v_h) = (p^{n+1} - q_h^{n+1}, \nabla \cdot v_h)$ since $p_h^{n+1} \in Q_h$. We can estimate this term as follows

$$|(p^{n+1} - q_h^{n+1}, \nabla \cdot v_h)| \leq \sqrt{d}\|p^{n+1} - q_h^{n+1}\|\|\nabla v_h\|.$$

Further, using the usual techniques employed earlier, we have

$$|-Pr(\nabla e_u^{n+1}, \nabla v_h)| \leq Pr\|\nabla e_u^{n+1}\|\|\nabla v_h\|,$$

$$|PrRa(\gamma e_T^{n+1}, v_h)| \leq PrRaC_{PF,2}\|e_T^{n+1}\|\|\nabla v_h\|,$$

$$|\tau(u^{n+1}; v_h)| \leq C_{PF,2}\Delta t\|u_{tt}\|^2_{L^\infty(t^n, t^{n+1}; L^2(\Omega))}\|\nabla v_h\|.$$

Combining all estimates and dividing by $\|\nabla v_h\|$ on both sides leads to

$$\begin{aligned}
\frac{1}{\Delta t}\frac{(e_u^{n+1} - e_u^n, v_h)}{\|\nabla v_h\|} &\leq C(\|\nabla u^{n+1}\| + \|\nabla u'^n_h\| + Pr)\|\nabla e_u^{n+1}\| \\
&+ C(\|\nabla u_h^{n+1}\| + \|\nabla u'^n_h\|)\|\nabla e_u^n\| \\
&+ C(\|\nabla u'^n_h\| + C_{PF,2} + \|\nabla u_h^{n+1}\|)\Delta t\|\nabla u_t\|^2_{L^\infty(t^n, t^{n+1}; L^2(\Omega))} \\
&+ \sqrt{d}\|p^{n+1} - q_h^{n+1}\| + PrRaC_{PF,2}\|e_T^{n+1}\| + C_{PF,2}\Delta t\|u_{tt}\|^2_{L^\infty(t^n, t^{n+1}; L^2(\Omega))}.
\end{aligned}$$

Taking the supremum over all $0 \neq v_h \in V_h$,

$$\begin{aligned}
\frac{1}{\Delta t}\|e_u^{n+1} - e_u^n\|_* &\leq C(\|\nabla u^{n+1}\| + \|\nabla u'^n_h\| + Pr)\|\nabla e_u^{n+1}\| \\
&+ C(\|\nabla u_h^{n+1}\| + \|\nabla u'^n_h\|)\|\nabla e_u^n\| \\
&+ C(\|\nabla u'^n_h\| + C_{PF,2} + \|\nabla u_h^{n+1}\|)\Delta t\|\nabla u_t\|^2_{L^\infty(t^n, t^{n+1}; L^2(\Omega))} \\
&+ \sqrt{d}\|p^{n+1} - q_h^{n+1}\| + PrRaC_{PF,2}\|e_T^{n+1}\| + C_{PF,2}\Delta t\|u_{tt}\|^2_{L^\infty(t^n, t^{n+1}; L^2(\Omega))}.
\end{aligned}$$

Now that we have a bound for this term, consider the error equation for velocity and decompose $p^{n+1} - p_h^{n+1} = (p^{n+1} - q_h^{n+1})$ - $(p_h^{n+1} - q_h^{n+1})$. Isolate terms involving the former,

$$\begin{aligned}(p_h^{n+1} - q_h^{n+1}, \nabla \cdot v_h) = &-(\frac{e_u^{n+1} - e_u^n}{\Delta t}, v_h) - b(u^{n+1}, e_u^{n+1}, v_h) - b(e^n, u_h^{n+1}, v_h) \\ &- b(u^{n+1} - u^n, u_h^{n+1}, v_h) - b(u'^n_h, e_u^n, v_h) + b(u'^n_h, e_u^{n+1}, v_h) \\ &- b(u'^n_h, u^{n+1} - u^n, v_h) - Pr(\nabla e_u^{n+1}, \nabla v_h) + (p^{n+1} - q_h^{n+1}, \nabla \cdot v_h) \\ &+ PrRa(\gamma e_T^{n+1}, v_h) + \tau(u^{n+1}; v_h).\end{aligned}$$

Using previous estimates on the right hand side terms, dividing by $\|\nabla v_h\|$ on both sides,

$$\begin{aligned}\frac{(p_h^{n+1} - q_h^{n+1}, \nabla \cdot v_h)}{\|\nabla v_h\|} \leq &\, C(\|\nabla u^{n+1}\| + \|\nabla u'^n_h\| + Pr)\|\nabla e_u^{n+1}\| \\ &+ C(\|\nabla u_h^{n+1}\| + \|\nabla u'^n_h\|)\|\nabla e_u^n\| \\ &+ C(\|\nabla u'^n_h\| + C_{PF,2} + \|\nabla u_h^{n+1}\|)\Delta t\|\nabla u_t\|^2_{L^\infty(t^n, t^{n+1}; L^2(\Omega))} \\ &+ 2\sqrt{d}\|p^{n+1} - q_h^{n+1}\| + 2PrRaC_{PF,2}\|e_T^{n+1}\| \\ &+ 2C_{PF,2}\Delta t\|u_{tt}\|^2_{L^\infty(t^n, t^{n+1}; L^2(\Omega))}.\end{aligned}$$

Take the supremum over all $0 \neq v_h \in X_h$ and use the inf-sup condition,

$$\begin{aligned}\beta\|p_h^{n+1} - q_h^{n+1}\| \leq &\, C\Big(\|\nabla u^{n+1}\| + \|\nabla u'^n_h\| + Pr\Big)\|\nabla e_u^{n+1}\| \\ &+ C\Big(\|\nabla u_h^{n+1}\| + \|\nabla u'^n_h\|\Big)\|\nabla e_u^n\| \\ &+ C\Big(\|\nabla u'^n_h\| + C_{PF,2} + \|\nabla u_h^{n+1}\|\Big)\Delta t\|\nabla u_t\|^2_{L^\infty(t^n, t^{n+1}; L^2(\Omega))} \\ &+ 2\sqrt{d}\|p^{n+1} - q_h^{n+1}\| + 2PrRaC_{PF,2}\|e_T^{n+1}\| \\ &+ 2C_{PF,2}\Delta t\|u_{tt}\|^2_{L^\infty(t^n, t^{n+1}; L^2(\Omega))}.\end{aligned}$$

Applying the triangle inequality, multiplying by Δt, summing over n from 0 to $N-1$ yields the result. □

Theorem 4.5.3. *For (u,p,T) satisfying (4.1)-(4.5), suppose the approximation assumptions hold and that $(u_h^0, p_h^0, T_h^0) \in (X_h, Q_h, W_h)$ are approximations of (u^0, p^0, T^0) to within the accuracy of the interpolant. Further, suppose that $\frac{C\Delta t}{h}\|\nabla u_h^n\|^2 \leq 1$, holds for all $j = 1, ..., J$. Then there exists a constant C such that*

$$\begin{aligned}
&\|e_T^N\|^2 + \|e_u^N\|^2 + \frac{1}{2}\sum_{n=0}^{N-1}\left(\|e_T^{n+1} - e_T^n\|^2 + \|e_u^{n+1} - e_u^n\|^2\right) + \frac{\kappa\Delta t}{2}\|\nabla e_T^N\|^2 + \frac{Pr\Delta t}{2}\|\nabla e_u^N\|^2 \\
&\leq C\Big\{\Delta t h^{2k}|||T|||^2_{\infty,k+1} + \Delta t h^{2k}|||u|||^2_{\infty,k+1} + \Delta t h^{2k+2}|||T_t|||^2_{\infty,k+1} \\
&+ \Delta t^3|||\nabla u_t|||^2_{\infty,k+1} + \Delta t^3|||\nabla T_t|||^2_{\infty,0} + \Delta t^3|||T_{tt}|||^2_{\infty,0} + \Delta t h^{2k}|||p|||^2_{\infty,k} + \Delta t h^{2k+2}|||u_t|||^2_{\infty,k+1} \\
&+ \Delta t^3|||u_{tt}|||^2_{\infty,0}\Big\} + C\big(\|\zeta_h^0\|^2 + \frac{\kappa\Delta t}{2}\|\nabla\zeta_h^0\|^2 + \|\eta_h^0\|^2 + \frac{Pr\Delta t}{2}\|\nabla\eta_h^0\|^2\big) \\
&+ \|e_T^0\|^2 + \|e_u^0\|^2 + \frac{\kappa\Delta t}{2}\|\nabla e_T^0\|^2 + \frac{Pr\Delta t}{2}\|\nabla e_u^0\|^2 \\
&\leq C(\Delta t h^{2k} + \Delta t h^{2k+2} + \Delta t^3 + \Delta t\|\nabla\eta_h^0\|^2 + \Delta t\|\nabla\zeta_h^0\|^2 + \|\eta_h^0\|^2 \\
&+ \|\zeta_h^0\|^2 + \|e_T^0\|^2 + \|e_u^0\|^2 + \Delta t\|\nabla e_T^0\|^2 + \Delta t\|\nabla e_u^0\|^2).
\end{aligned}$$

Proof. We follow the same methodology as in the previous theorem. The error equations are

$$\begin{aligned}
&(\frac{e_u^{n+1} - e_u^n}{\Delta t}, v_h) - b(u_h^n - u'^n_h, u_h^{n+1}, v_h) - b(u'^n_h, u_h^n, v_h) + Pr(\nabla e_u^{n+1}, \nabla v_h) \\
&\quad - (e_p^{n+1}, \nabla\cdot v_h) = PrRa\Big\{(\gamma T^{n+1}, v_h) - (\gamma T_h^n, v_h)\Big\} + \tau(u^{n+1}, v_h) \ \ \forall v_h \in X_h, \quad (4.88)
\end{aligned}$$

$$(q_h, \nabla e_u^{n+1}) = 0 \ \ \forall q_h \in Q_h, \quad (4.89)$$

$$\begin{aligned}
&(\frac{e_T^{n+1} - e_T^n}{\Delta t}, S_h) + b^*(u^{n+1}, T^{n+1}, S_h) - b^*(u_h^n - u'^n_h, T_h^n, S_h) - b^*(u'^n_h, T_h^n, S_h) \\
&\quad + \kappa(\nabla e_T^{n+1}, \nabla S_h) = (u_1^{n+1}, S_h) - (u_{1h}^n, S_h) + \tau(T^{n+1}, S_h) \ \ \forall S_h \in W_h. \quad (4.90)
\end{aligned}$$

Add/subtract $PrRa(\gamma T^n, v_h)$ in the velocity error equation and (u_1^n, S_h) in the temperature error equation,

$$\begin{aligned}
&(\frac{e_u^{n+1} - e_u^n}{\Delta t}, v_h) - b(u_h^n - u'^n_h, u_h^n, v_h) - b(u'^n_h, u_h^n, v_h) + Pr(\nabla e_u^{n+1}, \nabla v_h) \\
&- (e_p^{n+1}, \nabla\cdot v_h) = PrRa\Big\{(\gamma(T^{n+1} - T^n), v_h) - (\gamma e_T^n, v_h)\Big\} + \tau(u^{n+1}, v_h) \ \ \forall v_h \in X_h, \quad (4.91)
\end{aligned}$$

$$(\frac{e_T^{n+1}-e_T^n}{\Delta t},S_h)+b^*(u^{n+1},T^{n+1},S_h)-b^*(u_h^n-u'^n_h,T_h^n,S_h)-b^*(u'^n_h,T_h^n,S_h)$$
$$+\kappa(\nabla e_T^{n+1},\nabla S_h)=(u_1^{n+1}-u_1^n,S_h)-(e_{u1}^n,S_h)+\tau(T^{n+1},S_h)\ \ \forall S_h\in W_h. \quad (4.92)$$

Estimate the new terms using similar techniques as in Theorem 4.4.1:

$$\begin{aligned}|PrRa(\gamma(T^{n+1}-T^n),v_h)| &\leq \tfrac{Pr^2Ra^2C_{PF,1}^2C_r}{\epsilon}\|T^{n+1}-T^n\|^2+\tfrac{\epsilon}{r}\|\nabla v_h\|^2\\ &\leq \tfrac{const.\Delta t^2}{\epsilon}\|T_t\|^2_{L^\infty(t^n,t^{n+1};L^2(\Omega))}+\tfrac{\epsilon}{r}\|\nabla v_h\|^2,\end{aligned}$$

$$\begin{aligned}|PrRa(\gamma e_T^n,v_h)| &= |PrRa(\gamma\zeta^n,v_h)-PrRa(\gamma\psi_h^n)|\\ &\leq \tfrac{Pr^2Ra^2C_{PF,1}^2C_r}{\epsilon}(\|\zeta^n\|^2+\|\psi_h^n\|^2)+\tfrac{2\epsilon}{r}\|\nabla v_h\|^2,\end{aligned}$$

$$\begin{aligned}|(u_1^{n+1}-u_1^n,S_h)| &\leq \tfrac{C_{PF,2}^2C_r}{\epsilon}\|u_1^{n+1}-u_1^n\|^2+\tfrac{\epsilon}{r}\|\nabla S_h\|^2\\ &\leq \tfrac{const.\Delta t^2}{\epsilon}\|u_t\|^2_{L^\infty(t^n,t^{n+1};L^2(\Omega))}+\tfrac{\epsilon}{r}\|\nabla S_h\|^2,\end{aligned}$$

$$\begin{aligned}|(e_{u1}^n,S_h)| &= |(\eta_1^n,S_h)+(\phi_{1h}^n,S_h)|\\ &\leq \tfrac{Pr^2Ra^2C_{PF,1}^2C_r}{\epsilon}(\|\eta^n\|^2+\|\phi_h^n\|^2)+\tfrac{2\epsilon}{r}\|\nabla S_h\|^2.\end{aligned}$$

Apply estimates in previous theorem as well as the above estimates to arrive, sum over n from 0 to $N-1$, apply Lemma 2.0.3, triangle inequality and arrive at the result. □

Theorem 4.5.4. *Suppose the assumptions of Theorem 4.4.1 hold. Then the error in the pressure satisfies*

$$\Delta t\sum_{n=0}^{N-1}\|e_p^{n+1}\|\leq C\Delta t\sum_{n=0}^{N-1}\Big\{\|\nabla e_u^{n+1}\|+\|\nabla e_u^n\|+\Delta t\|\nabla u_t\|_{L^\infty(t^n,t^{n+1};L^2(\Omega))}$$
$$+\Delta t\|T_t\|_{L^\infty(t^n,t^{n+1};L^2(\Omega))}+\|p^{n+1}-q_h^{n+1}\|+\|e_T^n\|+\Delta t\|u_{tt}\|_{L^\infty(t^n,t^{n+1};L^2(\Omega))}\Big\}.$$

Proof. We follow the same strategy as in the proof above; we need only estimate two different terms and incorporate them in the analysis,

$$\begin{aligned}|PrRa(\gamma(T^{n+1}-T^n),v_h)| &\leq PrRaC_{PF,1}\|T^{n+1}-T^n\|\|\nabla v_h\|\\ &\leq \Delta tPRRaC_{PF,1}\|T_t\|_{L^\infty(t^n,t^{n+1};L^2(\Omega))}\|\|\nabla v_h\|,\end{aligned}$$

$$|PrRa(\gamma e_T^n,v_h)|\leq PrRaC_{PF,1}\|e_T^n\|\|\nabla v_h\|.$$

□

4.6 NUMERICAL EXPERIMENTS

In this section, we test the stability and accuracy of the numerical scheme described by (4.28)-(4.29), using Taylor-Hood elements to approximate the average velocity (piecewise continuous quadratic elements), the pressure (piecewise continuous linear elements), and the average temperature (piecewise continuous quadratic elements). The software used for all tests is FreeFem++ [93]. In these tests, $e = u - u_h$ and all errors are relative.

4.6.1 The double pane window problem

This example is taken from [21], where no exact solution is given. We solve the problem first on a fine mesh (128×128) for spatial convergence testing. The problem being considered is that of the two-dimensional flow of a Boussinesq fluid of Prandtl number 0.71 in an upright square cavity of side L. Both velocity components are zero on the boundaries. The horizontal walls are insulated, and the vertical sides are at temperatures T_h and T_c. We set $T_h = 1.0$ and $T_c = 0.0$. The gravitational vector is pointing downwards.

The solutions of this problem have been obtained for Rayleigh numbers of 10^3, 10^4, 10^5, and 10^6 at a final time $T_f = 1.0$ (Figures 11, 12, 13, 14). An 31×31 mesh is used for the Rayleigh numbers of 10^3, 10^4 and 10^5, with a time step of 10^{-2}. For $Ra = 10^6$, a finer mesh (51×51) is used, with $\Delta t = 10^{-3}$. We consider two different initial conditions for the velocity, $u_1(x, y)$ and $u_2(x, y)$. The velocity and temperature initial conditions are, respectively, $u_1 = (0.0 - \epsilon, 0.0 - \epsilon)$, $u_2 = (0.0 + \epsilon, 0.0 + \epsilon)$ and $T_0 = 0.0$, for $\epsilon = 10^{-3}$. The solutions converge to a steady state solution before the final time, and the figures are in accordance to the ones presented in [21].

Figure 10 shows the iso-values used in the results presented.

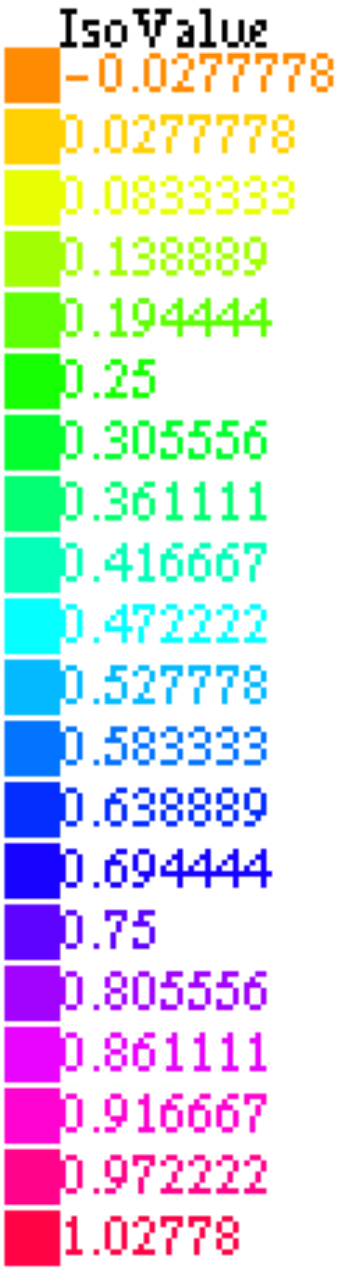

Figure 10: isovalues used for tests 1 and 2

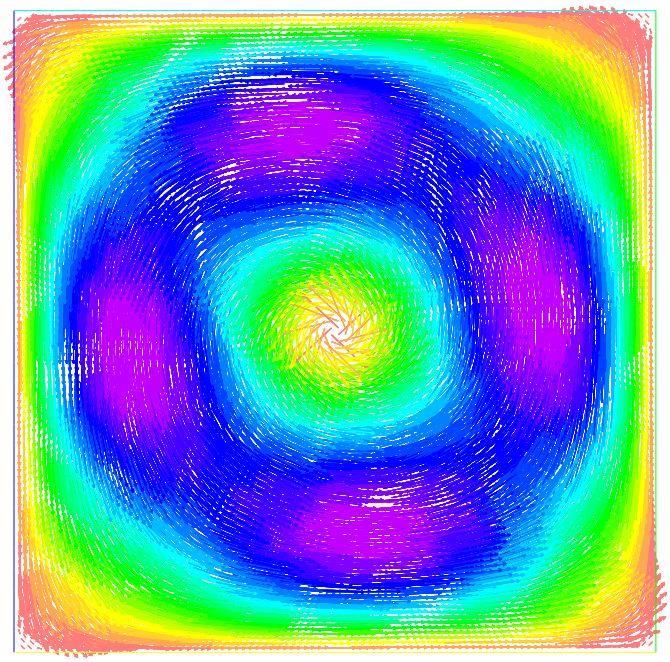

(a) Velocity

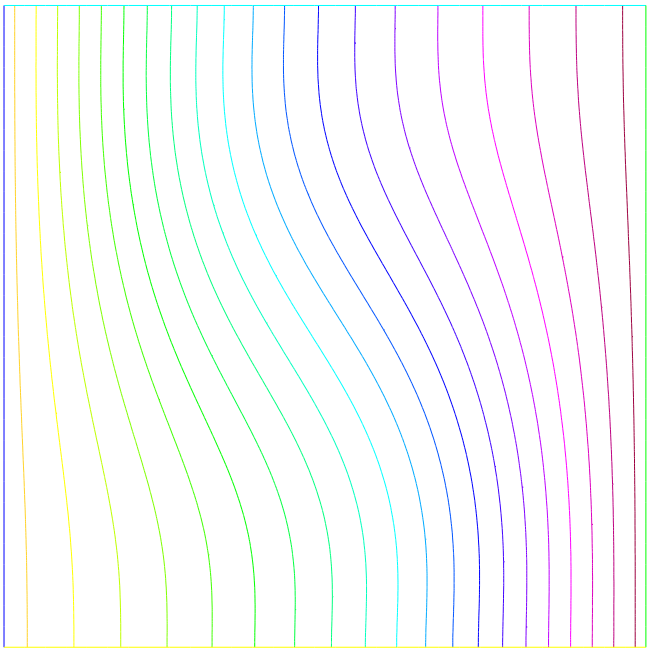

(b) Temperature

Figure 11: Average velocity (a) and temperature(b) for $Ra = 10^3$

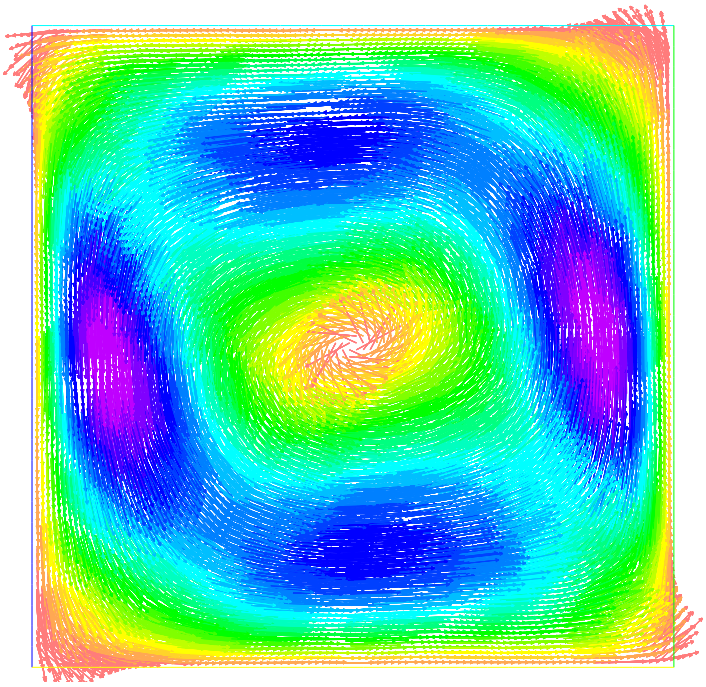

(a) Velocity

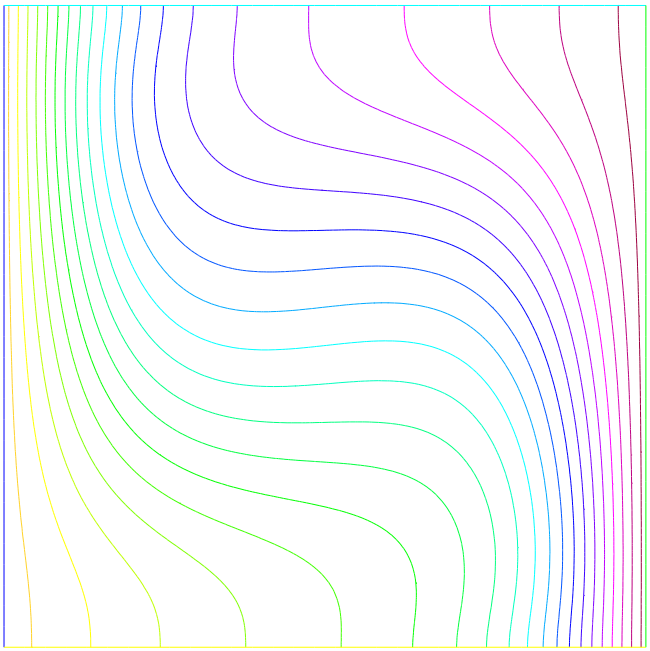

(b) Temperature

Figure 12: Average velocity (a) and temperature(b) for $Ra = 10^4$

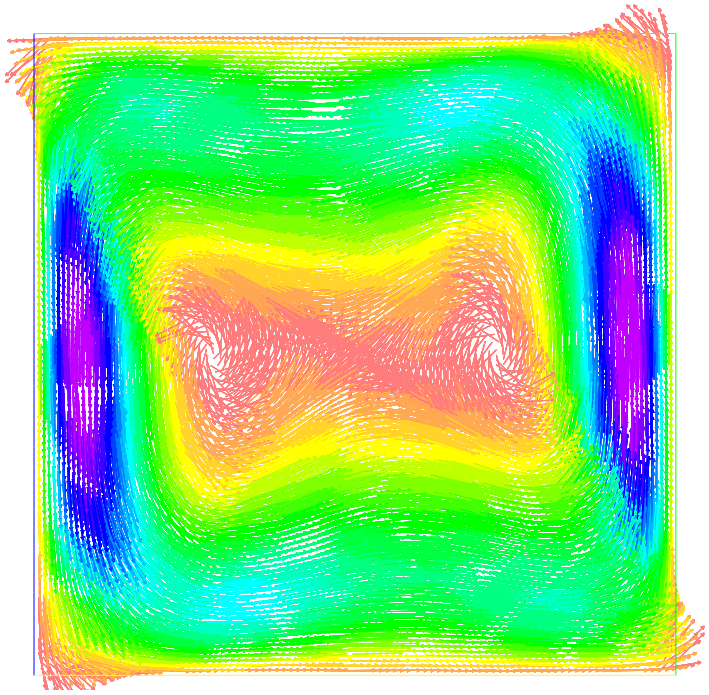

(a) Velocity

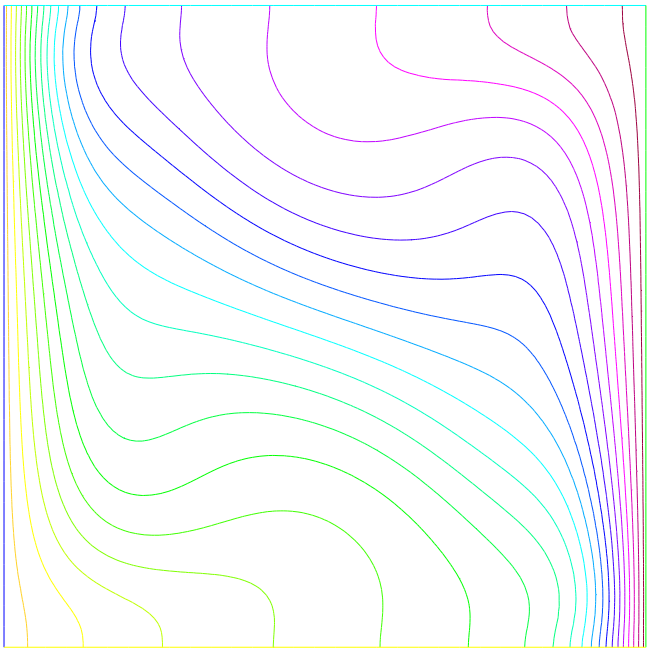

(b) Temperature

Figure 13: Average velocity (a) and temperature(b) for $Ra = 10^5$

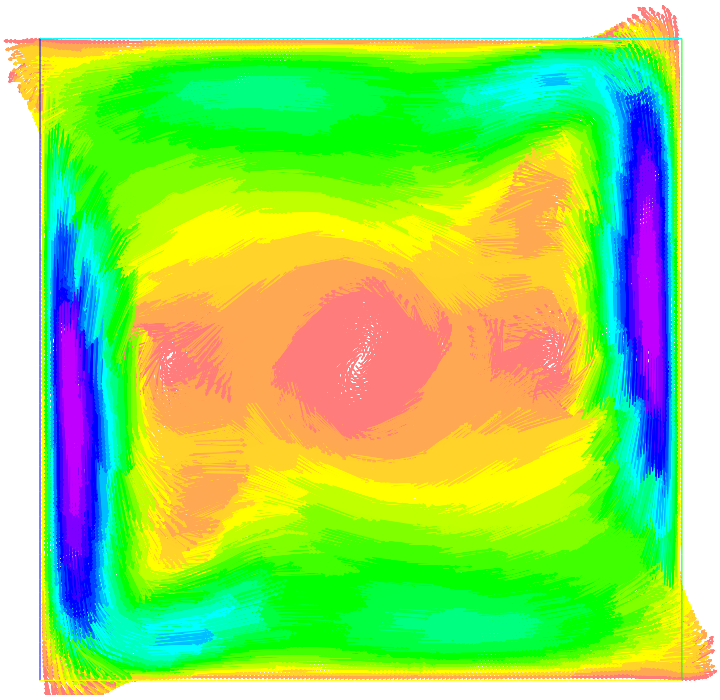

(a) Velocity

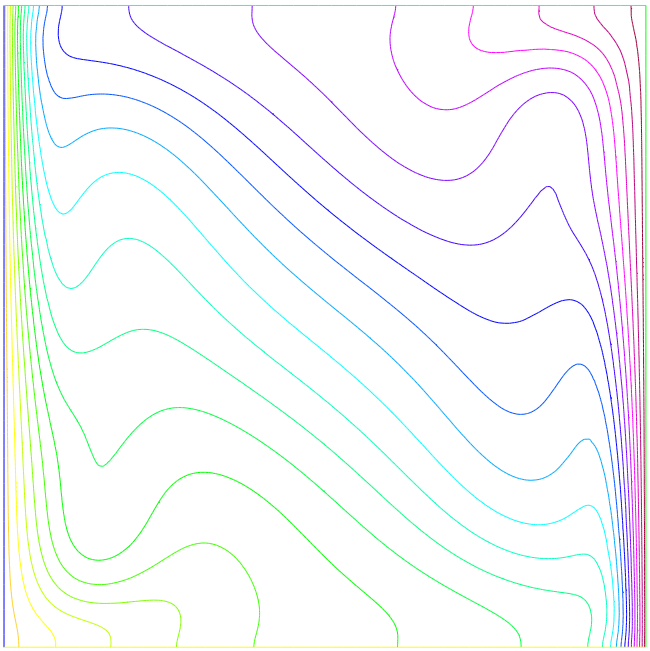

(b) Temperature

Figure 14: Average velocity (a) and temperature(b) for $Ra = 10^6$

Figures 11, 12, 13, and 14 show a circular motion of the velocity vectors: the fluid goes upwards near the hot wall gets cooler as it approaches the cold boundary and then goes downwards near the cold wall, the fact that creates a circular motion; a phenomenon that is well explained by the physics of nature.

Table 4 shows the spatial and temporal convergence rates. As predicted by the theory, the numerical tests confirm second order accuracy in space and first order in time (for the H_1 norm). To test spatial convergence, 4 meshes of different sizes were considered with h ranging from 2^{-5} to 2^{-2}. As for the temporal convergence, 5 different time steps were used, ranging from $\Delta t = 10^{-1}$ to $\Delta t = \frac{10^{-1}}{2^4}$. The errors are being evaluated at a final time $T_F = 1.0$. The norm used to calculate the error for each h is the L^2 norm. Letting $\tilde{u} = (\tilde{u}_1, \tilde{u}_2)$ be the solution for the fine 128×128 mesh, which is considered as the reference solution; and let $u_h = (u_1, u_2)$ be the approximate solution obtained by the algorithm for a certain h, then, for the mesh ThF,

$$\|u_h - \tilde{u}\|_{L^2} = \sqrt{\int_{ThF} ((u_1 - \tilde{u}_1)^2 + (u_2 - \tilde{u}_2)^2) dxdy};$$

Similarly, letting $\tilde{T}$ be the solution for the fine 128×128 mesh, which is considered as the reference solution; and let T_h be the approximate solution obtained by the algorithm for a certain h, then, for the mesh ThF,

$$\|T_h - \tilde{T}\|_{L^2} = \sqrt{\int_{ThF} (T_h - \tilde{T})^2 dxdy};$$

	Spatial convergence rate	Temporal convergence rate
velocity	2.0	1.4
temperature	2.3	1.26

Table 4: Spatial and temporal convergence rates, Double pane window

4.6.2 The annulus example

We consider an annular domain Ω, with $\partial\Omega = C_1 \cup C_2$, where C_1 is the circle of center $(0,0)$ and radius r and C_2 the circle of center $(0,0)$ and radius $2r$ (we take $r = 1.0$). The normalized gravity vector $\vec{g} = (0,-1)$ is pointing downwards. We discretize the mesh using 50 points on C_1 and 100 on C_2, with a time step $\Delta t = 0.01$. The final result is obtained at $T_f = 0.5$, for $Ra = 10^3$ and $Pr = 0.71$, with initial conditions $u_1 = (0.0-\epsilon, 0.0-\epsilon)$, $u_2 = (0.0+\epsilon, 0.0+\epsilon)$ and $T_0 = 0.0$, for $\epsilon = 10^{-3}$. The right hand sides are set to $f_1 = (0,0)$ and $f_2 = 0$. The velocity components are set to 0.0 on the boundaries. The temperature boundary conditions satisfy $T_{C_1} = 1.0$ corresponding to the hot boundary and $T_{C_2} = 0.0$ corresponding to the cold boundary. Figure 15 shows the steady state solution after convergence.

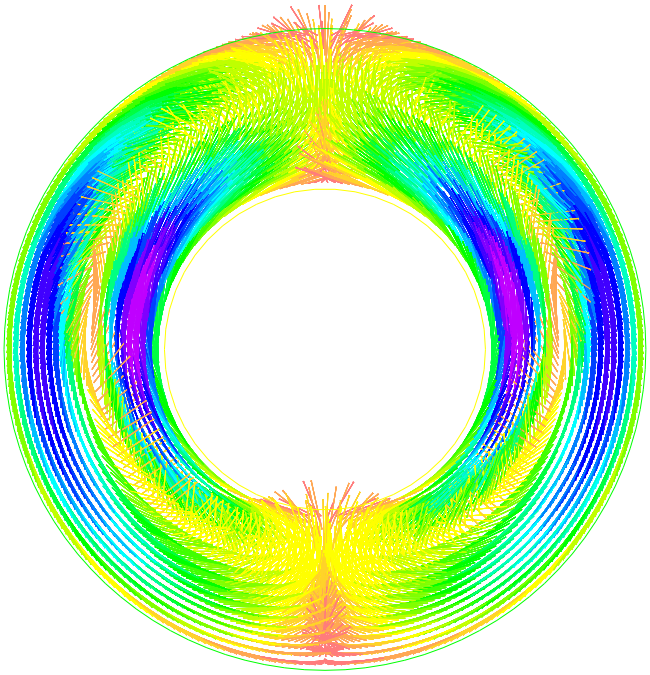

(a) Velocity

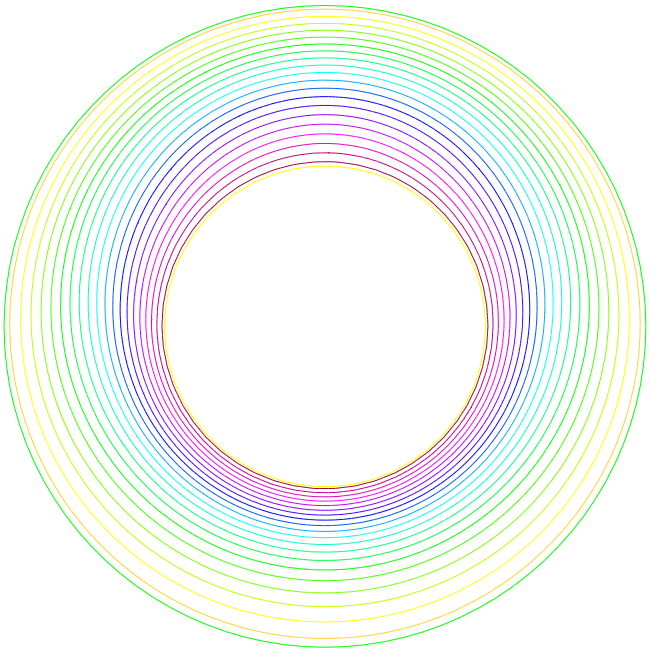

(b) Temperature

Figure 15: Average velocity (a) and temperature(b) for $Ra = 4.8e4$

4.6.3 The Earth-like example

We consider an Earth-like domain Ω, with $\partial\Omega = C_1 \cup C_2$, where C_1 is the circle of center $(0, 0)$ and radius r, representing the Earth with hot boundary; and C_2 the circle of center $(0, 0)$ and radius $2.6 \times r$ (we take $r = 1.0$), representing the atmosphere with cold boundary. The gravity vector $\vec{g} = (-x, -y)$ is pointing inwards. We discretize the mesh using 40 points on C_1 and 104 points on C_2, with a time step $\Delta t = 10^{-2}$. We set $Ra = 4.8e4$ and $Pr = 0.706$, with initial conditions $u_1 = (0.0, 0.0)$, $u_2 = (0.0 + \epsilon, 0.0 + \epsilon)$ and $T_0 = 0.0$, for $\epsilon = 10^{-3}$. The velocity components are set to 0.0 on the boundaries. The temperature boundary conditions satisfy $T_{C_1} = 5.0$ and $T_{C_2} = 0.0$. The velocity and temperature at $T_F = 1.0$ and $T_F = 0.3$ are shown in Figures 17 and 18 respectively. The Earth-like example has no documented exact solution.

Figure 16 show the isovalues used for the Earth-like test.

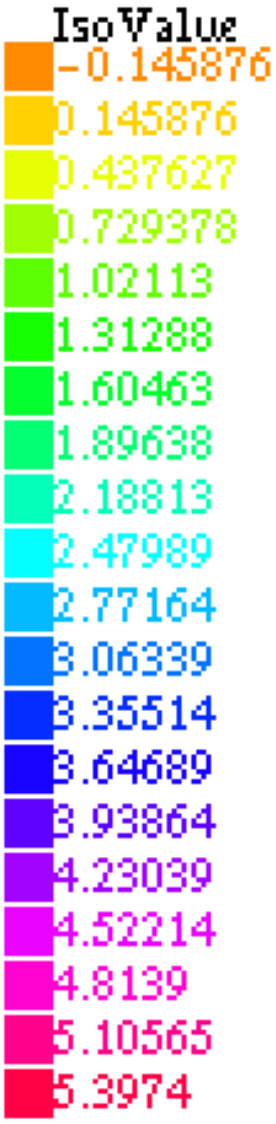

Figure 16: isovalues used for tests 1 and 2

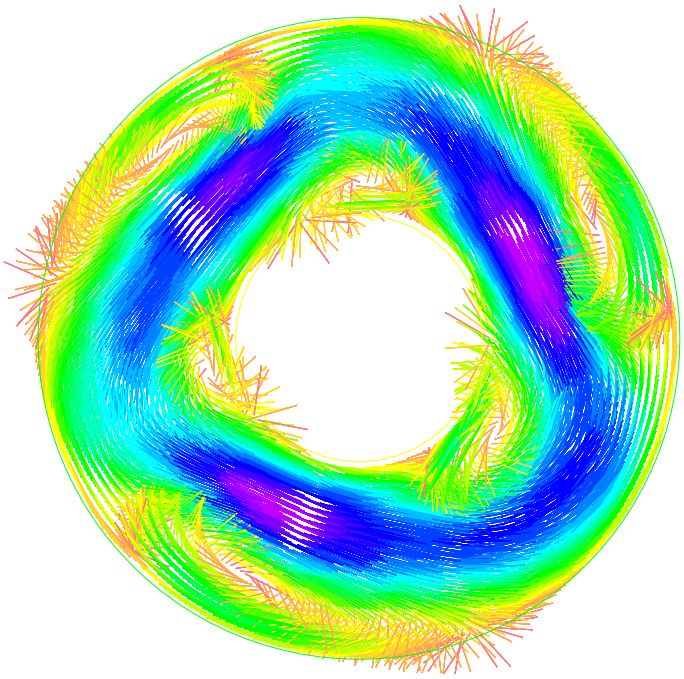

(a) Velocity, $Ra = 4.8e4$

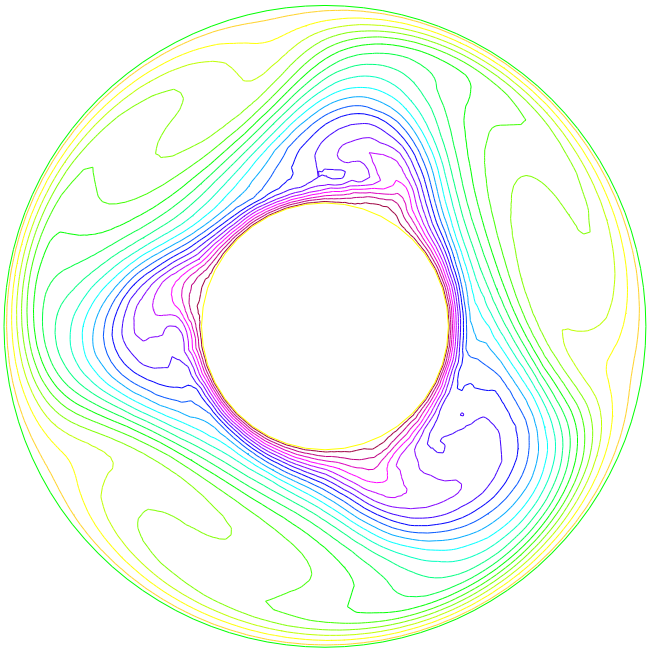

(b) Temperature, $Ra = 4.8e4$

Figure 17: Earth-like example at $T_F = 1.0$.

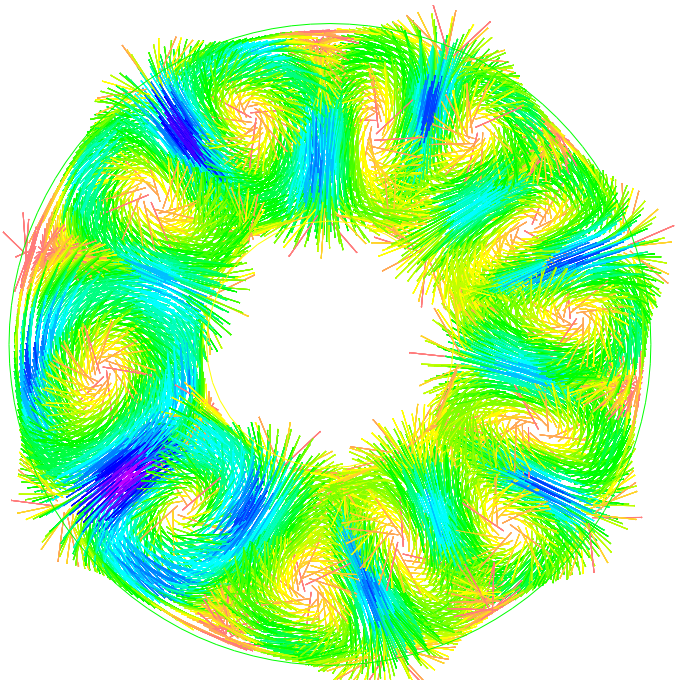

(a) Velocity, $Ra = 4.8e4$

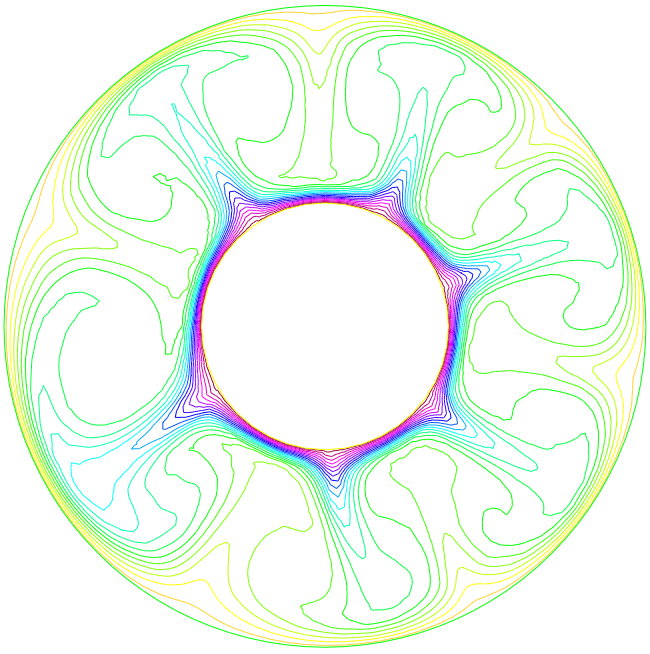

(b) Temperature, $Ra = 4.8e4$

Figure 18: Earth-like example at $T_F = 0.3$.

Figures 17 and 18 show a circular motion of the velocity vectors and the development of some eddies: the fluid goes upwards near the hot boundary gets cooler as it reaches higher altitudes, and therefore gets heavier. The fluid then goes downwards near the cold boundary (the atmosphere) until it reaches again the hot boundary (the Earth) and so on, the fact that creates a circular motion; a phenomenon that is well explained by the physics of nature.

5.0 PREDICTABILITY OF AVERAGE TEMPERATURES

The instability of the atmosphere with respect to perturbations of small amplitude places an upper bound on the predictability of instantaneous weather patterns. The lack of complete periodicity in the atmosphere's behavior is sufficient evidence for instability, but it does not reveal the range at which the uncertainty in prediction must become large. Most estimates of this range have been based on numerical integrations of systems of equations of varying degrees of complexity, starting from two or more rather similar initial states. It has become common practice to measure the error which would be made by assuming one of these states to be correct, when in fact another is correct, by the root-mean-square difference between the two fields of wind, temperature, or some other element, and to express the rate of amplification of small errors in terms of a doubling time. The available models then were those of Smagorinsky (1963), Mintz (1964), and Leith (1965); predictability studies which they subsequently performed with these models were described by Charney et al. (1966), who concluded that a reasonable estimate of the doubling time was five days. A landmark study was that of Smagorinsky (1969), whose numerical integrations indicated a three-day doubling time for the smallest errors.

A basic characteristic of chaotic dynamical systems is especially relevant to predictability: the leading Lyapunov number, or its logarithm, the leading Lyapunov exponent. The Lyapunov exponent of a dynamical system is a quantity that characterizes the rate of separation of infinitesimally close trajectories. The characteristic Lyapunov exponents are somehow an extension of the linear stability analysis to the case of aperiodic motions. Roughly speaking, they measure the typical rate of exponential divergence of nearby trajectories. In this sense they give information on the rate of growth of a very small error on the initial state of a system.

The ensemble code for the Natural Convection problem was used to study the predictability of average temperatures. Different temperature initial conditions were used . We first run the experiments with a constant initial perturbation of the velocities and the temperatures; we choose the norm of the perturbation to be $O(10^{-3})$. In Section 5.2, we repeat the same predictability experiment using initial perturbations generated by the Bred Vector algorithm, keeping the same norm mentioned above. The difference in the solutions was recorded for many final times. The Lyupanov exponents and the doubling times, which in the case of squeezing of solutions are called "half-lives", are then computed as follows:

Let ΔZ_0 and $\Delta Z(T_f)$ denote the separation of the solution at the initial time $t = 0$ and the final time $t = T_f$, respectively. Let λ denote the Lyapunov exponent and $T_{1/2}$ the doubling time (or half-life, if the flow is not turbulent), then

$$\lambda = \frac{1}{T_f} ln \left(\frac{|\Delta Z(T_f)|}{|\Delta Z_0|} \right), \text{ and}$$

$$T_{1/2} = \frac{ln(2)}{\lambda}$$

The norm used in the calculation of λ is the L^2 norm.

We intend to study the separation between two trajectories, starting from two close initial conditions.

If $\lambda > 0$, we have a rapid (exponential) amplification of an error on the initial condition. In such a case, the system is chaotic and unpredictable on the long times.

Let us stress that the Lyapunov exponents give information on the typical behaviors along a generic trajectory, followed for infinite time and keeping the perturbation infinitesimally small. In this respect, they are global quantities characterizing fine-grained properties of a system [24].

5.1 NUMERICAL RESULTS FOR CONSTANT INITIAL PERTURBATIONS

The Earth-like example described in Section 4.7.3 is the core of the predictability numerical tests that were conducted. We discretize the domain using 20 points on the inner circle and

104 points on the outer circle. We set the Rayleigh number to $4.8e3$, the initial deviation to $\epsilon = 10^{-3}$, $\Delta t = 0.01$, $Pr = 0.706$, $\kappa = 1$, $f_1 = (0,0)^T$, $f_2 = 0$, and we calculated the average temperature using

$$T_{avg} = \frac{1}{area} \int_{\Omega} T(x, y, T_f) dxdy$$

We first show in Table 5 the numerical values of the Lyapunov exponent and the half-life for the Earth-like example described above at different final times.

T_f	Deviation	λ	$T_{1/2}$
0.5	0.0002	-4.6052	-0.1505
1.0	0.00005	-3.6889	-0.1879
2.0	0.00002	-2.3026	-0.3010

Table 5: λ and $T_{1/2}$ for different final times, entire domain

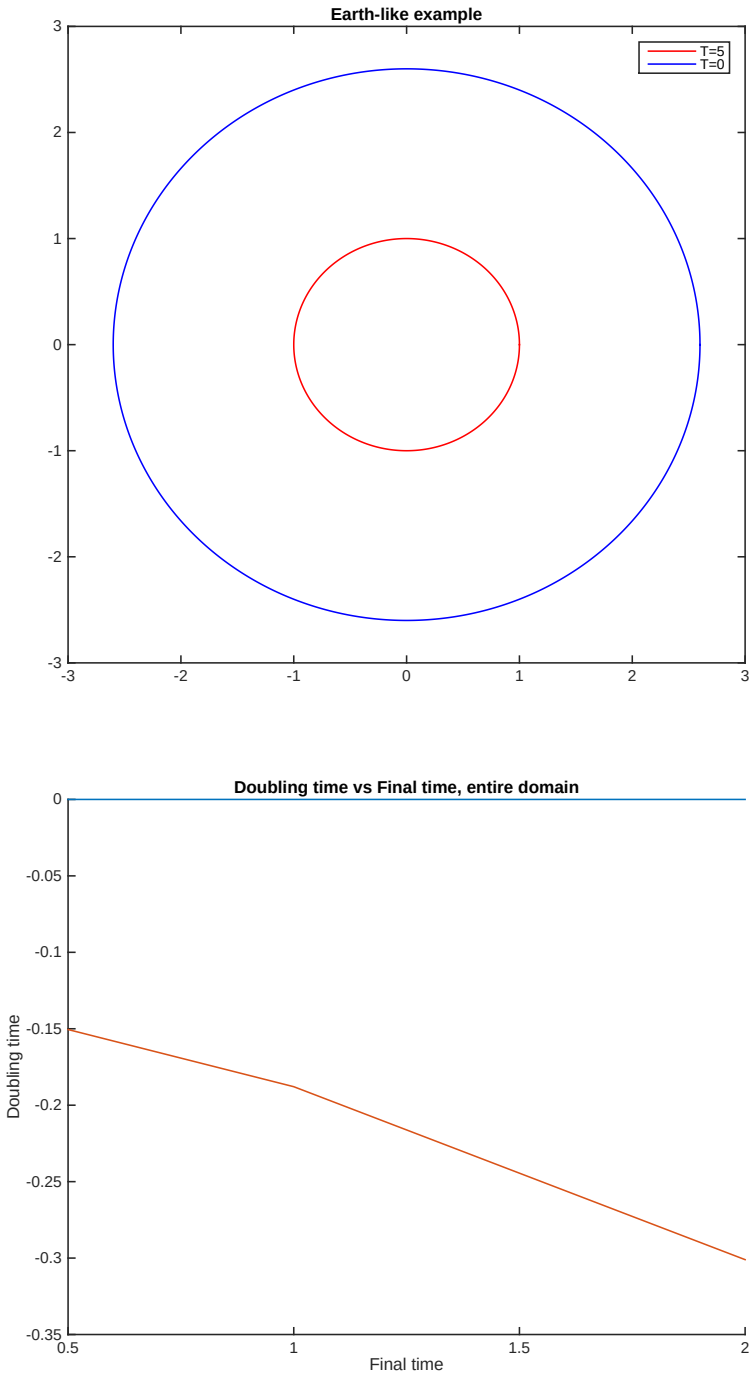

Figure 19: Average Temperature Predictability results

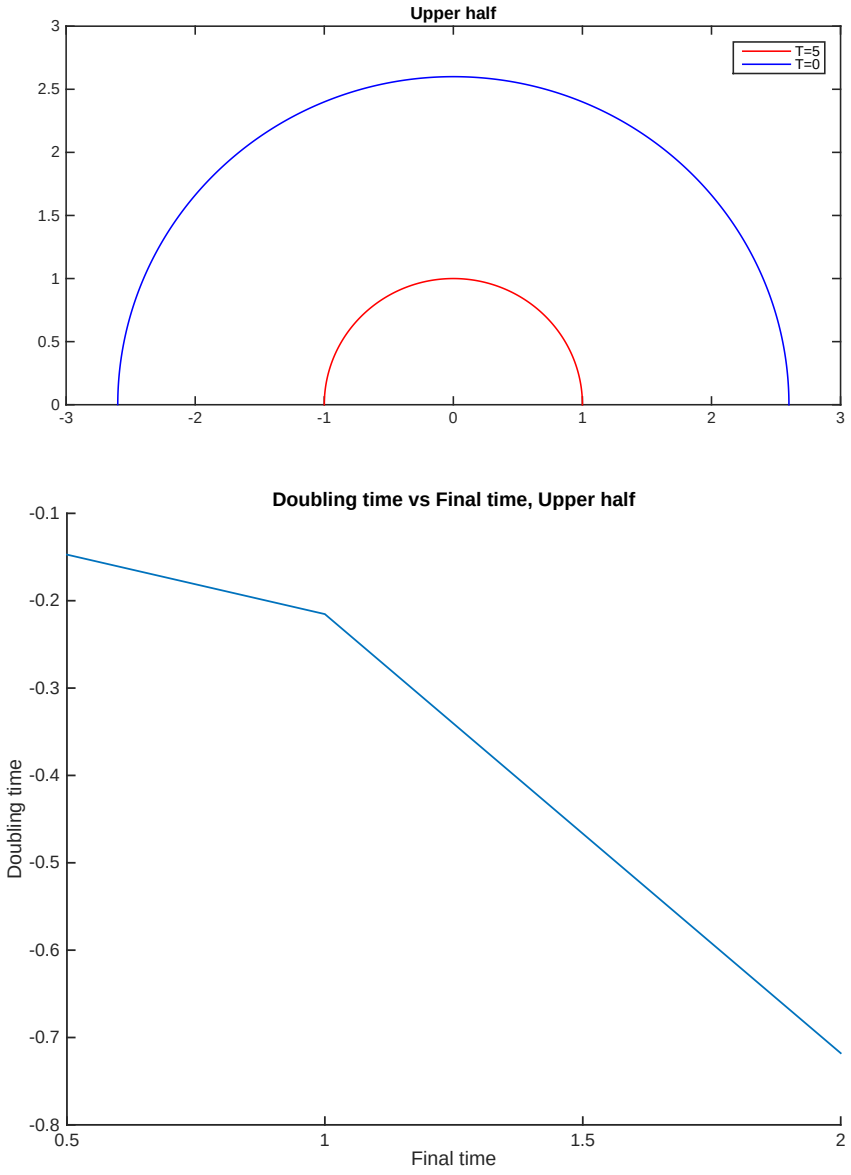

Figure 20: Predictability results for the Upper Half subdomain

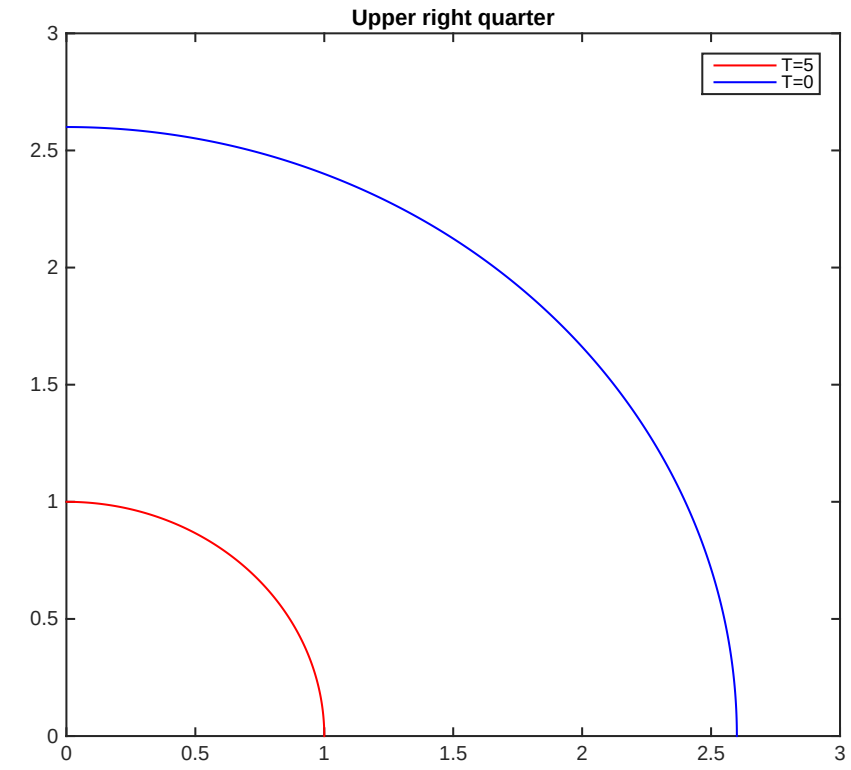

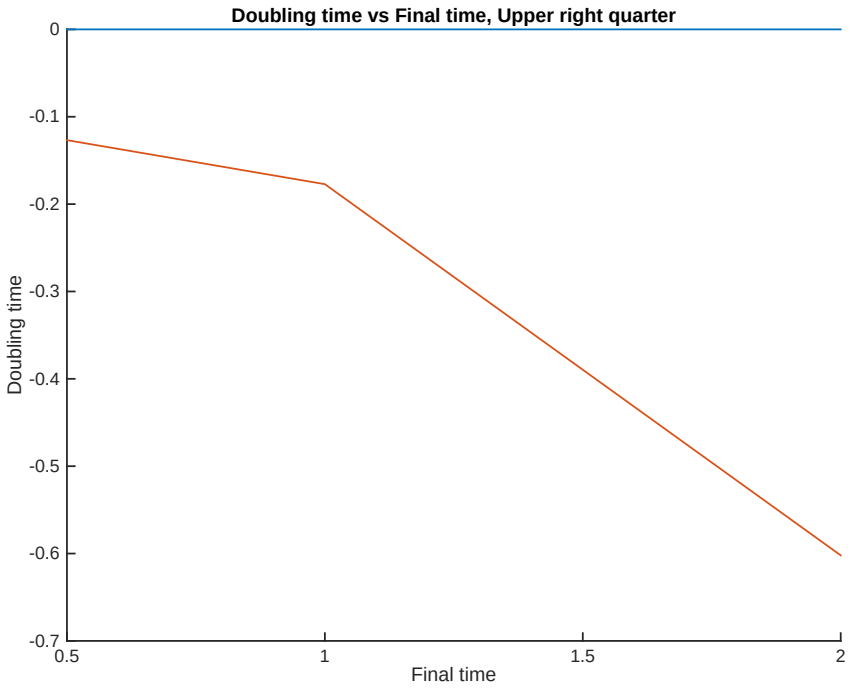

Figure 21: Predictability results for the Upper Right Quarter subdomain

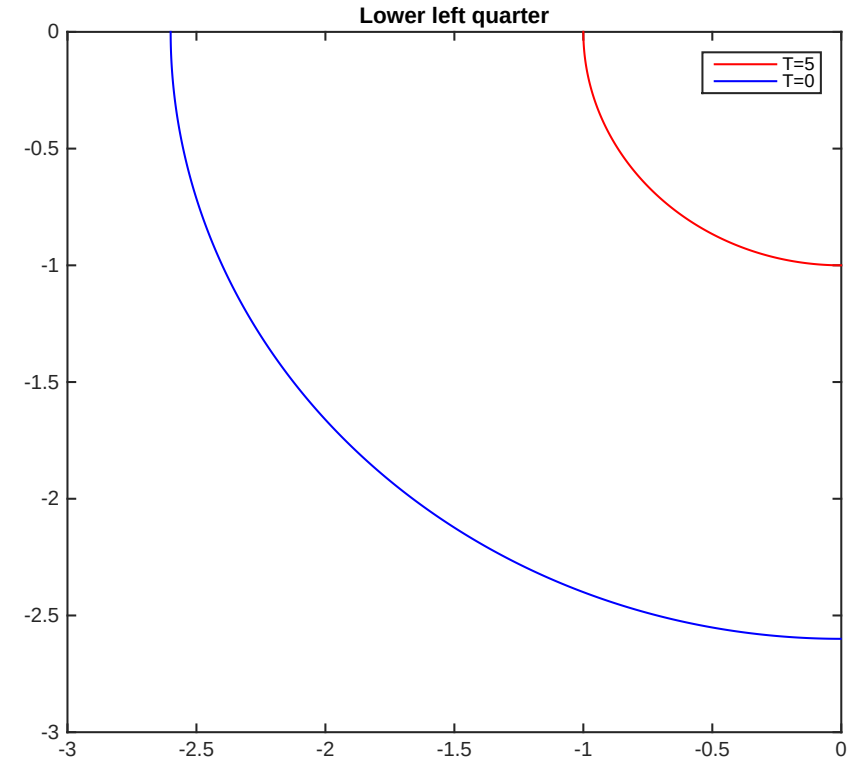

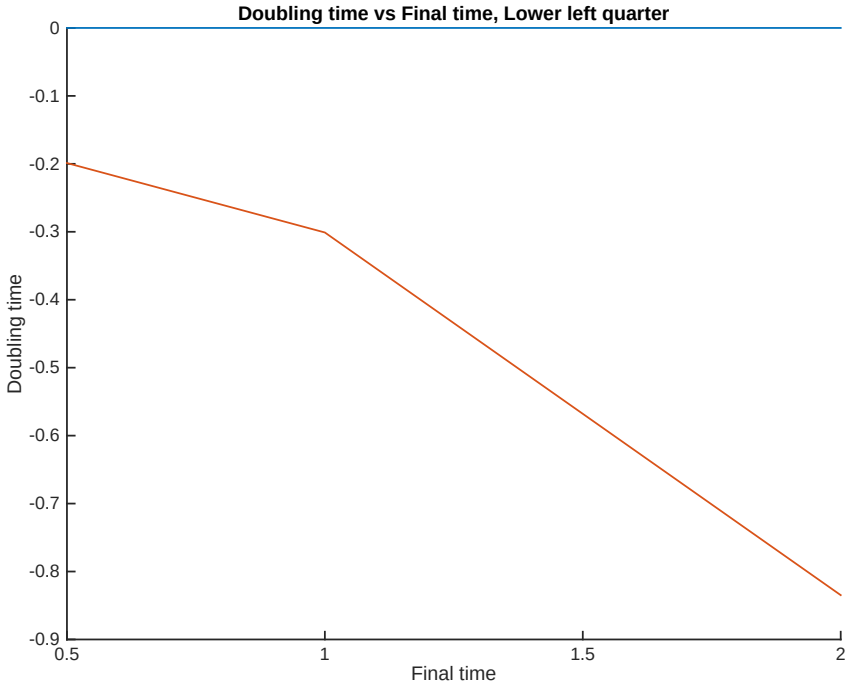

Figure 22: Predictability results for the Lower Left Quarter subdomain

Figure 19 shows the results listed in Table 5, for the entire domain.

The same experiment was conducted for the upper half (Figure 20), upper right quarter (Figure 21), and lower left quarter (Figure 22) subdomains. The half-lives were recorded and plotted into a graph versus the final times for each subdomain.

Figure 23 gathers the above information in one graph, showing that the half-life gets closer and closer to zero as the subdomain approaches the entire domain. The latter brings us to one of the most important points of that thesis: Predictability by scale.

Figure 24 shows the half-lives versus the scale. A scale of 1 denotes the entire domain, 0.5 half of the domain, and so on. Nevertheless, the results shown in this chapter are only preliminary; and thus a definite conclusion cannot be drawn until the predictability of turbulent flows is tested.

The negative half-life shown in the above numerical tests is a numerical evidence that the average temperature in the Earth-like example is stable and predictable; which means that the total heat in the earth is stable. This is due to the fact that the system we studied is a stable system under some respected time-step condition. In the case of a turbulent system, the temperature is expected not to be predictable and the doubling time to be positive (Chapter 6).

5.2 NUMERICAL RESULTS USING THE BRED VECTOR ALGORITHM

In the results shown above, the initial perturbation ϵ was fixed to $10e-3$. A closer way to the reality of dynamical systems is to generate the initial perturbation using the Bred Vector algorithm [9]. In her book entitled *Atmospheric Modeling, Data Assimilation and Predictability*, Kalnay discusses a breeding cycle that generates initial perturbations. Given an evolving atmospheric flow (either a series of atmospheric analyses, or a long model run), a breeding cycle is started by introducing a random initial perturbation ("random seed") with a given initial size. It should be noted that the random seed is introduced only once. The same nonlinear model is integrated from the control and from the perturbed initial conditions. From then on at fixed time intervals (e.g., every 6 hours or every 24 hours), the

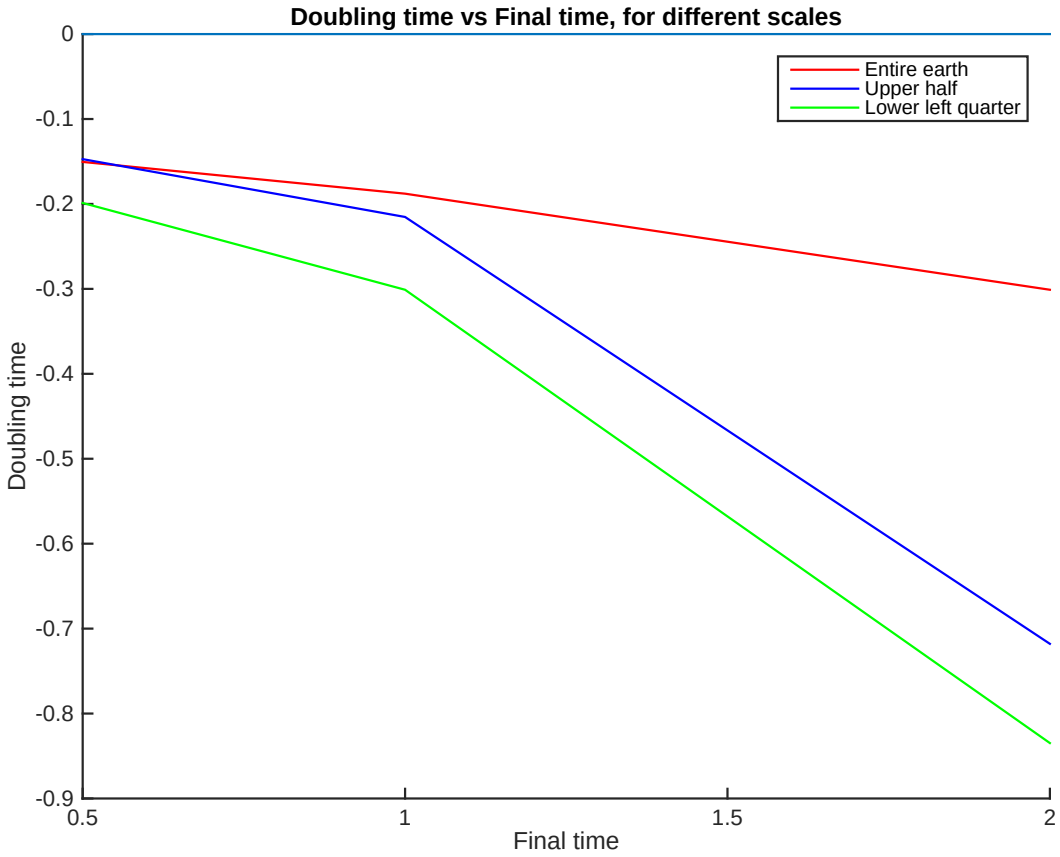

Figure 23: Half-life versus final time for different scales

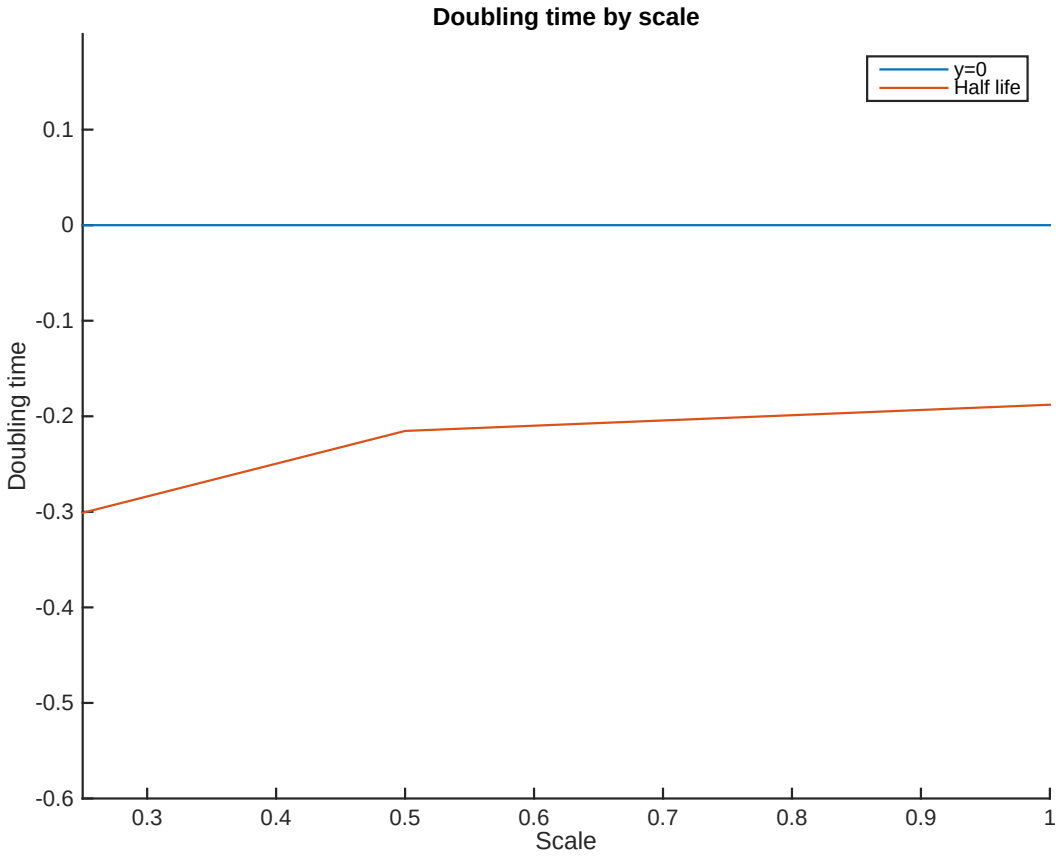

Figure 24: Half-life by scale

control forecast is subtracted from the perturbed forecast. The difference is scaled down so that it has the same amplitude (defined using the same arbitrary norm) as the initial perturbation, and then added to the corresponding new analysis or model state. It was found that beyond an initial transient period of 3-4 days after random perturbations were introduced, the perturbations generated in the breeding cycle (denoted bred vectors), acquired a large growth rate, faster than the growth rate of Monte Carlo forecasting or even scaled lagged average forecasting and forecast differences [9].

Toth and Kalnay (1993 [91], 1997 [92]) also found that (after the transient period of 3-4 days) the shape or structure of the perturbation bred vectors did not depend on either the norm used for the rescaling or the length of the scaling period. The breeding cycle has been designed to model how the growing errors are "bred" and maintained in a conventional analysis cycle through the successive use of short-range forecasts. The bred modes should thus offer a good estimate of possible growing error fields in the analysis. Results from extensive experiments indicate that ensembles of just two BGM forecasts achieve better results than much larger random Monte Cado or lagged average forecast (LAF) ensembles [91].

The Bred Vector algorithm reads as follows:

Let $\phi^n(x,t)$ denote the perturbation at time t^n. Without loss of generality, we assume $u_1(x,t)$ is velocity we are perturbing around.

Given u_1^n and u_2^n, let $\epsilon = \|u_1^n - u_2^n\|$

Then $\phi^n = u_1^n - u_2^n$, $\phi^n \leftarrow \epsilon \times \frac{\phi^n}{\|\phi^n\|}$ and $u_2^n \leftarrow u_2^n + \phi^n$.

In brief, the norm of the perturbation is preserved and determined by the norm of the initial perturbation picked. It is the direction of the perturbation that is being changed using that algorithm.

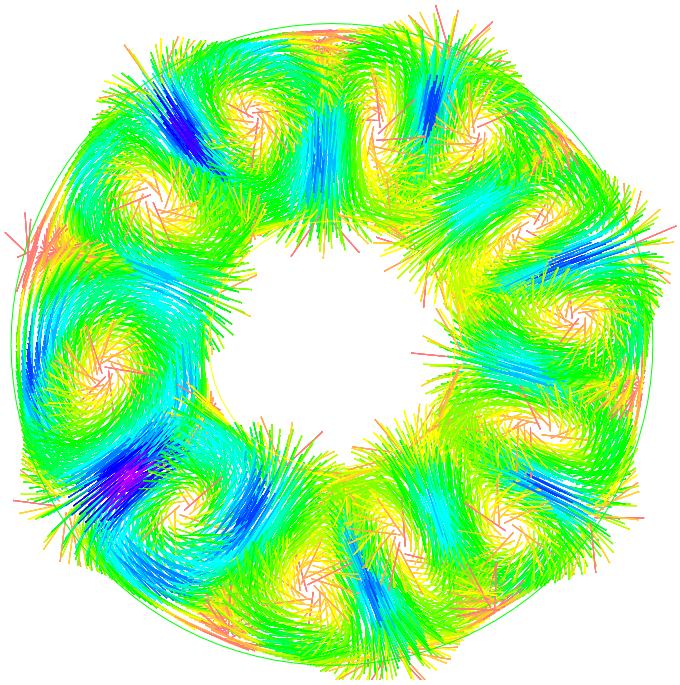

(a) Velocity, $Ra = 4.8e4$

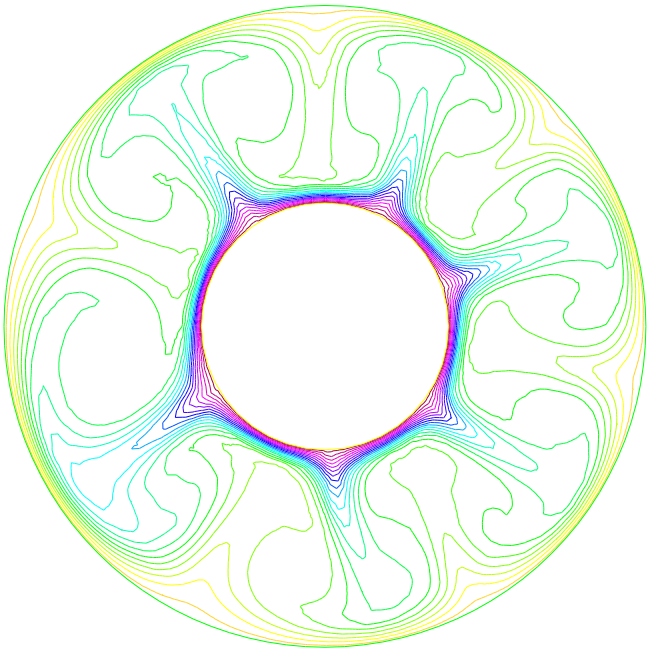

(b) Temperature, $Ra = 4.8e4$

Figure 25: Earth-like example using Bred Vectors at $T_F = 0.3$.

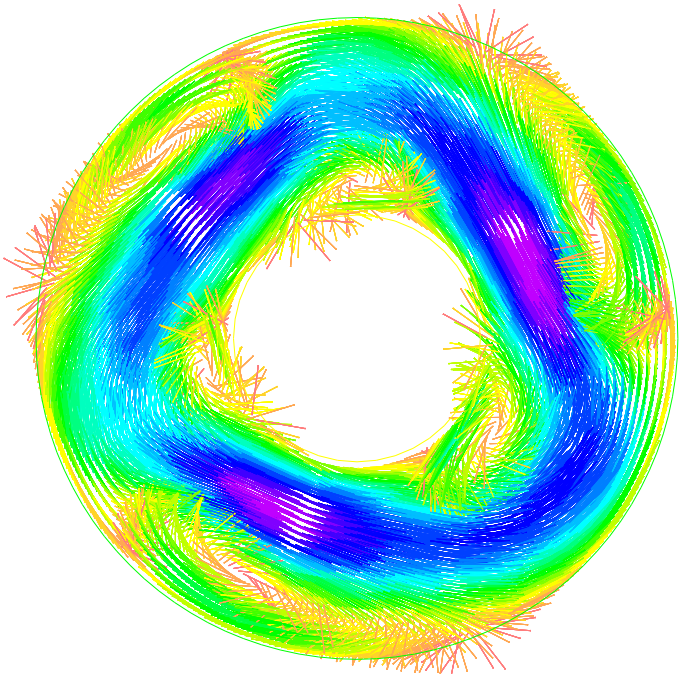

(a) Velocity, $Ra = 4.8e4$

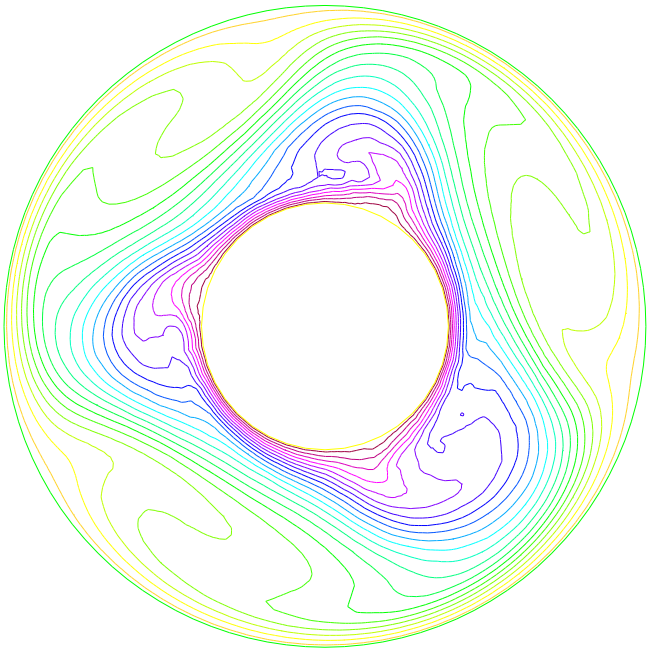

(b) Temperature, $Ra = 4.8e4$

Figure 26: Earth-like example using Bred Vectors at $T_F = 1$.

We repeat the iterations 5 times to generate u_2^5, that will be used as the initial condition u_2^0 in the ensemble algorithm for predictability, instead of $u_2^0 = u_1^0 + (10^{-3}, 10^{-3})^T$.

We repeat the half-life calculations for the The earth-like example performed in section 5.1. To obtain an accurate comparison, we use the same data, with the exception of the initial perturbations of the velocity and temperature; which are obtained using the Bred Vector algorithm then imported into the main FreeFem++ code. We set the Rayleigh number to $4.8e3$, the initial deviation to $\epsilon = 2 \times 10^{-3}$, $\Delta t = 0.01$, $Pr = 0.706$, $\kappa = 1$, $f_1 = (0, 0)^T$, $f_2 = 0$, and we calculated the average temperature using

$$T_{avg} = \frac{1}{area} \int_\Omega T(x, y, T_f) dxdy$$

T_f	Deviation	λ	$T_{1/2}$
0.5	0.00005	-11.983	-0.0578
1.0	0.00002	-7.824	-0.0886
1.5	0.00005	-1.997	-0.3471

Table 6: λ and $T_{1/2}$ for different final times using Bred Vectors, for the entire domain

Figure 5.2 compares the half-lives obtained for different final times for the Earth-like example, using a constant initial perturbation of the temperature versus an initial perturbation generated by a Bred Vector algorithm. In such a case of a predictable system, we notice that the Bred Vector algorithm give half-lives that a slightly closer to zero. It is worth mentioning though that the results for both perturbations become comparable for high final times.

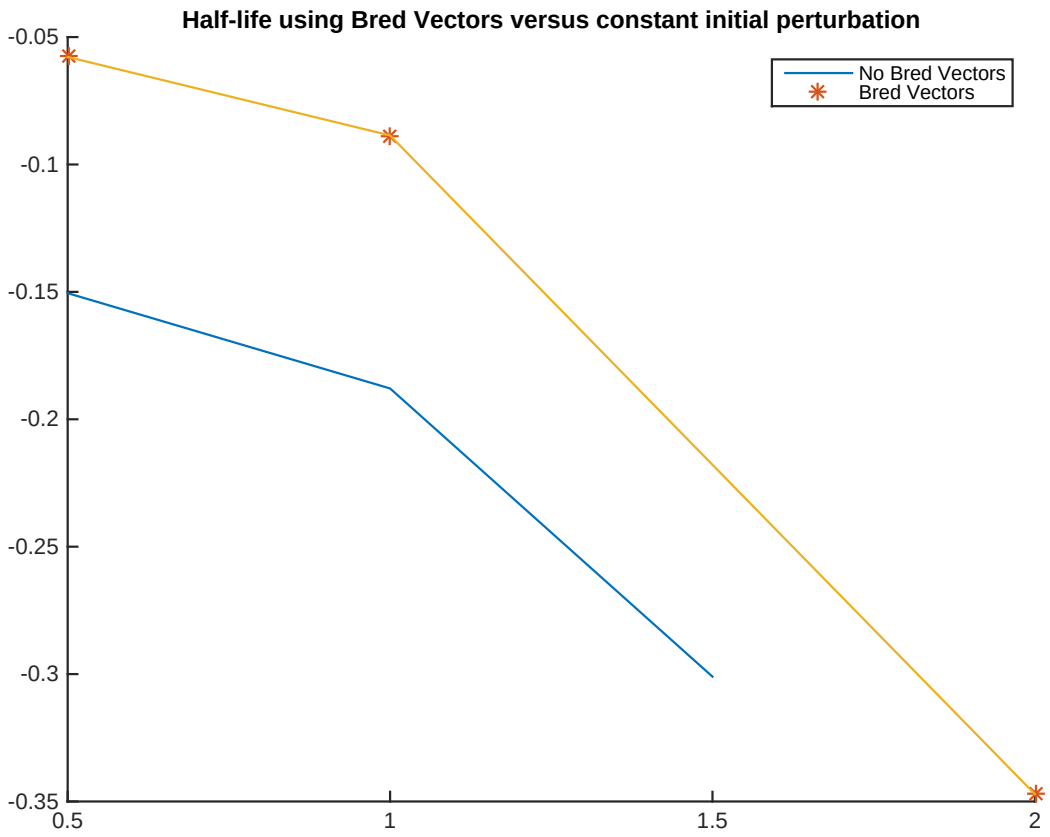

Figure 27: Half-life using constant initial perturbation versus Bred Vectors

6.0 ENSEMBLES FOR TURBULENT NATURAL CONVECTION

Time stepping methods have been developed in Chapter 3 for the Natural Convection problem with oscillating viscosity. Moreover, an ensemble algorithm for the Natural Convection problem has been studied in details in Chapter 4. The latter was a preparation for the predictability study presented in Chapter 5, using the ensemble algorithm for the Natural Convection problem; showing stability and predictability of average temperatures in the Earth-like model.

The natural next step is to extend our ensemble algorithm to the turbulent Natural Convection problem, with oscillating Prandtl number and heat conductivity. The latter occurs in flows with high Reynolds numbers. This is the case of an eddy viscosity model. The transport of heat within turbulent flows is a fundamental physical process in many natural and engineered systems. Historically, engineering approaches to modeling such systems employed a turbulence closure scheme for the momentum field based on either an eddy viscosity or a mixing length formulation. The calculation of the scalar transport then often made use of the so-called Reynolds analogy, whereby the scalar dispersivity was assumed to be proportional to the eddy viscosity [90].

The difference between laminar and turbulent flows can be seen if a filament of dye is injected near the center-line of a pipe. In laminar flow, the filament remains straight and coherent but, with the onset of turbulent flow, it meanders, winds itself up into tight coils and is diffused rapidly over the whole section of the pipe. Although the transition from laminar to turbulent flow is not as simple as this and similar descriptions make it appear, the phenomenon illustrates very well the fundamental differences in character between laminar and turbulent flow, particularly the ability of a turbulent flow to transmit larger shear stresses and to diffuse heat and matter more rapidly than the corresponding laminar flow. It is

well known that differences arise from an intricate and eddying motion of the fluid which convects momentum, heat and matter from one part of the flow to another, the direction of net transport being in general down the gradient of the quantity concerned. Formally, the overall effect is equivalent to increasing greatly the effective coefficients of viscosity, heat conductivity and diffusion.

As a consequence of the irregularity and complexity of the motion, it is only practicable to consider mean values of functions of the instantaneous and local values of the fluid velocities, pressures and temperatures. The most important theories developed were the various forms of the mixing-length theory [95] [96] by L. Prandtl and by G.I. Taylor, which served a purpose in providing a framework for current theoretical and experimental work, but they were admittedly incomplete and contained internal inconsistencies [94].

Following Prandtl's assumption that the eddy viscosity is proportional to the mixing length multiplied by a turbulence characteristic velocity, and the relation of the Prandtl number and heat conductivity to the viscosity, we define the fluctuating, time and space-dependent, Prandtl number and heat conductivity.

Recall the definitions of the average $< u >$ in 4.6 and the fluctuation $|u'|$ in 4.27:

$$< u >^n := \frac{1}{J} \sum_{j=1}^{J} u^n \text{ and,}$$

$$u'^n_j = u^n_j - < u_h >^n .$$

Definition 1. *Let $|\cdot|$ denote the Euclidean length of a vector and Frobenius norm of an array. Then the magnitude of the fluctuation (the characteristic velocity) is defined by*

$$|u'^n| = \sqrt{\sum_{j=1}^{J} |u'^n_j|^2}$$

We also define the mixing length, which will be used in the definitions of the fluctuating Prandtl number and heat conductivity.

Definition 2. *The distance that a fluctuating eddy travels in one time step is called the mixing length and is defined by*

$$l = |u'|\Delta t$$

Definition 3. *The fluctuating, time and space-dependent, Prandtl number and heat conductivity are respectively defined by*

$$Pr_T = \gamma_{Pr}(l \cdot |u'|)$$

$$\kappa_T = \gamma_\kappa(l \cdot |u'|)$$

Consider the natural convection problem enclosed in a medium with non-zero wall thickness. Let $\Omega_e \subset \Omega$ be polyhedral domains in $\mathbb{R}^d (d = 2, 3)$ with boundaries $\partial\Omega_e$ and $\partial\Omega$, respectively, such that dist($\partial\Omega_e$,$\partial\Omega$) > 0. The boundary $\partial\Omega$ is partitioned such that $\partial\Omega = \Gamma_1 \cup \Gamma_2$ with $\Gamma_1 \cap \Gamma_2 = \emptyset$ and measure $(\Gamma_2) > 0$. Let $u(x,t) : \Omega \times [0,t^*] \to \mathbb{R}^d$, $p(x,t) : \Omega \times [0,t^*] \to \mathbb{R}$, and $T(x,t) : \Omega \times [0,t^*] \to \mathbb{R}$ satisfy

$$u_t + u \cdot \nabla u - Pr\Delta u - \nabla \cdot (Pr_T \nabla u) + \nabla p = PrRa\gamma T + f \ \ in\ \Omega_e, \tag{6.1}$$

$$\nabla \cdot u = 0 \ \ in\ \Omega_e, \tag{6.2}$$

$$T_t + u \cdot \nabla T - \nabla \cdot (\kappa \nabla T) - \nabla \cdot (\kappa_T \nabla T) = g \ \ in\ \Omega, \tag{6.3}$$

$$u(x,0) = u^0(x)\ and\ T(x,0) = T^0(x) \ \ in\ \Omega, \tag{6.4}$$

$$u = 0 \ \ on\ \partial\Omega_e, \ \ u = 0 \ \ in\ \Omega - \Omega_e, \ \ T = 0 \ \ on\ \Gamma_2 \ \ and \ \ n \cdot \nabla T = 0 \ \ on\ \Gamma_1, \tag{6.5}$$

where n denotes the usual outward normal to Ω, $\gamma = \frac{g}{|g|}$, Pr is the Prandtl number, Ra is the Rayleigh number, and $\kappa = \kappa_e$ in Ω_e is the thermal conductivity; all of which are positive constants. Further, f and g are forcing terms dependent on space and time. We now combine the ensembles studied in Chapter 4 with the turbulent Natural convection problem. We consider J systems of the above equations with J slightly perturbed initial conditions u_j^0 and T_j^0 and body forces f_j and g_j. Let $u_j(x,t) : \Omega \times [0,t^*] \to \mathbb{R}^d$, $p_j(x,t) : \Omega \times [0,t^*] \to \mathbb{R}$,

and $T_j(x,t) : \Omega \times [0,t^*] \to \mathbb{R}$ satisfy

$$u_{j,t} + u_j \cdot \nabla u_j - Pr\Delta u_j - \nabla \cdot (Pr_T \nabla u_j) + \nabla p_j = PrRa\gamma T_j + f_j \ \ in\ \Omega_e, \tag{6.6}$$

$$\nabla \cdot u_j = 0 \ \ in\ \Omega_e, \tag{6.7}$$

$$T_{j,t} + u_j \cdot \nabla T_j - \nabla \cdot (\kappa \nabla T_j) - \nabla \cdot (\kappa_T \nabla T_j) = g_j \ \ in\ \Omega, \tag{6.8}$$

$$u_j(x,0) = u_j^0(x)\ and\ T_j(x,0) = T_j^0(x) \ \ in\ \Omega, \tag{6.9}$$

$$u_j = 0 \ \ on\ \partial\Omega_e, \ \ u_j = 0 \ \ in\ \Omega - \Omega_e, \ \ T_j = 0 \ \ on\ \Gamma_2 \ \ and \ \ n \cdot \nabla T_j \ \ on\ \Gamma_1, \tag{6.10}$$

Keeping the spatial dependence suppressed and using an implicit-explicit time-discretization, while keeping the coefficient matrix independent of the ensemble members, as in Section 4.3, leads to the method:

$$\begin{aligned} &\frac{u_j^{n+1} - u_j^n}{\Delta t} - Pr\triangle u_j^{n+1} - \nabla \cdot (Pr_T^n \nabla u_j^{n+1}) + < u >^n \cdot \nabla u_j^{n+1} \\ &\qquad + (u_j^n - < u >^n) \cdot \nabla u_j^n + \nabla p_j^{n+1} = PrRa\gamma T_j^{n+1} + f_j^{n+1}, \\ &\qquad \nabla \cdot u_j^{n+1} = 0, \\ &\frac{T_j^{n+1} - T_j^n}{\Delta t} - \kappa \Delta T_j^{n+1} - \nabla \cdot (\kappa_T^n \nabla T_j^{n+1}) + < u >^n \cdot \nabla T_j^{n+1} + (u_j^n - < u >^n) \cdot \nabla T_j^n = g_j^{n+1}. \end{aligned} \tag{6.11}$$

The weak formulation of the above system will be useful in the stability analysis. It reads: Find $u_j : [0,t^*] \to X$, $p_j : [0,t^*] \to Q$, $T_j : [0,t^*] \to W$ for almost every $t \in (0,t^*]$ satisfying for $j = 1, ..., J$:

$$\begin{aligned} (u_{j,t}, v) + b(u_j, u_j, v) + Pr(\nabla u_j, \nabla v) + \int_\Omega \gamma_{Pr} \Delta t |u'^n|^2 \nabla u_j^{n+1} \nabla v dx - (p_j, \nabla \cdot v) \\ = PrRa(\gamma T_j, v) + (f_j, v) \ \ \forall v \in X, \end{aligned} \tag{6.12}$$

$$(q, \nabla \cdot u_j) = 0 \ \ \forall q \in Q, \tag{6.13}$$

$$\begin{aligned} (T_{j,t}, S) + \kappa(\nabla T_j, \nabla S) + \int_\Omega \gamma_\kappa \Delta t |u'^n|^2 \nabla T_j^{n+1} \nabla S dx + b^*(u_j, T_j, S) \\ = (g_j, S) \ \ \forall S \in W. \end{aligned} \tag{6.14}$$

6.1 NUMERICAL SCHEME

We should now discuss those aspects relevant to finite element approximation. We consider the same finite element spaces X_h, Q_h, W_h described in Chapter 4.

The aforementioned finite element spaces satisfy the approximation properties in (2.1) and the discrete inf-sup condition (2.4). Recall that the space of discretely divergence free functions, V_h, is defined by

$$V_h := \{v_h \in X_h : (q_h, \nabla \cdot v_h) = 0, \forall q_h \in Q_h\}.$$

We assume that the mesh and finite element spaces satisfy the following inverse inequality:

$$\|\nabla \chi_{1,2}\| \leq C_{inv,1,2} h^{-1} \|\chi_{1,2}\| \quad \forall \chi_1 \in X_h, \ \forall \chi_2 \in W_h.$$

The Poincaré-Friedrichs inequality is also satisfied:

$$\|\chi_{1,2}\| \leq C_{PF,1,2} \|\nabla \chi_{1,2}\| \quad \forall \chi_1 \in X_h, \ \forall \chi_2 \in W_h.$$

Recall the explicitly skew-symmetric bilinear forms, $b(u, v, w)$ and $b^*(u, T, S)$.

Lemma 6.1.1. *Let $u_h, v_h,$ and $w_h \in X_h$ and $T_h, S_h \in W_h$, then the following identities hold*

$$b(u_h, v_h, w_h) = \int_\Omega u_h \cdot \nabla v_h \cdot w_h dx + \frac{1}{2} \int_\Omega (\nabla \cdot u_h)(v_h \cdot w_h) dx,$$

$$b(u_h, T_h, S_h) = \int_\Omega u_h \cdot \nabla T_h S_h dx + \frac{1}{2} \int_\Omega (\nabla \cdot u_h)(T_h S_h) dx.$$

Proof. Use integration by parts. □

Remark: The integral is taken over Ω_e due to the fluid velocity being identically zero in $\Omega - \Omega_e$, the solid wall enclosing the fluid.

The discrete time analysis will utilize the following norms $\forall\ 1 \leq k \leq \infty$:

$$|||v|||_{\infty,k} := \max_{0\leq n\leq N} \|v^n\|_k,$$

$$|||v|||_{p,k} := \big(\Delta t \sum_{0}^{N} \|v^n\|_k^p\big)^{1/p}.$$

In subsequent discussion, the ensemble number is suppressed and the following notational simplicities are enforced:

$$u(x,t;\omega_j) := u_j(x,t),$$
$$p(x,t;\omega_j) := p_j(x,t),$$
$$T(x,t;\omega_j) := T_j(x,t),$$
$$U_h^n = u_h^n - < u_h >^n .$$

Denote the fully discrete solutions u_h^n, p_h^n, and T_h^n at time levels $t^n = n\Delta t$, $n = 0, 1, ..., N$, such that $t^* = N\Delta t$. Introducing the finite element approximation in space and applying a backward Euler discretization in time, the fully discrete approximation of (6.11) is:
Given $u_h^n(x,t;\omega_j)$, $p_h^n(x,t;\omega_j)$, and $T_h^n(x,t;\omega_j)$, find $u_h^{n+1} \in X_h$, $p_h^{n+1} \in Q_h$, and $T_h^{n+1} \in W_h$ satisfying, for every $n = 0, 1, ..., N$,

$$\begin{aligned}
(\frac{u_h^{n+1} - u_h^n}{\Delta t}, v_h) + b(< u_h >^n, u_h^{n+1}, v_h) + b(U_h^n, u_h^n, v_h) + Pr(\nabla u_h^{n+1}, \nabla v_h) \\
+ \int_\Omega \gamma_{Pr}\Delta t |u'^n|^2 \nabla u_h^{n+1} \nabla v_h dx - (p_h^{n+1}, \nabla \cdot v_h) \\
= PrRa(\gamma T_h^{n+1}, v_h) + (f^{n+1}, v_h)\ \ \forall v_h \in X_h, \\
(q_h, \nabla \cdot u_h^{n+1}) = 0\ \ \forall q_h \in Q_h, \\
(\frac{T_h^{n+1} - T_h^n}{\Delta t}, S_h) + b^*(< u_h >^n, T_h^{n+1}, S_h) + b^*(U_h^n, T_h^n, S_h) + \kappa(\nabla T_h^{n+1}, \nabla S_h) \\
+ \int_\Omega \gamma_\kappa \Delta t |u'^n|^2 \nabla T_h^{n+1} \nabla S_h dx = (g^{n+1}, S_h)\ \ \forall S_h \in W_h.
\end{aligned} \tag{6.15}$$

6.2 NUMERICAL ANALYSIS

In this section, we present two stability conditions for the numerical scheme (6.15).The first stability condition, stated in Theorem 6.2.1 depends mainly on the constants in the fluctuating Prandtl number Pr_T and heat conductivity κ_T. The second stability condition depends on κ, Pr and the space discretization h.

6.2.1 Stability Analysis (method 1)

We state and prove herein the first condition for the stability of the scheme (6.15).

Theorem 6.2.1. *The scheme* (6.15) *is conditionally stable with respect to the timestep* Δt *in the following sense: Suppose* $f \in L^\infty(0,t^*;H^{-1}(\Omega)^d)$, $g \in L^\infty(0,t^*;H^{-1}(\Omega))$, $\gamma_{Pr} > 1$, $\gamma_\kappa > 1$, *and for all* $N \geq 1$ *and* $j = 1, ..., J$ *if*

$$\Delta t \|\nabla \cdot u_j'^n\|_{L^4}^2 \leq \min\{\frac{\gamma_{Pr}-1}{2C_s\gamma_{Pr}}, \frac{\gamma_\kappa - 1}{2C_s\gamma_\kappa}\} \tag{6.16}$$

where C_s *is the constant arising from the Sobolev embedding theorem, then*

$$\begin{aligned}\frac{1}{2}\|u_h^{N+1}\|^2 + \frac{1}{4}\sum_{n=0}^{N}\|u_h^{n+1}-u_h^n\|^2 + \Delta t\sum_{n=0}^{N}\int_\Omega\left(\frac{Pr}{2}+\gamma_{Pr}|u_h'^n|^2\Delta t\right)|\nabla u_h^{n+1}|^2dx \\ - \Delta t^2\sum_{n=0}^{N}\int_\Omega\left(\frac{1}{\gamma_{Pr}}|u_h'^n|^2|\nabla u_h^{n+1}|^2 + \frac{1}{1-\gamma_{Pr}}|\nabla\cdot u_h'^n|^2|u_h^{n+1}|^2\right)dx \\ \leq \frac{1}{2}\|u_h^0\|^2 + \Delta t PrRa^2\gamma^2\sum_{n=0}^{N}\|T_h^{n+1}\|_*^2 + \frac{2\Delta t}{Pr}\sum_{n=0}^{N}\|f^{n+1}\|_*^2, \text{ and,}\end{aligned} \tag{6.17}$$

$$\begin{aligned}\frac{1}{2}\|T_h^{N+1}\|^2 + \frac{1}{4}\sum_{n=0}^{N}\|T_h^{n+1}-T_h^n\|^2 + \Delta t\sum_{n=0}^{N}\int_\Omega\left(\frac{\kappa}{2}+\gamma_\kappa|u_h'^n|^2\Delta t\right)|\nabla u_h^{n+1}|^2dx \\ - \Delta t^2\sum_{n=0}^{N}\int_\Omega\left(\frac{1}{\gamma_\kappa}|u_h'^n|^2|\nabla T_h^{n+1}|^2 + \frac{1}{1-\gamma_\kappa}|\nabla\cdot u_h'^n|^2|T_h^{n+1}|^2\right)dx \\ \leq \frac{1}{2}\|T_h^0\|^2 + \frac{2\Delta t}{\kappa}\sum_{n=0}^{N}\|g^{n+1}\|_*^2.\end{aligned} \tag{6.18}$$

Proof. We begin by proving the stability result of the temperature equation.

Let $S_h = T_h^{n+1}$, multiply by Δt and use the polarization identity. Then,

$$\frac{1}{2}(\|T_h^{n+1}\|^2 - \|T_h^n\|^2) + \frac{1}{2}\|T_h^{n+1} - T_h^n\|^2 + \Delta t\kappa\|\nabla T_h^{n+1}\|^2 \tag{6.19}$$

$$+ \Delta t \int_\Omega \gamma_\kappa \Delta t |u'^n|^2 |\nabla T_h^{n+1}|^2 dx$$

$$= \Delta t(g^{n+1}, T_h^{n+1}) - \Delta t b^*(u_h'^n, T_h^n, T_h^{n+1}), \tag{6.20}$$

Using Young's inequality with $\epsilon = \kappa$, the right-hand side is bounded by

$$\Delta t(g^{n+1}, T_h^{n+1}) \leq \frac{\Delta t\kappa}{2}\|\nabla T_h^{n+1}\|^2 + \frac{\Delta t}{2\kappa}\|g^{n+1}\|_*^2 \tag{6.21}$$

and the term $\frac{\Delta t\kappa}{2}\|\nabla T_h^{n+1}\|^2$ is moved to the left hand side.

Next, the trilinear term $|-\Delta t b^*(u_h'^n, T_h^n, T_h^{n+1})|$ is bounded by, for any $0 < \alpha < 1$,

$$|-\Delta t b^*(u_h'^n, T_h^n, T_h^{n+1})| = |\Delta t b^*(u_h'^n, T_h^n - T_h^{n+1}, T_h^{n+1})| \tag{6.22}$$

$$= |\Delta t b^*(u_h'^n, T_h^{n+1}, T_h^{n+1} - T_h^n)|$$

$$= |\Delta t(u_h'^n \cdot \nabla T_h^{n+1}, T_h^{n+1} - T_h^n) + \frac{1}{2}\Delta t(\nabla \cdot u_h'^n, T_h^{n+1} \cdot (T_h^{n+1} - T_h^n))|$$

$$\leq \frac{\Delta t^2}{\alpha}\int_\Omega |u_h'^n|^2 |\nabla T_h^{n+1}|^2 dx + \frac{\alpha}{4}\|T_h^{n+1} - T_h^n\|^2$$

$$+ \frac{\Delta t^2}{1-\alpha}\int_\Omega |\nabla \cdot u_h'^n|^2 |T_h^{n+1}|^2 dx + \frac{1-\alpha}{4}\|T_h^{n+1} - T_h^n\|^2$$

$$= \Delta t^2 \int_\Omega \left(\frac{1}{\alpha}|u_h'^n|^2|\nabla T_h^{n+1}|^2 + \frac{1}{1-\alpha}|\nabla \cdot u_h'^n|^2|T_h^{n+1}|^2\right) dx + \frac{1}{4}\|T_h^{n+1} - T_h^n\|^2.$$

The stability follows provided there is an $\alpha, 0 < \alpha < 1$, such that

$$\Delta t \int_\Omega \left(\frac{\kappa}{2} + \gamma_\kappa |u_h'^n|^2 \Delta t\right) |\nabla T_h^{n+1}|^2 dx \tag{6.23}$$

$$- \Delta t^2 \int_\Omega \left(\frac{1}{\alpha}|u_h'^n|^2|\nabla T_h^{n+1}|^2 + \frac{1}{1-\alpha}|\nabla \cdot u_h'^n|^2|T_h^{n+1}|^2\right) dx \geq 0.$$

For $0 \leq \theta \leq \frac{1}{2}$, (6.23) is equivalent to

$$\int_\Omega \left(\theta\kappa + \Delta t(\gamma_\kappa - \frac{1}{\alpha})|u_h'^n|^2\right) |\nabla T_h^{n+1}|^2 \tag{6.24}$$

$$+ \int_\Omega \left((\frac{1}{2} - \theta)\kappa|\nabla T_h^{n+1}|^2 - \frac{\Delta t}{1-\alpha}|\nabla \cdot u_h'^n|^2|T_h^{n+1}|^2\right) dx \geq 0.$$

A sufficient condition for (6.24) is

$$\theta\kappa + \Delta t(\gamma_\kappa - \frac{1}{\alpha})|u_h'^n|^2 \geq 0 \text{ and} \tag{6.25}$$
$$(\frac{1}{2} - \theta)\kappa\|\nabla T_h^{n+1}\|^2 - \frac{\Delta t}{1-\alpha}\|\nabla \cdot u_h'^n\|_{L^4}^2\|T_h^{n+1}\|_{L^4}^2 \geq 0.$$

By Sobolev embedding theorem, (6.25) holds if

$$\theta\kappa + \Delta t(\gamma_\kappa - \frac{1}{\alpha})|u_h'^n|^2 \geq 0 \text{ and} \tag{6.26}$$
$$(\frac{1}{2} - \theta)\kappa\|\nabla T_h^{n+1}\|^2 - \frac{C_s\Delta t}{1-\alpha}\|\nabla \cdot u_h'^n\|_{L^4}^2\|T_h^{n+1}\|_{L^4}^2 \geq 0.$$

In particular, let $\gamma_\kappa > 1$, $\alpha = \frac{1}{\gamma_\kappa}$ and $\theta = 0$, then (6.26) reduces to

$$\gamma_\kappa \geq 0 \text{ and } \frac{1}{2}\kappa - \frac{C_s\gamma_\kappa}{\gamma_\kappa - 1}\Delta t\|\nabla \cdot u_h'^n\|_{L^4}^2 \geq 0, \tag{6.27}$$

which is equivalent to

$$\gamma_\kappa \geq 1 \text{ and } \Delta t\|\nabla \cdot u_h'^n\|_{L^4}^2 \leq \frac{(\gamma_\kappa - 1)\kappa}{2C_s\gamma_\kappa}. \tag{6.28}$$

Given (6.21), (6.22) and (6.28), sum (6.19) from 0 to N and stability of the temperature approximation follows.

The stability proof of the velocity approximation is similar to the temperature one. Let $v_h = u_h^{n+1} \in V_h$, multiply by Δt and use the polarization identity. Then,

$$\frac{1}{2}(\|u_h^{n+1}\|^2 - \|u_h^n\|^2) + \frac{1}{2}\|u_h^{n+1} - u_h^n\|^2 + \Delta t b^*(u_h'^n, u_h^n, u_h^{n+1}) + \Delta t Pr\|\nabla u_h^{n+1}\|^2 \tag{6.29}$$
$$+ \Delta t\int_\Omega \gamma_{Pr}\Delta t|u'^n|^2|\nabla u_h^{n+1}|^2 dx = \Delta t Pr Ra\gamma(T_h^{n+1}, u_h^{n+1}) + \Delta t(f^{n+1}, u_h^{n+1}).$$

Using Young's inequality with $\epsilon = \frac{1}{2}$ and $\epsilon = \frac{Pr}{2}$ respectively, the right-hand side is bounded by

$$\Delta t Pr Ra\gamma(T_h^{n+1}, u_h^{n+1}) = \Delta t Pr(Ra\gamma T_h^{n+1}, u_h^{n+1}) \tag{6.30}$$
$$\leq \Delta t\frac{Pr}{4}\|\nabla u_h^{n+1}\|^2 + \Delta t Pr Ra^2\gamma^2\|T_h^{n+1}\|_*^2 \tag{6.31}$$

$$\Delta t(f^{n+1}, u_h^{n+1}) \leq \frac{\Delta t Pr}{4}\|\nabla u_h^{n+1}\|^2 + \frac{2\Delta t}{\mathrm{Pr}}\|f^{n+1}\|_*^2 \tag{6.32}$$

and the resulting term $\frac{\Delta t Pr}{2}\|\nabla u_h^{n+1}\|^2$ is moved to the left hand side.

Next, the trilinear term $|-\Delta t b^*(u_h'^n, T_h^n, T_h^{n+1})|$ is bounded by

$$
\begin{aligned}
|-\Delta t b^*(u_h'^n, u_h^n, u_h^{n+1})| &= |\Delta t b^*(u_h'^n, u_h^n - u_h^{n+1}, u_h^{n+1})| \\
&= |\Delta t b^*(u_h'^n, u_h^{n+1}, u_h^{n+1} - u_h^n)| \\
&= |\Delta t(u_h'^n \cdot \nabla u_h^{n+1}, u_h^{n+1} - u_h^n) + \frac{1}{2}\Delta t(\nabla \cdot u_h'^n, u_h^{n+1} \cdot (u_h^{n+1} - u_h^n))| \\
&\le \frac{\Delta t^2}{\alpha}\int_\Omega |u_h'^n|^2 |\nabla u_h^{n+1}|^2 dx + \frac{\alpha}{4}\|u_h^{n+1} - u_h^n\|^2 \\
&+ \frac{\Delta t^2}{1-\alpha}\int_\Omega |\nabla \cdot u_h'^n|^2 |u_h^{n+1}|^2 dx + \frac{1-\alpha}{4}\|u_h^{n+1} - u_h^n\|^2 \text{ for any } 0 < \alpha < 1 \\
&= \Delta t^2 \int_\Omega \left(\frac{1}{\alpha}|u_h'^n|^2 |\nabla u_h^{n+1}|^2 + \frac{1}{1-\alpha}|\nabla \cdot u_h'^n|^2 |u_h^{n+1}|^2\right) dx + \frac{1}{4}\|u_h^{n+1} - u_h^n\|^2.
\end{aligned} \tag{6.33}
$$

The stability follows provided there is an $\alpha, 0 < \alpha < 1$, such that

$$
\begin{aligned}
&\Delta t \int_\Omega \left(\frac{Pr}{2} + \gamma_{Pr}|u_h'^n|^2 \Delta t\right) |\nabla u_h^{n+1}|^2 \\
&\quad - \Delta t^2 \int_\Omega \left(\frac{1}{\alpha}|u_h'^n|^2 |\nabla u_h^{n+1}|^2 + \frac{1}{1-\alpha}|\nabla \cdot u_h'^n|^2 |u_h^{n+1}|^2\right) dx \ge 0.
\end{aligned} \tag{6.34}
$$

For $0 \le \theta \le \frac{1}{2}$, (6.34) is equivalent to

$$
\int_\Omega \left(\theta Pr + \Delta t(\gamma_{Pr} - \frac{1}{\alpha})|u_h'^n|^2\right) |\nabla u_h^{n+1}|^2 \tag{6.35}
$$

$$
+ \int_\Omega \left((\frac{1}{2} - \theta)Pr|\nabla u_h^{n+1}|^2 - \frac{\Delta t}{1-\alpha}|\nabla \cdot u_h'^n|^2 |u_h^{n+1}|^2\right) dx \ge 0. \tag{6.36}
$$

A sufficient condition for (6.35) is

$$
\begin{aligned}
\theta Pr + \Delta t(\gamma_{Pr} - \frac{1}{\alpha})|u_h'^n|^2 \ge 0 \text{ and} \\
(\frac{1}{2} - \theta)Pr\|\nabla u_h^{n+1}\|^2 - \frac{\Delta t}{1-\alpha}\|\nabla \cdot u_h'^n\|_{L^4}^2 \|u_h^{n+1}\|_{L^4}^2 \ge 0.
\end{aligned} \tag{6.37}
$$

By Sobolev embedding theorem, (6.37) holds if

$$
\begin{aligned}
\theta Pr + \Delta t(\gamma_{Pr} - \frac{1}{\alpha})|u_h'^n|^2 \ge 0 \text{ and} \\
(\frac{1}{2} - \theta)Pr\|\nabla u_h^{n+1}\|^2 - \frac{C_s \Delta t}{1-\alpha}\|\nabla \cdot u_h'^n\|_{L^4}^2 \|u_h^{n+1}\|_{L^4}^2 \ge 0.
\end{aligned} \tag{6.38}
$$

In particular, let $\gamma_{Pr} > 1$, $\alpha = \frac{1}{\gamma_{Pr}}$ and $\theta = 0$, then (6.38) reduces to

$$\gamma_{Pr} \geq 0 \text{ and } \frac{1}{2}Pr - \frac{C_s\gamma_{Pr}}{\gamma_{Pr}-1}\Delta t\|\nabla \cdot u_h'^n\|_{L^4}^2 \geq 0, \tag{6.39}$$

which is equivalent to

$$\gamma_{Pr} \geq 1 \text{ and } \Delta t\|\nabla \cdot u_h'^n\|_{L^4}^2 \leq \frac{(\gamma_{Pr}-1)Pr}{2C_s\gamma_{Pr}}. \tag{6.40}$$

Given (6.30), (6.32), (6.33) and (6.40), sum (6.29) from 0 to N and stability of the velocity approximation follows.

□

6.2.2 Stability Analysis (method 2)

We state and prove herein a second stability condition for (6.15).

Theorem 6.2.2. *The scheme (6.15) is conditionally stable with respect to the timestep Δt in the following sense: Suppose $f \in L^\infty(0,t^*;H^{-1}(\Omega)^d)$, $g \in L^\infty(0,t^*;H^{-1}(\Omega))$, $\gamma_\kappa \geq 0$, $\gamma_{Pr} \geq 0$ and for all $N \geq 1$ and $j = 1,...,J$ if*

$$\|\nabla \cdot u_j'^n\|^2 \leq \min\{\frac{\kappa h}{C^*\Delta t}, \frac{Prh}{C^*\Delta t}\} \tag{6.41}$$

where $C* = C(\Omega, C_{PF}, C_{inv}, C_2)$, then

$$\begin{aligned}
&\frac{1}{2}\|u_h^{N+1}\|^2 + \frac{1}{4}\sum_{n=0}^{N}\|u_h^{n+1}-u_h^n\|^2 + \frac{Pr\Delta t}{2}\|\nabla u_h^{N+1}\|^2 \\
&+ \frac{Pr\Delta t}{2}\sum_{n=0}^{N}\|\nabla u_j^n\|^2\left(1 - \frac{C*\Delta t}{Prh}\|\nabla u_h'^n\|^2\right) + \Delta t\sum_{n=0}^{N}\int_\Omega \gamma_{Pr}\Delta t|u_h'^n|^2|\nabla u_j^{n+1}|^2 dx \\
&\leq \frac{1}{2}\|u_h^0\|^2 + \frac{Pr\Delta t}{2}\|\nabla u_j^0\|^2 + \frac{2\Delta t}{Pr}\sum_{n=0}^{N}\|f^{n+1}\|_*^2 + \Delta t PrRa^2\gamma^2\sum_{n=0}^{N}\|T_h^{n+1}\|_*^2.
\end{aligned} \tag{6.42}$$

$$\frac{1}{2}\|T_h^{N+1}\|^2 + \frac{1}{4}\sum_{n=0}^{N}\|T_h^{n+1}-T_h^n\|^2 + \frac{\kappa\Delta t}{2}\|\nabla T_h^{N+1}\|^2 \tag{6.43}$$
$$+ \frac{\kappa\Delta t}{2}\sum_{n=0}^{N}\|\nabla T_j^n\|^2\left(1-\frac{C*\Delta t}{\kappa h}\|\nabla u_h'^n\|^2\right) - \Delta t\sum_{n=0}^{N}\int_\Omega \gamma_\kappa \Delta t|u_h'^n|^2|\nabla T_j^{n+1}|^2 dx$$
$$\leq \frac{1}{2}\|T_h^0\|^2 + \frac{\kappa\Delta t}{2}\|\nabla T_j^0\|^2 + \frac{\Delta t}{2\kappa}\sum_{n=0}^{N}\|g^{n+1}\|_*^2.$$

Proof. We begin by proving the stability result of the temperature equation.
Let $S_h = T_h^{n+1}$, multiply by Δt and use the polarization identity. Then,

$$\frac{1}{2}(\|T_h^{n+1}\|^2 - \|T_h^n\|^2) + \frac{1}{2}\|T_h^{n+1}-T_h^n\|^2 + \Delta t\kappa\|\nabla T_h^{n+1}\|^2 \tag{6.44}$$
$$+ \Delta t\int_\Omega \gamma_\kappa\Delta t|u'^n|^2|\nabla T_h^{n+1}|^2 dx$$
$$= \Delta t(g^{n+1}, T_h^{n+1}) - \Delta t b^*(u_h'^n, T_h^n, T_h^{n+1}),$$

Using Young's inequality with $\epsilon = \kappa$, the right-hand side is bounded by

$$\Delta t(g^{n+1}, T_h^{n+1}) \leq \frac{\Delta t\kappa}{2}\|\nabla T_h^{n+1}\|^2 + \frac{\Delta t}{2\kappa}\|g^{n+1}\|_*^2 \tag{6.45}$$

and the term $\frac{\Delta t\kappa}{2}\|\nabla T_h^{n+1}\|^2$ is moved to the left hand side.
Next, the trilinear term $|-\Delta t b^*(u_h'^n, T_h^n, T_h^{n+1})|$ is bounded by

$$\begin{aligned}|-\Delta t b^*(u_h'^n, T_h^n, T_h^{n+1})| &\leq \Delta t\overline{C_2}\|\nabla u_h'^n\|\|\nabla T_h^n\|\sqrt{\|T_h^{n+1}-T_h^n\|\|\nabla T_h^{n+1}-T_h^n\|} \\ &\quad + \frac{C\Delta t}{2}\|\nabla u_h'^n\|\|T_h^n(T_h^{n+1}-T_h^n)\| \\ &\leq \Delta t\overline{C_2}\|\nabla u_h'^n\|\|\nabla T_h^n\|\sqrt{\|T_h^{n+1}-T_h^n\|\|\nabla T_h^{n+1}-T_h^n\|} \\ &\quad + C\Delta t\frac{C_{PF,2}^{\frac{3}{2}}}{2}\|\nabla u_h'^n\|\|\nabla T_h^n\|\sqrt{\|T_h^{n+1}-T_h^n\|\|\nabla T_h^{n+1}-T_h^n\|},\end{aligned} \tag{6.46}$$

where Cauchy-Schwarz is used on $\|T_h^n(T_h^{n+1}-T_h^n)\|$, then split the $\|(T_h^{n+1}-T_h^n)\|$ into two terms to the one half power and applied Poincaré-Friedrichs on the second term and one of these terms. We now apply the inverse inequality to the pertinent terms,

$$\begin{aligned}
&\leq \Delta t\overline{C_2}\|\nabla u_h'^n\|\|\nabla T_h^n\|C_{inv,2}h^{-\frac{1}{2}}\|T_h^{n+1}-T_h^n\| \\
&\qquad + C\Delta t\frac{C_{PF,2}^{\frac{3}{2}}}{2}\|\nabla u_h'^n\|\|\nabla T_h^n\|C_{inv,2}h^{-\frac{1}{2}}\|T_h^{n+1}-T_h^n\| \\
&\qquad\leq \frac{(\overline{C_2}+0.5C_{PF,2}^{\frac{3}{2}}C)\Delta tC_{inv,2}}{h^{\frac{1}{2}}}\|\nabla u_h'^n\|\|\nabla T_h^n\|\|T_h^{n+1}-T_h^n\|, \quad (6.47)
\end{aligned}$$

where we have regrouped in the last inequality. Lastly, apply Cauch-Schwartz-Young to the right hand side,

$$|-\Delta tb^*(u_h'^n,T_h^n,T_h^{n+1})| \leq \frac{\overline{C}^*\Delta t^2}{h}\|\nabla u_h'^n\|^2\|\nabla T_h^n\|^2+\frac{1}{4}\|T_h^{n+1}-T_h^n\|^2, \quad (6.48)$$

where $\overline{C}^* \equiv \overline{C}^*(\Omega_e, C_{PF,2}, C_{inv,2}, \overline{C_2})$. Regrouping all terms leads to

$$\begin{aligned}
&\frac{1}{2}(\|T_h^{n+1}\|^2-\|T_h^n\|^2)+\frac{1}{4}\|T_h^{n+1}-T_h^n\|^2+\frac{\kappa\Delta t}{2}(\|\nabla T_h^{n+1}\|^2-\|\nabla T_h^n\|^2) \\
&+\frac{\kappa\Delta t}{2}\|\nabla T_h^n\|^2\left(1-\frac{C^*\Delta t}{\kappa h}\|\nabla u_h'^n\|^2\right)+\Delta t\int_\Omega \gamma_\kappa\Delta t|u_h'^n|^2|\nabla T_h^{n+1}|^2dx \\
&\quad\leq \frac{\Delta t}{2\kappa}\|g^{n+1}\|_*^2.
\end{aligned}$$

Taking the sum from $n=0$ to $n=N$ gives (6.43).

Next we prove the stability of the velocity using the stability of the temperature.

Let $v_h = u_h^{n+1}$, multiply by Δt and use the polarization identity. Then,

$$\begin{aligned}
&\frac{1}{2}(\|u_h^{n+1}\|^2-\|u_h^n\|^2)+\frac{1}{2}\|u_h^{n+1}-u_h^n\|^2+\Delta tPr\|\nabla u_h^{n+1}\|^2 \quad (6.49)\\
&\qquad+\Delta t\int_\Omega \gamma_{Pr}\Delta t|u'^n|^2|\nabla u_h^{n+1}|^2dx \\
&\qquad=\Delta t(f^{n+1},T_h^{n+1})+\Delta tPrRa\gamma(T_h^{n+1},u_h^{n+1})-\Delta tb^*(u_h'^n,u_h^n,u_h^{n+1}),
\end{aligned}$$

Using Young's inequality with $\epsilon = \frac{Pr}{2}$ and $\epsilon = \frac{1}{2}$ respectively, the right-hand side is bounded by

$$\begin{aligned}\Delta t(f^{n+1}, u_h^{n+1}) &\leq \frac{\Delta t Pr}{4}\|\nabla u_h^{n+1}\|^2 + \frac{2\Delta t}{Pr}\|f^{n+1}\|_*^2 \qquad (6.50)\\ \Delta t Pr Ra\gamma(T_h^{n+1}, u_h^{n+1}) &= \Delta t Pr(Ra\gamma T_h^{n+1}, u_h^{n+1})\\ &\leq \Delta t\frac{Pr}{4}\|\nabla u_h^{n+1}\|^2 + \Delta t Pr Ra^2\gamma^2\|T_h^{n+1}\|_*^2,\end{aligned}$$

and the combined terms $\frac{\Delta t Pr}{2}\|\nabla u_h^{n+1}\|^2$ are moved to the left hand side.
Next, the trilinear term $|-\Delta t b^*(u_h'^n, u_h^n, u_h^{n+1})|$ is bounded by

$$\begin{aligned}|-\Delta t b^*(u_h'^n, u_h^n, u_h^{n+1})| &\leq \Delta t\overline{C_2}\|\nabla u_h'^n\|\|\nabla u_h^n\|\sqrt{\|u_h^{n+1}-u_h^n\|\|\nabla u_h^{n+1}-u_h^n\|}\\ &\quad + \frac{C\Delta t}{2}\|\nabla u_h'^n\|\|u_h^n(u_h^{n+1}-u_h^n)\|\\ &\leq \Delta t\overline{C_2}\|\nabla u_h'^n\|\|\nabla u_h^n\|\sqrt{\|u_h^{n+1}-u_h^n\|\|\nabla u_h^{n+1}-u_h^n\|}\\ &\quad + C\Delta t\frac{C_{PF,2}^{\frac{3}{2}}}{2}\|\nabla u_h'^n\|\|\nabla u_h^n\|\sqrt{\|u_h^{n+1}-u_h^n\|\|\nabla u_h^{n+1}-u_h^n\|}, \qquad (6.51)\end{aligned}$$

where Cauchy-Schwarz is used on $\|u_h^n(u_h^{n+1}-u_h^n)\|$, then split the $\|(u_h^{n+1}-u_h^n)\|$ into two terms to the one half power and applied Poincaré-Friedrichs on the second term and one of these terms. We now apply the inverse inequality to the right hand side,

$$\begin{aligned}|-\Delta t b^*(u_h'^n, u_h^n, u_h^{n+1})| &\leq \Delta t\overline{C_2}\|\nabla u_h'^n\|\|\nabla u_h^n\|C_{inv,2}h^{-\frac{1}{2}}\|u_h^{n+1}-u_h^n\|\\ &\quad + C\Delta t\frac{C_{PF,2}^{\frac{3}{2}}}{2}\|\nabla u_h'^n\|\|\nabla u_h^n\|C_{inv,2}h^{-\frac{1}{2}}\|u_h^{n+1}-u_h^n\|\\ &\leq \frac{(\overline{C_2}+0.5C_{PF,2}^{\frac{3}{2}}C)\Delta t C_{inv,2}}{h^{\frac{1}{2}}}\|\nabla u_h'^n\|\|\nabla u_h^n\|\|u_h^{n+1}-u_h^n\|, \qquad (6.52)\end{aligned}$$

where we have regrouped in the last inequality. Lastly, apply Cauchy-Schwartz-Young to the right hand side,

$$|-\Delta t b^*(u_h'^n, u_h^n, u_h^{n+1})| \leq \frac{\overline{C}^*\Delta t^2}{h}\|\nabla u_h'^n\|^2\|\nabla u_h^n\|^2 + \frac{1}{4}\|u_h^{n+1}-u_h^n\|^2, \qquad (6.53)$$

where $\overline{C}^* \equiv \overline{C}^*(\Omega_e, C_{PF,2}, C_{inv,2}, \overline{C_2})$. Regrouping all terms leads to

$$\begin{aligned}
&\frac{1}{2}(\|u_h^{n+1}\|^2 - \|u_h^n\|^2) + \frac{1}{4}\|u_h^{n+1} - u_h^n\|^2 + \frac{Pr\Delta t}{2}(\|\nabla u_h^{n+1}\|^2 - \|\nabla u_h^n\|^2) \\
&+\frac{Pr\Delta t}{2}\|\nabla u_h^n\|^2\left(1 - \frac{C^*\Delta t}{Prh}\|\nabla u_h'^n\|^2\right) + \Delta t\int_\Omega \gamma_{Pr}\Delta t|u_h'^n|^2|\nabla u_h^{n+1}|^2 dx \\
&\quad\leq \frac{2\Delta t}{Pr}\|f^{n+1}\|_*^2 + \Delta t Pr Ra^2\gamma^2\|T_h^{n+1}\|_*^2.
\end{aligned}$$

Taking the sum from $n = 0$ to $n = N$ gives (6.42).

□

Remark 1. *A more precise stability condition, which combines the two methods shown above, reads*

$$\frac{\kappa\Delta t}{2}\|\nabla T_h^n\|^2\left(1 - \frac{C*\Delta t}{\kappa h}\|\nabla u_h'^n\|^2\right) + \Delta t\int_\Omega \gamma_\kappa\Delta t|u_h'^n|^2|\nabla T_h^{n+1}|^2 dx \geq 0$$

and

$$\frac{Pr\Delta t}{2}\|\nabla u_h^n\|^2\left(1 - \frac{C*\Delta t}{Prh}\|\nabla u_h'^n\|^2\right) + \Delta t\int_\Omega \gamma_{Pr}\Delta t|u_h'^n|^2|\nabla u_h^{n+1}|^2 dx \geq 0$$

leading to

$$\|\nabla u_h'^n\|^2 \leq \min\{\frac{\kappa h}{C^*\Delta t + \kappa h\gamma_\kappa C_{PF}}, \frac{Prh}{C^*\Delta t + Prh\gamma_{Pr}C_{PF}}\}. \tag{6.54}$$

7.0 COMPRESSION/RECONSTRUCTION OF TURBULENT DATA

The following chapter is based on a joint work with Professor William Layton [69].

There are a multitude of models of turbulence of various types, RANS, URANS, LES (large eddy simulation), DES, VLES, (and so on) e.g., [70, 73, 77, 83, 84], with sporadic attempts at model assessment and comparison, e.g., [74, 81, 82, 86, 87, 88]. For large eddy simulation, DNS data (e.g., time averaged velocities $u(x)$[1]) can be explicitly filtered by the chosen LES filter and the magnitude of the residual stresses, [76, 86, 88], calculated to quantify model consistency errors. This calculation (accessing raw DNS data and filtering it) is time consuming and computationally expensive. Both time and storage can be reduced substantially by precalculating and storing the needed filtered values (e.g., $\overline{u}(x)$) from which the needed quantities of interest can be calculated, greatly reducing the amount of data that needs to be sifted through. For example, with the stored filtered values, the magnitude of the residual stresses in LES closures can then be quickly calculated.

Storing and accessing only filtered values is a large reduction in the complexity of accessing and manipulating data but not a complete solution because:

1. Filtered values are needed for every filter width that is computationally interesting,

2. Filtered values are needed for every filter commonly used in LES practice (e.g., the Gaussian, box, spectral cutoff and Pao filters and more, [83, 84].

3. Approximation of filtered values for different filter widths from one stored $\overline{u}(x)$ is computationally expensive as it requires repeated filtering (if required width $>$ stored width) or deconvolution (if required width $<$ stored width), e.g.,[77].

4. Practical simulations lead to intricate computational techniques to deal with either

[1] Actually, $u = \overrightarrow{u}(x,t)$; scalar and tensor valued quantities are also important. We suppress the dependence on time and component index since they are extraneous to the methods and analysis.

filtering through a boundary,[71, 72, 78], or variable filter radii that may shrink to zero at walls, [85].

We therefore consider the problem of quickly reconstructing filtered values for a selected filter radius δ from stored values for a few radii δ_1, δ_2, etc. seeking a local formula to obviate the problems of variable radii and boundaries. Therefore we consider herein the simplest idea of (local) extrapolation from the stored radii to the new radii. This is the first step in this new problem so, while the methods are selected to be useful in the final, desired application, an ideal case is considered in the analysis: one dimension, no mesh or boundaries (so $u \in L^2(\mathbb{R})$), and constant filter radii. However, the method itself is local and does not require any of these restrictions used in the analysis of the method.

To begin, let $g(x)$ denote a filter kernel. We assume $g(x)$ is a smooth, even function decaying rapidly as $|x| \to \infty$, $g(0) = 1$, and $\int_{\mathbb{R}} g(x)dx = 1$. (Specific choices of $g(x)$ are made below.) Choose $\delta > 0$ and define

$$g_\delta(x) := \frac{1}{\delta} g(\frac{x}{\delta}), \text{ for } 0 < \delta < 1.$$

Let $L^2(\mathbb{R})$ denote the set of all measurable functions with finite norm $||u||^2 := \int_{\mathbb{R}} |u(x)|^2 dx < \infty$. Given $u(x) \in L^2(\mathbb{R})$ define

$$\overline{u}^\delta(x) = (g_\delta \star u)(x) := \int_{\mathbb{R}} g_\delta(x - x')u(x')dx'.$$

The problem is then:

Given $\overline{u}^{\delta_1}, \overline{u}^{\delta_2}$, reconstruct $\overline{u}^\delta$ approximately with bounds on error committed with low complexity and without further filtering.

Viewing $\overline{u}(x) = u(x; \delta)$ we analyze linear approximation in the scale variable δ given by (7.1) below. The error in this approximation is estimated under general assumptions on the filter and specifically for the three commonly used filters in the table below. These share the properties that $\widehat{g}_\delta(k)$ is a bounded, even function that is differentiable at $k = 0$.

Filter:	$g_\delta(x)$	$\widehat{g}_\delta(k)$
Gaussian	$\left(\frac{\gamma}{\pi}\right)^{1/2} e^{-\gamma x^2}$	$e^{-\frac{(k\delta)^2}{4\gamma}}$
Box / Top Hat	$g_\delta(x) = \begin{cases} \frac{1}{\delta} \text{ if } \lvert x\rvert < \delta/2 \\ 0 \text{ if } \lvert x\rvert \geq \delta/2 \end{cases}$	$\frac{\sin(\frac{k\delta}{2})}{(\frac{k\delta}{2})}$
Spectral Cutoff	$\frac{\sin(k_c x)}{k_c x}$	$\widehat{g}_\delta(k) = \begin{cases} 1 \text{ if } \lvert k\rvert < k_c \\ 0 \text{ if } \lvert k\rvert \geq k_c \end{cases}$

Table 1: Three common filters and their transfer functions

To minimize storage and the cost of accessing it, we analyze the reconstruction formula

$$\overline{u}^\delta(x) \simeq \overline{u}^\delta_{App}(x) := \theta \overline{u}^{\delta_1}(x) + (1-\theta)\overline{u}^{\delta_2}(x), \text{ where } \theta = \frac{\delta_2^2 - \delta^2}{\delta_2^2 - \delta_1^2}. \tag{7.1}$$

Selection of the parameter θ by different principles is discussed in Remark 3 below. The corresponding cases are

$$\begin{aligned} \text{upscaling: } & 0 < \delta_1 < \delta_2 < \delta \Rightarrow \theta < 0 \\ \text{downscaling: } & 0 < \delta < \delta_1 < \delta_2 \Rightarrow \theta > 1 \\ \text{inscaling: } & 0 < \delta_1 < \delta < \delta_2 \Rightarrow 0 < \theta < 1. \end{aligned}$$

Formula (7.1) holds down to $\delta_1 = 0$ and $\delta = 0$, giving

$$\begin{aligned} \overline{u}^\delta(x) \simeq \overline{u}^\delta_{App}(x) &:= \theta u(x) + (1-\theta)\overline{u}^{\delta_2}(x), \text{ where } \theta = 1 - \left(\frac{\delta}{\delta_2}\right)^2, \\ u(x) \simeq u_{App}(x) &:= \theta \overline{u}^{\delta_1}(x) + (1-\theta)\overline{u}^{\delta_2}(x), \text{ where } \theta = \frac{\delta_2^2}{\delta_2^2 - \delta_1^2}. \end{aligned}$$

7.1 ERROR ANALYSIS

Averaging by convolution naturally fits the tools of Fourier transforms, denoted by $\widehat{\cdot}$, with dual variable (wavenumber) k. Define

$$g_{App}(x) := \theta g_{\delta_1}(x) + (1-\theta) g_{\delta_2}(x) \text{ so that}$$
$$\overline{u}^{\delta}_{App}(x) = \int_{\mathbb{R}} g_{App}(x-x')u(x')dx' = (g_{App} \star u)(x).$$

We then have the following.

Proposition 4. *If $\widehat{g}(k)$ is a bounded, even function that is differentiable at $k=0$, $\widehat{g}_\delta(k) = \widehat{g}(k\delta)$ and*

$$\theta = \frac{\delta_2^2 - \delta^2}{\delta_2^2 - \delta_1^2}$$

then

$$\widehat{g}_{App}(k)|_{k=0} = \widehat{g}_\delta(k)|_{k=0},$$
$$\frac{d}{dk}\widehat{g}_{App}(k)|_{k=0} = \frac{d}{dk}\widehat{g}_\delta(k)|_{k=0},$$
$$\frac{d^2}{dk^2}\widehat{g}_{App}(k)|_{k=0} = \frac{d^2}{dk^2}\widehat{g}_\delta(k)|_{k=0}.$$

Proof. This is a direct calculation. Indeed, $\int g(x)dx = 1$ so $\widehat{g}(k)|_{k=0} = 1$, for $g = g_\delta, g_{\delta_1}, g_{\delta_2}, g_{App}$. Since $\widehat{g}_\delta(k)$ is an even function $\frac{d}{dk}\widehat{g}(k)|_{k=0} = 0$ for $g = g_\delta, g_{\delta_1}, g_{\delta_2}, g_{App}$ and the first derivatives also match at $k=0$. Since $\widehat{g}_\delta(k) = \widehat{g}(k\delta)$, second derivatives matching at $k=0$ is equivalent to

$$\delta^2 \frac{d^2\widehat{g}(0)}{dk^2} = \theta\delta_1^2 \frac{d^2\widehat{g}(0)}{dk^2} + (1-\theta)\delta_2^2 \frac{d^2\widehat{g}(0)}{dk^2},$$

or

$$\delta^2 = \theta\delta_1^2 + (1-\theta)\delta_2^2,$$

yielding to the chosen value of θ.
If $\frac{d^2\widehat{g}(0)}{dk^2} = 0$ then matching of second derivatives at $k=0$ holds trivially. Otherwise it follows provided $\delta^2 = \theta\delta_1^2 + (1-\theta)\delta_2^2$ which is satisfied for the specified value of θ. □

Remark 5. *Third derivatives at $k = 0$ match since $\frac{d^3\widehat{g}(0)}{dk^3} = 0$. Fourth derivatives match at $k = 0$ provided $\theta\delta_1^4 + (1-\theta)\delta_2^4 = \delta^4$ which does not hold generally. Such matching could be enforced by storing more filtered values and using 2 parameters.*

Remark 6. *[The general case]The general approach is as follows. Write*

$$\overline{u}^{\delta}(x) \simeq \overline{u}^{\delta}_{App}(x) := \sum_{j=0}^{J} \theta_j \overline{u}^{\delta_j}(x), \text{ and}$$
$$g_{App}(x) := \sum_{j=0}^{J} \theta_j g_{\delta_j}(x)$$

where θ_j are chosen to maximize accuracy on smooth components. Following Proposition (4), so that

$$\frac{d^j}{dk^j}\widehat{g}_{App}(k)|_{k=0} = \frac{d^j}{dk^j}\widehat{g}_{\delta}(k)|_{k=0}, j = 0, \cdots, 2J.$$

For the filters where $\widehat{g}(k)$ is a smooth function near $k = 0$, that is even, matching odd order derivatives at $k = 0$ is automatic (because it reduces to $0 = 0$). Matching even derivatives at $k = 0$ up to order $2J$ requires

$$\sum_{j=0}^{J} \delta_j^{2l}\theta_j = \delta^{2l}, \text{ for } l = 0, \cdots, J.$$

For the simplest case herein of $J = 1$, $l = 0, 1$, this gives the equations

$$\theta_0 + \theta_1 = 1 \text{ and } \delta_0^2\theta_0 + \delta_1^2\theta_1 = \delta^2$$

whose solution is above.

We let $M(k) = \widehat{g}_{\delta}(k) - \widehat{g}_{App}(k)$.

Proposition 5. *Set $\theta = \frac{\delta_2^2 - \delta^2}{\delta_2^2 - \delta_1^2}$. For any $\kappa \geq 0$ and any fixed but arbitrary cutoff frequency π/α we have*

$$||\overline{u}^{\delta} - \overline{u}^{\delta}_{App}||^2 \leq \frac{1}{576}\left(\max_{|k|<\pi/\alpha} |M^{(iv)}(k)|^2\right)||\frac{d^4u}{dx^4}||^2 + C\alpha^{2\kappa}||\frac{d^{\kappa}u}{dx^{\kappa}}||^2$$

Proof. By Parseval's equality, we have the error representation

$$||\overline{u}^{\delta} - \overline{u}^{\delta}_{App}||^2 = \int_{\mathbb{R}} M(k)^2 |\widehat{u}(k)|^2 dk.$$

Pick π/α and decompose the error by

$$||\overline{u}^{\delta} - \overline{u}^{\delta}_{App}||^2 = \left(\int_{|k|<\pi/\alpha} + \int_{|k|\geq\pi/\alpha} \right) M(k)^2 |\widehat{u}(k)|^2 dk = I_1 + I_2.$$

For I_2 use $|M(k)| \leq 2$, and $|\pi/\alpha|^{-2\kappa}|k|^{+2\kappa} \geq 1$ for $|k| \geq \pi/\alpha$ and $\kappa \geq 0$. This yields

$$\begin{aligned} I_2 &\leq 2 \int_{|k|\geq\pi/\alpha} |\widehat{u}(k)|^2 dk \leq 2 \left(\frac{\alpha}{\pi}\right)^{2\kappa} \int_{|k|\geq\pi/\alpha} |k|^{+2\kappa} |\widehat{u}(k)|^2 dk \\ &\leq 2 \left(\frac{\alpha}{\pi}\right)^{2\kappa} \int_{\mathbb{R}} |k|^{+2\kappa} |\widehat{u}(k)|^2 dk \leq C\alpha^{2\kappa} ||\frac{d^{\kappa} u}{dx^{\kappa}}||^2, \text{ where } C = C(\kappa). \end{aligned}$$

For I_1 we have, by Taylor's theorem, using $M(0) = M'(0) = M''(0) = M'''(0) = 0$,

$$\begin{aligned} I_1 &= \int_{|k|<\pi/\alpha} \left[\frac{k^4}{4!} M^{(iv)}(k^*) \right]^2 |\widehat{u}(k)|^2 dk, \text{ for some } k^*, 0 < k^* < \frac{\pi}{\alpha}, \\ &\text{thus } I_1 \leq \frac{1}{576} \max_{|k|<\pi/\alpha} |M^{(iv)}(k)|^2 \int_{|k|<\pi/\alpha} k^8 |\widehat{u}(k)|^2 dk, \\ &\text{thus } I_1 \leq \frac{1}{576} \max_{|k|<\pi/\alpha} |M^{(iv)}(k)|^2 ||\frac{d^4 u}{dx^4}||^2. \end{aligned}$$

Combining the bounds for I_1 and I_2 completes the proof. □

The error in reconstruction depends (modulo the second, higher order term $C\alpha^{2\kappa}||\frac{d^{\kappa}u}{dx^{\kappa}}||^2$) on $\max_{|k|<\pi/\alpha} |\widehat{g}_{\delta}(k) - \widehat{g}_{App}(k)|^2$. This depends on the exact filter used and α in the choice of cutoff frequency.

Remark 7 (A min-max problem for θ)**.** *Since* $M(k) = \widehat{g}_\delta(k) - \theta\widehat{g}_{\delta_1}(k) - (1-\theta)\widehat{g}_{\delta_2}(k)$ *an alternate approach to determining* θ *is via the non-standard min-max problem*

$$\min_\theta \max_{|k|<\pi/\alpha} \left|\widehat{g}_\delta(k) - \theta\widehat{g}_{\delta_1}(k) - (1-\theta)\widehat{g}_{\delta_2}(k)\right|.$$

The min-max problem simplifies for the gaussian filter. Let $z = e^{-\frac{(k\delta_2)^2}{4\gamma}}$*, then it becomes*

$$\min_\theta \max_{0<z<1} \left|z^a - \theta z^b - (1-\theta)z\right| \quad \textit{where } a = \left(\frac{\delta}{\delta_1}\right)^2, b = \left(\frac{\delta_1}{\delta_2}\right)^2.$$

We do not have a solution of even this simplified problem. If the problem is changed to least squares

$$\min_\theta \int_0^1 \left|z^a - \theta z^b - (1-\theta)z\right|^2 dz$$

then the solution is

$$\theta = \frac{-\frac{1}{a+b+1} + \frac{1}{a+2} + \frac{1}{b+1} - \frac{1}{2}}{-\frac{1}{2b+1} - \frac{2}{b+2} + \frac{1}{3}}.$$

The Spectral Cutoff Filter.

Proposition (5) already yields an estimate for the reconstruntion error in spectral cutoff. The exponential accuracy of spectral cutoff is shared by the approximation. We find that $M(k) = 0$ for all k.

Theorem 1 (Reconstruction of spectral cutoff filtering)**.** *For any* $\kappa \geq 0$ *and any fixed but arbitrary cutoff frequency* π/α *we have*

$$||\overline{u}^\delta - \overline{u}^\delta_{App}||^2 \leq C\alpha^{2\kappa}||\frac{d^\kappa u}{dx^\kappa}||^2$$

Definition 8. *Let*

$$\varepsilon_1(\theta,\delta,\delta_1,\delta_2) = |\theta|\left(|\delta_1^4 - \delta^4| + \frac{|\delta_1^6 - \delta^6|}{\delta_2^2}\right) + |1-\theta||\delta_2^4 - \delta^4|$$

$$\varepsilon_2(\theta,\delta,\delta_1,\delta_2) = |\theta||\delta_1^4 - \delta^4| + |1-\theta|\left(|\delta_2^4 - \delta^4| + \frac{|\delta_1^6 - \delta^6|}{\delta_2^2}\right)$$

Define ε *by* $\varepsilon = \max\{\varepsilon_1, \varepsilon_2\}$.

The Gaussian Filter.

Filtering by a Gaussian has special theoretical importance, [76, 81, 78]. We thus consider **the Gaussian filter.** We have

$$\begin{aligned} M(k) &= e^{-\frac{(k\delta)^2}{4\gamma}} - \theta e^{-\frac{(k\delta_1)^2}{4\gamma}} - (1-\theta)e^{-\frac{(k\delta_2)^2}{4\gamma}} \\ &= \theta\left[e^{-\frac{(k\delta)^2}{4\gamma}} - e^{-\frac{(k\delta_1)^2}{4\gamma}}\right] + (1-\theta)\left[e^{-\frac{(k\delta)^2}{4\gamma}} - e^{-\frac{(k\delta_2)^2}{4\gamma}}\right]. \end{aligned}$$

We prove the error is $\mathcal{O}(FilterRadius^4)$.

Theorem 2. *For the Gaussian filter with $\delta_1 < \delta < \delta_2$ we have*

$$||\overline{u}^{\delta} - \overline{u}^{\delta}_{App}||^2 \leq C_1\varepsilon^2||\frac{d^4u}{dk^4}||^2 + C_2\delta_2^{2\kappa}||\frac{d^\kappa u}{dk^\kappa}||^2 \text{ for any } \kappa \geq 0$$

Proof. The estimate for $\mathcal{I}_2$ is already in Proposition (5). For $\mathcal{I}_1$, we must estimate $\max_{|k|<\pi/\alpha}|M^{(iv)}(k)|$.

$$\begin{aligned} M(k) &= \hat{g}_\delta(k) - \hat{g}_{App}(k) \\ &= \hat{g}_\delta(k) - \theta\hat{g}_{\delta_1}(k) - (1-\theta)\hat{g}_{\delta_2}(k) \\ &= \theta\left[e^{\frac{-(k\delta)^2}{4\gamma}} - e^{\frac{-(k\delta_1)^2}{4\gamma}}\right] + (1-\theta)\left[e^{\frac{-(k\delta)^2}{4\gamma}} - e^{\frac{-(k\delta_2)^2}{4\gamma}}\right]. \end{aligned}$$

As $f(x) = e^x$ is analytic, $e_i(k) = f\left(\frac{\delta k}{2}\right) - f\left(\frac{\delta_i k}{2}\right)$ is also analytic. Thus, we calculate

$$e^{\frac{-(k\delta)^2}{4\gamma}} = 1 - \frac{\delta^2k^2}{4\gamma} + \frac{1}{2!}\frac{\delta^4k^4}{(4\gamma)^2} - \frac{1}{3!}\frac{\delta^6k^6}{(4\gamma)^3} + \cdots$$

therefore,

$$\begin{aligned} e_i(k) &= e^{\frac{-(k\delta)^2}{4\gamma}} - e^{\frac{-(k\delta_i)^2}{4\gamma}} \\ &= \frac{\delta_i^2 - \delta^2}{4\gamma}k^2 + \frac{1}{2!}\frac{\delta^4 - \delta_i^4}{(4\gamma)^2}k^4 + \frac{1}{3!}\frac{\delta_i^6 - \delta^6}{(4\gamma)^3}k^6 + \cdots. \end{aligned}$$

The series for derivatives of $e_i(k)$ also converge globally:

$$e_i^{(iv)}(k) = -\frac{3(\delta_i^4 - \delta^4)}{4\gamma^2} + \frac{15(\delta_i^6 - \delta^6)}{16\gamma^3}k^2 - \cdots$$

Since these are alternating series we observe:

- If $\delta_i > \delta$,
$$-\frac{3(\delta_i^4-\delta^4)}{4\gamma^2} \le e_i^{(iv)}(k) \le -\frac{3(\delta_i^4-\delta^4)}{4\gamma^2} + \frac{15(\delta_i^6-\delta^6)}{16\gamma^3}k^2$$
- If $\delta_i < \delta$,
$$-\frac{3(\delta_i^4-\delta^4)}{4\gamma^2} + \frac{15(\delta_i^6-\delta^6)}{16\gamma^3}k^2 \le e_i^{(iv)}(k) \le -\frac{3(\delta_i^4-\delta^4)}{4\gamma^2}$$

Recall that,
$$M^{(iv)}(k) = \theta e_1^{(iv)}(k) + (1-\theta)e_2^{(iv)}(k).$$

Therefore, for $\delta_1 < \delta < \delta_2$,

$$M_1 \le M^{(iv)}(k) \le M_2$$

where,
$$\begin{aligned} M_1 &= \theta\left(-\frac{3(\delta_1^4-\delta^4)}{4\gamma^2} + \frac{15(\delta_1^6-\delta^6)}{16\gamma^3}k^2\right) + (1-\theta)\left(-\frac{3(\delta_2^4-\delta^4)}{4\gamma^2}\right) \\ M_2 &= \theta\left(-\frac{3(\delta_1^4-\delta^4)}{4\gamma^2}\right) + (1-\theta)\left(-\frac{3(\delta_2^4-\delta^4)}{4\gamma^2} + \frac{15(\delta_2^6-\delta^6)}{16\gamma^3}k^2\right). \end{aligned}$$

This implies
$$|M^{(iv)}(k)| \le \max\{|M_1|, |M_2|\}$$

The next step is to bound $max_{|k|<\frac{\pi}{\alpha}}|M_1|$ and $max_{|k|<\frac{\pi}{\alpha}}|M_2|$.

$$max_{|k|<\frac{\pi}{\alpha}}|M_1| \le |\theta|\frac{3}{4\gamma^2}|\delta_1^4-\delta^4| + |\theta|\frac{15\pi^2}{16\alpha^2|\gamma|^3}|\delta_1^6-\delta^6| + |1-\theta|\frac{3}{4\gamma^2}|\delta_2^4-\delta^4|.$$

If we pick $\alpha = \delta_2$,
$$max_{|k|<\frac{\pi}{\alpha}}|M_1| \le C\varepsilon_1(\theta,\delta,\delta_1,\delta_2).$$

Similarly,
$$max_{|k|<\frac{\pi}{\alpha}}|M_2| \le C'\varepsilon_2(\theta,\delta,\delta_1,\delta_2)$$

Since $\varepsilon = \max\{\varepsilon_1,\varepsilon_2\}$, then $max_{|k|<\frac{\pi}{\alpha}}|M^{(iv)}(k)| \le C\epsilon(\theta,\delta,\delta_1,\delta_2)$.

Therefore,
$$I_1 \le C\varepsilon^2\int_{|k|<\pi/\alpha} k^8|\widehat{u}(k)|^2dk \le C\varepsilon^2||\frac{d^4}{dk^4}u||^2,$$
as claimed. □

Theorem 1 applies to downscaling and upscaling, with different ε_1 and ε_2

$$Downscaling\ (\delta < \delta_1):$$

$$\varepsilon_1 = |\theta||\delta_1^4 - \delta^4| + |1-\theta||\delta_2^4 - \delta^4|,$$
$$\varepsilon_2 = |\theta|\left(|\delta_1^4 - \delta^4| + \tfrac{|\delta_1^6 - \delta^6|}{\delta_2^2}\right) + |1-\theta|\left(|\delta_2^4 - \delta^4| + \tfrac{|\delta_2^6 - \delta^6|}{\delta_2^2}\right)$$

$$Upscaling\ (\delta > \delta_2):$$

$$\varepsilon_1 = |\theta|\left(|\delta_1^4 - \delta^4| + \tfrac{|\delta_1^6 - \delta^6|}{\delta_2^2}\right) + |1-\theta|\left(|\delta_2^4 - \delta^4| + \tfrac{|\delta_2^6 - \delta^6|}{\delta_2^2}\right)$$
$$\varepsilon_2 = |\theta||\delta_1^4 - \delta^4| + |1-\theta||\delta_2^4 - \delta^4|.$$

The proof of Theorem 1 also establishes the following result.

Theorem 3 (A general estimate)**.** *In addition to the assumptions of Proposition* (5)*, suppose* $\widehat{g}(k)$ *is analytic with its power series alternating sign. Then, the error estimate of Theorem 1 holds.*

The Box/Top Hat Filter.

We prove the error is $\mathcal{O}(FilterRadius^4)$

Theorem 4. *For the Box/Top Hat filter with* $\delta_1 < \delta < \delta_2$ *we have*

$$||\overline{u}^\delta - \overline{u}^\delta_{App}||^2 \leq C_1\varepsilon^2||\frac{d^4u}{dk^4}||^2 + C_2\delta_2^{2\kappa}||\frac{d^\kappa u}{dk^\kappa}||^2 \text{ for any } \kappa \geq 0$$

Proof. This follows from the general result in Theorem 2 above. Indeed, the power series of $sin(k)/k$ is

$$\frac{\sin k}{k} = 1 - \frac{k^2}{3!} + \frac{k^4}{5!} - \cdots$$

which alternates. Thus, as $\widehat{g}_\delta(k) = sin(\frac{k\delta}{2})/(\frac{k\delta}{2})$, its power series also alternates and the result follows. □

Theorem 3 holds for downscaling and upscaling, with different ε_1 and ε_2.

$$Downscaling\ (\delta < \delta_1):$$

$$\varepsilon_1 = |\theta||\delta_1^4 - \delta^4| + |1-\theta||\delta_2^4 - \delta^4|$$
$$\varepsilon_2 = |\theta|\left(|\delta_1^4 - \delta^4| + \tfrac{|\delta_1^6 - \delta^6|}{\delta_2^2}\right) + |1-\theta|\left(|\delta_2^4 - \delta^4| + \tfrac{|\delta_2^6 - \delta^6|}{\delta_2^2}\right)$$

$$Upscaling\ (\delta > \delta_2):$$

$$\varepsilon_1 = |\theta|\left(|\delta_1^4 - \delta^4| + \tfrac{|\delta_1^6 - \delta^6|}{\delta_2^2}\right) + |1-\theta|\left(|\delta_2^4 - \delta^4| + \tfrac{|\delta_2^6 - \delta^6|}{\delta_2^2}\right)$$
$$\varepsilon_2 = |\theta||\delta_1^4 - \delta^4| + |1-\theta||\delta_2^4 - \delta^4|$$

8.0 CONCLUSION

Does the flap of a butterfly's wings in Brazil set up a tornado in Texas? This question, raised by Edward N. Lorenz in 1972 [89], opened the door to a vast field in Fluid dynamics: Predictability.

If a single flap of a butterfly's wing can play a role in generating a tornado, so also can the flaps of the wings of millions of other butterflies, not to mention the activities of innumerable more powerful creatures, including our own species. More generally, we are proposing that over the years minuscule disturbances neither increase nor decrease the frequency of occurrences of various weather events such as tornados; the most they may do is to modify the sequences in which they occur. The question which really interests us is whether they can do even this— whether, for example, two particular weather situations differing by as little as the immediate influence of a single butterfly will generally after sufficient time evolve into two situations differing by as much as the presence of a tornado. In more technical language, is the behavior of the atmosphere unstable with respect to perturbations of small amplitude?

For the sake of this study, we developed an ensemble algorithm for the Natural Convection problem, that monitors the propagation of a small perturbation (of order of $10e^{-3}$) in the temperature initial conditions over different scales of the Earth. The latter was done in steps. First, a complete study of the Natural Convection problem, with oscillating viscosity, was made. We developed a first order and a nearly second order schemes (Chapter 3), proved their stability and led a complete error analysis.

We then moved to combining ensembles with the Natural Convection (Chapter 4). The need for ensemble calculations arises in calculation of sensitivities by differences, uncertainty quantification, stochastic NSE simulations, generation of bred vectors and their use in improving forecasting skill [6]. The most efficient way to calculate such an ensemble will vary

widely depending on the application, flow, computational resources and code used. We presented and analyzed an algorithm for computation of an ensemble of solutions such that each step requires the solution of one linear system with multiple right hand sides. Stability requires a timestep condition that can easily be imposed step by step. Experimental results under the stability condition were shown in Chapter 4, including an Earth-like example.

The above code is a closer step to our final objective. The Earth-like example was used, with different temperature initial conditions, to study the propagation of small perturbation with time. Given the negative resulting Lyapunov exponent, we provided evidence that the Earth average temperature is predictable and stable. The same experiment was performed on different sections of the Earth model, leading to the following observation: the larger the domain, the more predictable the temperature is.

Our second objective was to extend the predictability analysis to turbulent models, such as the Turbulent Natural Convection problem, with fluctuating Prandtl number and heat conductivity (Chapter 6). using an implicit-explicit time-discretization, we developed an ensemble algorithm for the turbulent Natural Convection problem and were able to prove its stability, under certain conditions mentioned in Chapter 6. The next natural step would be to develop a FreeFem++ code for the problem and study the temperature predictability in a way similar to what was done in Chapter 5.

Finally, some additional work was added to this thesis: the compression and reconstruction of turbulent flow data, showing a method of reconstruction of new averages given old ones.

The work presented in this thesis opens a wide door to research in predictability of average temperatures. As mentioned above, a code for the ensemble turbulent natural convection problem is now in progress. The Earth-like example will be of great interest for that study; in which case we expect a positive Lyapunov exponent and thus a positive doubling time; i.e, concluding that the average temperatures cannot be predicted in that case. The following step is the develop a Bred-Vector algorithm to generate the initial data for the ensemble studies.

BIBLIOGRAPHY

[1] E. N. Lorenz, *Atmospheric predictability experiments with a large numerical model*, TeNus (1982), 34,505-513.

[2] M. A. Belenli, S. Kaya, and L. G. Rebholz, *An Explicitly Decoupled Variational Multiscale Method for Incompressible, Non-Isothermal Flows*, Comput. Methods Appl. Math., 15 (2015), pp. 1-20.

[3] J. Boland and W. Layton, *An analysis of the finite element method for natural convection problems*, Numer. Methods Partial Diferential Equations, 2 (1990), pp. 115-126.

[4] J. Boland and W. Layton, *Error analysis for finite element methods for steady natural convection problems*, Numer. Funct. Anal. Optim., 11 (1990), pp. 449-483.

[5] S. Chandrasekhar, *Hydrodynamic and hydromagnetic stability*, Dover Publications, Inc., New York, 1981.

[6] N. Jiang and W. Layton, *An Algorithm for Fast Calculation of Flow Ensembles*, Int. J. Uncertain. Quantif., 4 (2014), pp. 273-301.

[7] N. Jiang and W. Layton, *Numerical analysis of two ensemble eddy viscosity numerical regularizations of fluid motion*, Numer Meth Part D E, 31 (2015), pp.630-651

[8] G. Karniadakis and J. Glimm, *Uncertainty quantification in simulation science*, J. Comput. Phys., 217 (2006), pp. 1-4.

[9] E. Kalnay, *Atmospheric modeling, data assimilation and predictability*, Cambridge University Press, New York, 2003.

[10] W. J. Layton, *Introduction to the Numerical Analysis of Incompressible Viscous Flows*, SIAM, Philadelphia, PA, 2008.

[11] W. J. Layton and E.P. Stephan, *Finite Element Method, Principles and Examples*, November 17, 1994.

[12] P. Lermusiaux et al., *Quantifying Uncertainties in Ocean Predictions*, Oceanography, 19 (2006)

[13] P. Lermusiaux, *Uncertainty estimation and prediction for interdisciplinary ocean dynamics*, J. Comput. Phys., 217 (2006), pp. 176-199

[14] M. Leutbecher and T. Palmer, *Ensemble Forecasting*, J. Comput. Phys., 227 (2008), pp. 3515-3539.

[15] J. M. Lewis, *Roots of Ensemble Forecasting*, Monthly Weather Review, 133 (2005), pp. 1865-1885.

[16] S. Lorca and J. Boldrini, *The initial value problem for a generalized Boussinesq model*, Nonlinear Analysis, 36 (1999), pp. 457-480.

[17] M. Malhotra and R. Freund, *A block QMR algorithm for non-Hermitian linear systems with multiple right-hand sides*, Linear Algebra Appl., 254 (1997), pp. 119-157.

[18] H. Morimoto, *Non-stationary Boussinesq equations*, J. Fac Sci. Univ. Tokyo, 39 (1992), pp. 61-75.

[19] D. P. O'Leary, *The Block Conjugate Gradient Algorithm and Related Methods*, Linear Algebra Appl., 29 (1980), pp. 293-332.

[20] Z. Toth and E. Kalnay, *Ensemble Forecasting at NMC: The Generation of Perturbations*, Bull. Am. Meteorol. Soc., 74 (1993), pp. 2317-2330.

[21] D. de Vahl Davis, *Natural convection of air in a square cavity: A benchmark solution*, Internat. J. Numer. Methods Fluids, 3 (1983), pp. 249-264.

[22] Y. Yu, M. Zhao, T. Lee, N. Pestieau, W. Bo, J. Glimm, and J. W. Grove, *Uncertainty quantification for chaotic computational fluid dynamics*, J. Comput. Phys., 217 (2006), pp. 200-216.

[23] Y. Zhang, Y. Hou, and J. Zhao, *Error analysis of a fully discrete finite element variational multiscale method for the natural convection problem*, Comput. Math. Appl., 67 (2014), pp. 543-567.

[24] G. Boffetta, M. Cencini, M. Falcioni, and A. Vulpiani, *Predictability: a way to characterize Complexity*, Physics Reports 356, 2002, pp. 367-474.

[25] S. Khankan, M. McLaughlin, and V. DeCaria, *Time-stepping methods for the Navier-Stokes equations with fluctuating viscosity*, in progress.

[26] S. Laplace, *Essai philosophique sur les probabilités*, Courcier, Paris 1812.

[27] N. Jiang, *A higher order ensemble simulation algorithm for fluid flows*, Journal of Scientific Computing, 64 (July 2014), pp. 264-288.

[28] M. Carney, P. Cunningham, J. Dowling and C. Lee, *Predicting Probability Distributions for Surf Height Using an Ensemble of Mixture Density Networks*, International Conference on Machine Learning, 2005.

[29] J.D. Giraldo and S.G. Garcıa Galiano, *Building hazard maps of extreme daily rainy events from PDF ensemble, via REA method, on Senegal River Basin*, Hydrology and Earth System Sciences, 15 (2011), 3605-3615.

[30] O.P Le Maitre and O.M. Kino, *Spectral methods for uncertainty quantification*, Springer, Berlin, 2010.

[31] M. Leutbecher and T.N. Palmer, *Ensemble forecasting*, J. Comp. Phys., 227 (2008), 3515-3539.

[32] J. A. Fiordilino, S. Khankan, and W. J. Layton, *Ensemble Method for Natural Convection Problem*, in progress

[33] W.J. Martin and M. Xue, *Initial condition sensitivity analysis of a mesoscale forecast using very-large ensembles*, Monthly Weather Rev., 134 (2006), 192-207.

[34] D. P. O'Leary, *The block conjugate gradient algorithm and related methods*, Linear Algebra and its Applications, 29 (1980), 293–322.

[35] Y. T. Feng, D. R. J. Owen and D. Peric, *A block conjugate gradient method applied to linear systems with multiple right hand sides*, Comp. Meth. Appl. Mech. & Engng. 127 (1995), 203-215.

[36] R. W. Freund and M. Malhotra, *A block QMR algorithm for non-Hermitian linear systems with multiple right-hand sides*, Linear Algebra and its Applications, 254 (1997), 119-157.

[37] E. Gallopulos and V. Simoncini, *Convergence of BLOCK GMRES and matrix polynomials*, Linear Algebra and its Applications, 247 (1996), 97-119.

[38] D. Chapelle and K.J. Bathe, *The inf-sup test*, Computers and Structures, Elsevier, 47 (1993), 537–545.

[39] K.J. Bathe, *The inf–sup condition and its evaluation for mixed finite element methods*, Computers and Structures, Elsevier, 79 (2001), 243–252.

[40] C. Bernardi, and Y. Maday, *Uniform inf-sup conditions for the spectral discretization of the Stokes problem*, Math. Models Methods Appl. Sci., World Scientific, 09 (1999), 395.

[41] M. Albers, *A local mesh refinement multigrid method for 3-D convection problems with strongly variable viscosity*, Journal of Computational Physics, Elsevier, 160 (2000), 126-150.

[42] G. Gui, and P. Zhang, *Global smooth solutions to the 2-D inhomogeneous Navier-Stokes equations with variable viscosity*, Chinese Annals of Mathematics, Series B, Springer, 30 (2009), 607-630.

[43] P. P. Grinevich, and M. A. Olshanskii, *An iterative method for the Stokes-type problem with variable viscosity*, SIAM Journal on Scientific Computing, SIAM, 31 (5), 2009, 3959-3978.

[44] V. John, and K. Kaiser, and J. Novo, *Finite element methods for the incompressible Stokes equations with variable viscosity*, ZAMM-Journal of Applied Mathematics and Mechanics/Zeitschrift für Angewandte Mathematik und Mechanik, SIAM, 2015.

[45] D. V. Georgievskii, *Hydrodynamical and computational aspects and stability problems for viscoplastic flows*, Journal of Mathematical Sciences, Springer, 189 (2), 2013, 223-256.

[46] M. Furuichi, and D. A. May, and P. J. Tackley, *Development of a Stokes flow solver robust to large viscosity jumps using a Schur complement approach with mixed precision arithmetic*, Journal of Computational Physics, Elsevier, 230 (24), 2011, 8835-8851.

[47] M. Renardy, *Mathematical analysis of viscoelastic flows*, CBMS-NSF Regional Conference Series in Applied Mathematics, SIAM, 2000, Philadelphia, PA.

[48] V. J. Ervin, and W. W. Miles, *Approximation of time-dependent viscoelastic fluid flow: SUPG approximation*, SIAM journal on numerical analysis, 41 (2), 2003, 457-486.

[49] V. J. Ervin, and N. Heuer, *Approximation of time-dependent, viscoelastic fluid flow: Crank-Nicolson, finite element approximation*, Numerical Methods for Partial Differential Equations, 20 (2), 2004, 248-283.

[50] V. J. Ervin, and H. Lee, *Defect correction method for viscoelastic fluid flows at high Weissenberg number*, Numerical Methods for Partial Differential Equations, 22 (1), 2006, 145-164.

[51] R. A. Trompert, and U. Hansen, *The application of a finite volume multigrid method to three-dimensional flow problems in a highly viscous fluid with a variable viscosity*, Geophysical & Astrophysical Fluid Dynamics, 83 (3-4), 1996, 261-291.

[52] P. J. Tackley, *Effects of strongly variable viscosity on three-dimensional compressible convection in planetary mantles*, Journal of Geophysical Research: Solid Earth (1978–2012), 101 (B2), 1996, 3311-3332.

[53] R. L. Cook, and H.E. King Jr, and C. A. Herbst, and D. R. Herschbach, *Pressure and temperature dependent viscosity of two glass forming liquids: glycerol and dibutyl phthalate*, The Journal of chemical physics, 100 (7), 1994, 5178-5189.

[54] M. A. Seddeek, and F. A. Salama, *The effects of temperature dependent viscosity and thermal conductivity on unsteady MHD convective heat transfer past a semi-infinite ver-*

tical porous moving plate with variable suction, Computational Materials Science, 40 (2), 2007, 186-192.

[55] R. Ellahi, *The effects of MHD and temperature dependent viscosity on the flow of non-Newtonian nanofluid in a pipe: analytical solutions*, Applied Mathematical Modelling, 37 (3), 2013, 1451-1467.

[56] J. T. Ratcliff, and P. J. Tackley, and G. Schubert, and A. Zebib, *Transitions in thermal convection with strongly variable viscosity*, Physics of the earth and planetary interiors, 102 (3), 1997, 201-212.

[57] K. Hooman, and H. Gurgenci, *Heatline visualization of natural convection in a porous cavity occupied by a fluid with temperature-dependent viscosity*, Journal of Heat Transfer, 130 (1), 2008.

[58] L. Moresi, and V. Solomatov, *Mantle convection with a brittle lithosphere: thoughts on the global tectonic styles of the Earth and Venus*, Geophysical Journal International, 133 (3), 1998, 669-682.

[59] U. Christensen, and H. Harder, *3-D convection with variable viscosity*, Geophysical Journal International, 104 (1), 1991, 213-226.

[60] J. M. Connors, and J. Howell, and W. Layton, *Decoupled time stepping methods for fluid-fluid interaction*, SIAM J. Numer. Anal., 50 (3), 2012, 1297-1319.

[61] N. Jiang W. Layton, *Numerical analysis of two ensemble eddy viscosity numerical regularizations of fluid motion*, Numerical Mathods for Partial Differential Equations, Volume 31, Issue 3, May 2015, pp 630–651

[62] M. Bulicek, and J. Malek, and K. R. Rajagopal, *Naviers slip and evolutionary Navier-Stokes-like systems with pressure and shear-rate dependent viscosity*, Indiana University mathematics journal, 56 (1), 2007, 51-85.

[63] J. Malek, and J. Necas, and K. R. Rajagopal, *Global Analysis of the Flows of Fluids with Pressure-Dependent Viscosities*, Archive for Rational Mechanics and Analysis, 165 (3), 2002, 243-269.

[64] T. Yea, and R. Mittala, and H. S. Udaykumar, and W. Shyy, *An Accurate Cartesian Grid Method for Viscous Incompressible Flows with Complex Immersed Boundaries*, Journal of Computational Physics, 156 (2), 1999, 209-240.

[65] K. Mahesha, and G. Constantinescu, and P. Moin, *A numerical method for large-eddy simulation in complex geometries*, Journal of Computational Physics, 197 (1), 2004, 215-240.

[66] V. Girault and P. A. Raviart, *Finite Element Approximation of the Navier-Stokes Equations*, Springer, Berlin, 1979.

[67] J.G. Heywood and R. Rannacher, *Finite-Element Approximation of the Nonstationary Navier-Stokes Problem Part IV: Error Analysis for Second-Order Time Discretization*, SIAM J. Numer. Anal., 27 (1990), pp. 353-384.

[68] D.S. Clark, *Short proof of a discrete gronwall inequality*, Discrete Applied Mathematics, Elsevier, Volume 16, Issue 3, March 1987, Pages 279-281.

[69] S. Khankan and W. Layton, *Upscaling, downscaling and inscaling spatial averages of turbulent flow data*, in progress.

[70] L.C. Berselli, T. Iliescu and W. Layton, *Mathematics of Large Eddy Simulation of Turbulent Flows*, Springer, Berlin, 2006.

[71] A. Bhattacharya, A. Das, and R.D. Moser. *A filtered-wall formulation for large-eddy simulation of wall-bounded turbulence*. Physics of Fluids (1994-present) 20.11 (2008): 115104.

[72] A. Dunca, V. John, & W. Layton, *The commutation error of the space averaged Navier-Stokes equations on a bounded domain* (pp. 53-78). Birkhäuser Basel, 2004.

[73] V. John, *Large Eddy Simulation of Turbulent Incompressible Flows. Analytical and Numerical Results for a Class of LES Models*, LN in CSE, 34, Springer-Verlag, Berlin, 2004

[74] V. John, *An assessment of two models for the subgrid scale tensor in the rational LES model.* Journal of computational and applied mathematics 173.1 (2005): 57-80.

[75] J.J. Koenderink, *The structure of images*, *Biol. Cybernetics*, 50 (1984), 363-370.

[76] W. Layton, and R. Lewandowski. *Residual stress of approximate deconvolution models of turbulence*. Journal of Turbulence 7 (2006) 1-21.

[77] W. Layton and L. Rebholz, *Approximation deconvolution models of turbulence*, Springer LNM, vol 2042, 2013.

[78] W. Layton, William, and C. Trenchea. *The Das–Moser commutator closure for filtering through a boundary is well-posed*. Mathematical and Computer Modelling 53.5 (2011): 566-573.

[79] R. Lewandowski, *The mathematical analysis of the coupling of a turbulent kinetic energy equation to the Navier-Stokes equation with an eddy viscosity*, Nonlinear Analysis, 28 (1997), 393-417.

[80] T. Lindeberg, *Scale-space theory in computer vision*, Kluwer, Dordrecht, (1994).

[81] J. Meyers, Bernard J. Geurts, and P. Sagaut. *A computational error-assessment of central finite-volume discretizations in large-eddy simulation using a Smagorinsky model.* Journal of Computational Physics 227.1 (2007): 156-173.

[82] J. Meyers, Bernard J. Geurts, and P. Sagaut, (eds.) *Quality and reliability of large-eddy simulations.* Vol. 12. Heidelberg: Springer, 2008.

[83] S.B. Pope, *Turbulent Flows*, Cambridge Univ. Press, Cambridge, 20002

[84] P. Sagaut, *Large eddy simulation for Incompressible flows*, Springer, Berlin, 2001.

[85] O.V. Vasilyev, T.S. Lund, and P. Moin. *A general class of commutative filters for LES in complex geometries.* Journal of Computational Physics 146.1 (1998): 82-104.

[86] B. Vreman, B. Geurts, and H. Kuerten. *A priori tests of large eddy simulation of the compressible plane mixing layer.* Journal of Engineering Mathematics 29.4 (1995): 299-327.

[87] G.S. Winckelmans, and Hervé Jeanmart. *Assessment of some models for LES without/with explicit filtering.* Direct and Large-Eddy Simulation IV. Springer Netherlands, 2001. 55-66.

[88] G.S. Winckelmans, T.S. Lund, D. Carati, & A.A. Wray, *A priori testing of subgrid-scale models for the velocity-pressure and vorticity-velocity formulations.* In Proceedings of the summer program (pp. 309-328) 1996.

[89] E.N. Lorenz, *Predictability: Does the flap of a butterfly's wing in Brazil set off a tornado in Texas?* American Association of Avdanced Science, December 1972.

[90] J.P. Crimaldi, J.R. Koseff, and S.G. Monismith, *A mixing-length formulation for the turbulent Prandtl number in wall-bounded flows with bed roughness and elevated scalar sources.* Physics of Fluids, 18, 2006.

[91] Z. Toth and E. Kalnay, *Ensemble Forecasting at NMC: The Generation of Perturbations.* American Meteorological Society, 1993.

[92] Z. Toth and E. Kalnay, *Ensemble Forecasting at NCEP and the Breeding Method.* American Meteorological Society, 1997.

[93] F. Hecht, *New development in FreeFem++.* Journal of Numerical Mathematics, vol 20 (3-4), pp 251-265, 2012.

[94] A.A. Townsend, *The structure of turbulent shear flow.* Second edition, Cambridge University Press, 1976.

[95] R. H. Kraichnan, *Turbulent Thermal Convection at Arbitrary Prandtl Number.* Phys. Fluids, Volume 4, issue 11, 1374, 1962.

[96] G. Maise and H. McDonald, *Mixing length and kinematic eddy viscosity in a compressible boundary layer.* AIAA Journal, Vol. 6, No. 1 (1968), pp. 73-80.

APPENDIX

DERIVATION OF ENSEMBLE NATURAL CONVECTION

The extra term u_1 or u_2 on the right hand side arises from setting the temperature boundary conditions to zero.We define θ to be equal to the temperature T at all time and (x, y), but with homogeneous boundary conditions. Thus if the domain is the unit square with $T = 0$ on $x = 0$ and $T = 1$ on $x = 1$, then we define $\theta(x, y, t) = T(x, y, t) - x$, which will make $\theta = 0$ on the left and right boundaries. Inside Ω, θ satisfies

$$\theta_t + \nabla \cdot (u(T - x) - \kappa \nabla (T - x) = f - \nabla \cdot (ux) + \nabla \cdot (\kappa \nabla x)$$

But $\nabla \cdot (\kappa \nabla x) = 0$ and

$$\begin{aligned} \nabla \cdot (ux) &= \frac{\partial u_1 x}{\partial x} + \frac{\partial u_2 x}{\partial y} \\ &= x u_{1,x} + u_1 \frac{\partial x}{\partial x} + x u_{2,y} + u_2 \frac{\partial x}{\partial y} \\ &= x \nabla \cdot u + u_1 \frac{\partial x}{\partial x} \\ &= u_1 \end{aligned}$$

since $\nabla \cdot u = 0$.